# MATHEMATICAL MODELS OF RESPIRATORY CONTROL IN HUMANS

Thesis submitted for the degree of Doctor of Philosophy at the University of Oxford

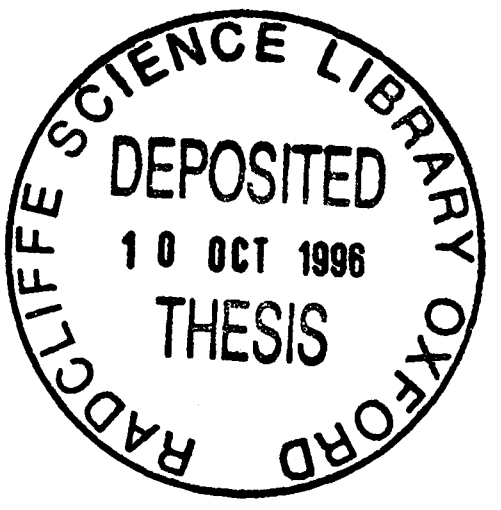


Pei-Ji Liang
Balliol College
Trinity Term, 1996

# Acknowledgements

I am deeply indebted to my supervisor Dr. Peter Robbins, whose meticulous supervision made this thesis possible.

I would particularly like to thank Dr. Jaideep Pandit, Dr. Daphne Bascom, Dr. Ian Clement, Dr. Rosemary Painter, and Mr. Ricardo Medina-Alvarez for their wonderful work on both the experimental and the modelling front. My studies have been firmly based on their work.

I would like to thank Dr. Marc Poulin for many useful discussions on the physiological front and thank Dr. Francis Marriott for his advice on many statistical matters.

I thank Dr. Jacob DeGoede, Prof. George Swanson and Prof. Denham Ward for their helpful suggestions.

I am very grateful to Dr. Piers Nye for his scientific advice and other support.

Last, but not least, I would like to thank Prof. Colin Blakemore FRS and Dr. Clive Ellory for providing me with space in the laboratory, and the Run Run Shaw and the O.R.S. foundations for awarding me my scholarships.

# Abstract

*Pei-Ji Liang*
*Balliol College*

*Mathematical Models of Respiratory Control in Humans*
*D.Phil. Thesis, Trinity Term, 1996*

This thesis is concerned with modelling the properties of human ventilation during steady-state conditions and during acute and sustained isocapnic hypoxia.

**Chapter 1** reviews some of the relevant studies in animals and humans.

**Chapter 2** describes the origins of the data studied in this thesis. In particular, it describes the experimental apparatus and the technique of dynamic end-tidal forcing used to gather the data, as well as the particular protocols employed.

**Chapter 3** studies the breath-to-breath variations in ventilation during steady breathing in both rest and during light exercise with the end-tidal gases controlled. The results suggest that: 1) both simple $ARMA$ models and a simple state-space model can describe the autocorrelation present in the data; 2) variations in spectral power were present in the data which cannot be described by these models; and 3) these variations were often due to a uniform modulation and did not significantly affect the coefficients of the models. For these kinds of data, a heteroscedastic form of state-space model provides an attractive theoretical structure for the noise processes.

**Chapter 4** studies human ventilation during sustained isocapnic hypoxia. Two models are used. The first, developed by Painter *et al.* (*J. Appl. Physiol.* 74:2007-2015, 1993) describes hypoxic ventilatory decline (HVD) as a decline in peripheral chemoreflex sensitivity. The second is an extended model which incorporates a component of HVD that is independent of peripheral chemoreflex sensitivity. The models incorporate a parallel noise structure. It is concluded that, in some subjects but not others, there is a component of HVD which is independent of peripheral chemoreflex sensitivity.

**Chapter 5** studies the human ventilatory response to cyclic isocapnic hypoxia. Both a simple proportional dynamic model suggested by Clement and Robbins (*Respir. Physiol.* 92:253-175, 1993), and an extended model with an additional non-linear rate-sensitive component are studied. The models incorporate a parallel noise structure. The results show that, although the extended model improves the fit to the data for some subjects, both models failed to explain the data fully, especially the occasional large breaths, which were shown to occur more frequently in some parts of the hypoxic cycle than other parts.

# Contents

# Chapter 1

# Introduction

知者不博　博者不知

老子・八十一

## 1.1 Brief Historical Overview

The role of breathing and the importance of its regulation has been realized since oxygen was discovered in 1779 by Lavoisier, and hypoxia (lack of oxygen) was first suggested by Lavoisier as a stimulus to respiration in 1790. Pflüger later (1868) confirmed by experiment that hypoxia stimulated ventilation and Miescher-Rüsch (1885) demonstrated that $CO_2$ pressure in the respiratory centre is another chemical factor which affects the lung-ventilation. Based on accurate measurement, Haldane and Priestley (1905) described a feedback process in respiratory control which regulates the alveolar fraction of $CO_2$. It has been from the work of Haldane that the quantitative tradition has been developed within the field of respiratory regulation.

## 1.2 Ventilatory Behaviour During Steady Breathing

### 1.2.1 Steady-state ventilatory response to chemical/exercise stimuli

Ventilation can be increased by chemical stimulation (hypoxia, hypercapnia and/or acidosis) and exercise.

Using a re-breathing technique, Haldane *et al.* (1919) demonstrated a progressive increase in ventilation during progressive hypercapnic hypoxia. Following this work, a number of studies have been focussed on the quantitative relationship between pulmonary ventilation and the partial pressure of alveolar carbon dioxide and/or oxygen. Essentially, it was found that, over a certain range, the relationship between ventilation and $P_{CO_2}$ is linear when $P_{O_2}$ is kept constant (Nielsen and Smith, 1951; Asmussen and Nielsen, 1957), while the relationship between ventilation and $P_{O_2}$ is non-linear, given constant $P_{CO_2}$ (Cormack *et al.*, 1957). Lloyd *et al.* (1958) later proposed a general relationship between ventilation and chemical stimuli as:

$$\dot{V}_E = D(P_{ET_{CO_2}} - B) + DA\frac{(P_{ET_{CO_2}} - B)}{(P_{ET_{O_2}} - C)}$$

which has become known as the Lloyd-Cunningham equation. One physiological interpretation of this equation is that hypoxia can be seen as stimulating ventilation via the peripheral chemoreflex only, while hypercapnia stimulates ventilation via both peripheral and central chemoreflexes.

By defining hypoxia as arterial desaturation, which can be approximated as an exponential function of $P_{O_2}$ for the upper part of the dissociation curve, ventilation during constant $P_{CO_2}$ was found to be linearly related to hypoxia (Kronenberg *et al.*, 1972; Rebuck and Campbell, 1974; Severinghaus, 1976). Thus the "peripheral" component of the Lloyd-Cunningham equation can be considered as a product of two components which are linearly related to hypoxia (desaturation here may be regarded as proportional to $1/(P_{ET_{O_2}} - C)$) and hypercapnia respectively.

Exercise is another factor affecting ventilation and ventilatory sensitivity to chemical stimuli. Ventilation increases during exercise. It is well recognised that, during moderate hypoxia, the ventilatory sensitivity to hypoxia is increased (Cunningham *et al.*, 1968; Weil *et al.*, 1972; Masson and Lahiri, 1974; Pandit and Robbins, 1991). An increase in the ventilatory sensitivity to hypercapnia has also been observed (Weil *et al.*, 1972; Cummin *et al.*, 1986).

### 1.2.2 Steady-state ventilatory variability

One important feature of ventilation during steady breathing is its breath-to-breath variability. The breath-to-breath variations in the pattern of breathing were first examined by Priban (1963). Tobin *et al.* (1988) reported that breath-to-breath measurements of the pattern of breathing display considerable variability, such variability has been shown to be related to age and disease (Cherniack, 1984). It has also been observed that there is more breath-to-breath variability in wakefulness and rapid-eye-movement sleep, compared with quiet sleep (Shea *et al.*, 1987; Shore *et al.*, 1985). It was thus suggested that the variability in breathing pattern is related to the central nervous system and/or the sensitivity of the chemoreflexes.

Although the underlying physiological processes for such variability still remain unclear, a number of studies have been carried out to determine whether variability in breathing pattern is caused by biological "noise" or is an integral component of respiratory control mechanisms. On analysing breath-by-breath tidal volumes and frequencies for human subjects during steady-state breathing, Priban (1963) found that both variables were correlated between successive breaths, which means that the variability in breathing was not purely "random". The autocorrelation within the respiratory variables in resting humans was confirmed by other authors (Lenfant, 1967; Bolton and Marsh, 1984) with the data collected with various compositions for the inspired gas. However, a negative correlation between the tidal volume and

frequency kept their product, the minute ventilation per breath, relatively stable (Priban, 1963; Kay *et al.*, 1975).

Further statistical studies were carried out, using the method of time-series analysis, to examine whether or not the structure of correlation could be considered as a combination of uncorrelated random (white) noise with additional components.

Benchetrit and Pham Dinh (1973) performed a statistical analysis on series of depths and durations for respiratory cycles recorded in man at rest. The results led to the conclusion that the depth and the duration of a cycle are not independent of those of the neighbouring cycle. A first order auto-regressive structure ($AR_1$) was proposed and positive coefficients were found for both tidal volume and breath duration. Jensen (1987) applied a multivariate time-series model to data from human subjects using tidal volume, and inspiratory and expiratory time durations as variables and found that the correlation could be modelled as an $AR_1$ structure. To avoid additional variability due to wakefulness influences on breathing, Modarreszadeh *et al.* (1990) studied ventilation and time-duration data obtained during stage 2 sleep. Their results showed that respiratory data records from sleeping humans generally exhibit an $AR_1$ structure with a positive $a_1$ coefficient.

Results from animal studies on the mechanism of auto-correlation have been more varied. Benchetrit and Bertrand (1975) analysed respiratory variables in bilaterally vagotomized cats, artificially ventilated under eucapnic and hypercapnic conditions at rest. Their finding was that the integrated phrenic activity and inspiratory/expiratory durations were all significantly autocorrelated with positive coefficients. They concluded that the auto-correlation was intrinsic to the respiratory control structures in the brain. In contrast to this finding, data collected from paralysed rats artificially ventilated with either 100% $O_2$ or 4% $CO_2$ in $O_2$ showed no correlation in phrenic activity during steady states of respiratory activity

(Khatib *et al.*, 1991), though in the same study, it was shown that in spontaneously breathing rats, tidal volume was positively correlated while inhaling either 100% $O_2$ or 4% $CO_2$ in $O_2$ and negatively correlated while breathing room air. The authors concluded that the autoregressive structure of ventilation is associated with the breath-to-breath changes in blood gases during spontaneous breathing. It was also suggested from these results that both central and peripheral chemical feedback loops contribute to the autoregressive behaviour, with positive and negative coefficients respectively.

## 1.3 Ventilatory Response to Acute Hypoxia

Brief exposure to hypoxia (for less than 2 minutes) results in a sharp increase in ventilation. This increase in ventilation is called the acute hypoxic response (AHR). It is well accepted that the carotid bodies are predominantly responsible for the ventilatory stimulation during hypoxia. Hypoxia produced by a reduction in arterial $P_{O_2}$ ($P_{a_{O_2}}$) initially causes an intense stimulation of the carotid chemoreceptors which in turn results in an increase in ventilation by affecting phrenic amplitude as well as respiratory duration (Fitzgerald and Lahiri, 1986). The hyperpnea of acute hypoxia is absent in human subjects who have undergone bilateral carotid-body resection (Lugliani *et al.*, 1971). In normal human subjects, the magnitude of ventilatory response to isocapnic hypoxia can be described as linearly related to the change in arterial saturation (Severinghaus, 1976). The dynamics of the ventilatory response to hypoxia will depend on the circulatory time delay from the lungs to the chemoreceptors, the dynamic properties of the chemoreceptors, and the dynamic responses of the respiratory centres to the afferent neural impulses.

### 1.3.1 Latency of ventilatory response to chemical stimuli

The latency of the peripheral chemoreflex response to the induction of a transient change in the alveolar gas (hypoxia/hypercapnia) may be viewed as the sum of the circulation time between the lungs and the carotid body, and the time then taken for a change in ventilation to result from the arrival of the stimulus at the carotid body. Latencies may be specified either in terms of breaths or time. Assessments can be made from the peripheral chemoreflex response to stimuli (Miller *et al.*, 1974; Gardner *et al.*, 1980; Clement and Robbins, 1993*b*). Estimates of the pure delay of peripheral chemoreflex have also been made with the delay as a parameter of a dynamic model (Bellville *et al.*, 1979; Dahan *et al.*, 1990; Ward *et al.* 1992; Clement

and Robbins, 1993*a*).

Using direct measurement, the mean circulatory time between the human pulmonary artery and the carotid body was estimated as 5.7 seconds by Jain *et al.* (1972). Miller *et al.* (1974) studied the transient respiratory effects in humans of sudden withdrawal of $CO_2$ and hypoxia from hypercapnic hypoxia and found the latencies to be 3 and 4 breaths respectively. Gardner *et al.* (1980) reported a similar finding for latencies during steps into isocapnic hypoxia and hypoxic hypercapnia. Clement and Robbins (1993*b*) used ventilatory data from experiments using square waves of hypoxia to estimate the latencies for the ventilatory response to isocapnic hypoxia. They reported that the measured latencies were generally shorter for the protocols with stronger stimuli, and also that the latency was slightly shorter for the off-steps than for the on-steps.

On the modelling side, studies on the human ventilatory response to a step change in $CO_2$ revealed that the latency was slightly shorter with a low $P_{O_2}$ background than that with a high $P_{O_2}$ background (Bellville *et al.*, 1979; Dahan *et al.*, 1990), the values were reported as less than 10 s. Ward *et al.* (1992) reported an estimated pure delay of 8.8 s for the ventilatory response to hypoxia. However, modelling the ventilatory response to cyclic hypoxia revealed a more complicated picture: the pure delay was significantly dependent on period for a sawtooth input but not for a square-wave input (Clement and Robbins, 1993*a*.)

### 1.3.2 Dynamic response to transient chemical stimuli and the mechanism of AHR

The dynamic characteristics of the ventilatory response to acute hypoxia have not been extensively reported in the literature, and previous research has been largely focussed on the the relationship between ventilatory behaviour and the acute change in the $CO_2$ level of the inspired and alveolar gas. However, since the ventilatory

responses to transient chemical stimuli (either hypoxia or hypercapnia) share common mechanisms, (*i.e.* a response via the peripheral chemoreflex loop), the model structure describing the ventilatory response to acute hypercapnia can be used as a starting point to describe the ventilatory response to acute hypoxia.

The dynamics of the ventilatory response to a change in inspired gas was the subject of an early report by Padget (1928). He reported that, when air containing an increased amount of $CO_2$ is breathed, the maximum increase in respiration would occur with some delay. The length of this "lag" varied with the concentration of $CO_2$ inspired. Initially, to assess the dynamics of the ventilatory response to acute $CO_2$ changes, step changes in the inspired gas mixture were used (Reynolds *et al.*, 1972). With the introduction of dynamic end-tidal forcing, step changes in alveolar gas composition could later be used as inputs to the respiratory system for the same sort of analysis (Swanson and Bellville, 1975). The advantage of controlling alveolar gas tensions is that, with the system in this open-loop condition, it makes it possible to study the chemoreflex dynamics without the feedback effect of ventilation on alveolar gas composition. From these studies, some of the dynamic features of the system — gain terms, time constants and pure delays — were estimated. Periodic stimuli have also been used. Sinusoidal variations of $CO_2$ in inspired air (Stoll, 1969) and alveolar gas (Swanson and Bellville, 1974) were used to analyse the fast response of respiratory system, and first-order dynamics were suggested for the relationship between the ventilatory response and the chemical stimulus.

In a similar manner to the models developed for changes in $P_{ET_{CO_2}}$, the dynamics of the ventilatory response to hypoxia have also been modelled by a first order system (Swanson and Bellville, 1974). This a model has been applied later on to sinusoidal (Robbins, 1984), square wave and saw-tooth wave inputs (Clement and Robbins, 1993*a*) of hypoxia at various frequencies. The results from these studies suggest

that a simple first-order linear dynamic model fails to predict ventilatory response satisfactorily and that the form of AHR is more complicated than is represented by this model.

## 1.4 Ventilatory Response to Sustained Hypoxia

In conscious humans, the ventilatory response to acute isocapnic hypoxia consists of a rapid increase in ventilation which is mediated by the peripheral chemoreflex, and which has been termed the acute hypoxic response AHR. However, this initial increase is not sustained when hypoxia is prolonged. After a brisk initial increase during the first 2-3 minutes of an isocapnic hypoxic exposure, ventilation declines over the next 20-30 mins (Edelman *et al.*, 1973; Weiskopf and Gabel, 1975; Weil and Zwillich, 1976; Kagawa *et al.*, 1982; Easton *et al.*, 1986). This second compartment of the response is generally referred to as roll-off or hypoxic ventilatory decline (HVD).

The mechanisms of HVD have not yet been clearly identified. However, hypotheses have been tested in relation to both anatomical and functional aspects and include the following: 1) whether HVD originates within the medulla or within the carotid bodies; 2) whether the mechanism results in any change in central and/or peripheral chemoreflex sensitivity; and 3) whether the mechanism results in a decline in ventilation independent of chemoreflex sensitivities. There is evidence both for and against each of these proposed mechanisms. Different dynamic mathematical models have been developed in respect of these hypotheses.

### 1.4.1 Hypothesis that HVD results from modulation of peripheral chemoreflex sensitivity

Evidence in support of HVD arising through a change in peripheral chemoreflex sensitivity has been observed in a number of different species.

Experiments performed on anaesthetised rabbits demonstrated an adaptation of the discharge from single carotid body chemoreceptor afferent fibre during prolonged hypoxia (Li *et al.*, 1990). On examining the ventilatory response to sustained isocapnic hypoxia in awake cats with and without carotid body denervation, Long *et*

*al.* (1993) found that in intact cats, ventilation exhibited a decline after a brisk increase. Such a response was not observed in chemodenervated cats. It was shown by the same group (Long *et al.*, 1994) that the peripheral chemosensitivity of awake cats was decreased after exposure to sustained hypoxia in the sense that: i) the magnitude of the rapid fall in ventilation at the relief of hypoxia is substantially smaller than the magnitude of the rapid rise in ventilation at the onset of hypoxia; and ii) after a brief period of euoxia, a rechallenge with hypoxia results in a rapid rise in ventilation that is of smaller magnitude than the response to the first exposure to hypoxia.

In conscious adult humans, HVD has been shown to be related to a change of peripheral chemoreflex sensitivity. The ventilatory response to a step out of hypoxia was observed to be smaller than that a step into the stimulus (Easton *et al.*, 1986; Khamnei and Robbins, 1990), and the response to a second step into hypoxia is smaller than that to the first step into hypoxia (Bascom *et al.*, 1992). Additionally, HVD has been found to be proportional to AHR (Easton *et al.*, 1986; Georgopoulos *et al.*, 1989; Bascom *et al.*, 1992). These findings all suggest that the process underlying HVD may involve an alteration of peripheral chemoreflex sensitivity. Furthermore, during HVD, peripheral hypercapnic sensitivity decreases (14%) less than hypoxic sensitivity (43%) (Bascom *et al.*, 1990), which supports the hypothesis that carotid bodies are involved in the development of HVD.

### 1.4.2 Hypothesis that HVD is of central original and does not affect peripheral chemoreflex sensitivity

There is a range of evidence supporting the hypothesis that HVD has a central origin, and that it causes a ventilatory decrease without affecting the peripheral chemoreflex sensitivity.

A decline in ventilation during prolonged hypoxia has been observed in exper-

iments performed on carotid-body denervated dogs (Morrill *et al.*, 1975) and cats (Lahiri, 1976; Millhorn *et al.*, 1984; Gallman and Millhorn, 1988). It has also been observed in anaesthetised cats (Vizek *et al.*, 1987; Andronikou *et al.*, 1988) that carotid sinus nerve discharge remained constant during sustained hypoxic exposure, while a decline in ventilation or phrenic nerve discharge was observed. These observations lead to the hypothesis that the central nervous system is involved in the development of HVD in a way which does not affect the sensitivity of the peripheral chemoreflex loop.

Evidence supporting this assumption has been also provided by a number of studies on the ventilatory response to central hypoxia, which eliminate the effect of peripheral chemoreflex. On performing a cross perfusion technique on intact dogs, Lee and Milhorn (1975) reported that cerebral hypoxia resulted in a ventilatory depression. Using an artificial brain stem preparation, Van Beek *et al.* (1984) showed that in cats, peripheral chemoreflex sensitivity to $CO_2$ was unchanged during ventilatory depression induced by central hypoxia. Results from a human study (Holtby *et al.*, 1988) revealed that the ventilation observed when hyperoxia succeeded hypoxia had a deeper nadir than that after room air breathing. The nadir could be deepened by a prolonged hypoxia. Since the function of the peripheral chemoreceptors is excluded by breathing pure $O_2$, this effect was suggested to have a central origin.

The possibility of HVD being caused by central hypocapnia has also been proposed. A number of relevant studies in cats have suggested that a hypoxia-induced increase in brain blood flow, washing out acid metabolites ($CO_2/H^+$) from central chemosensitive structures, plays an important role in the central depressant effect of hypoxia (Neubauer *et al.*, 1985; Ward *et al.*, 1990; Berkenbosch *et al.*, 1991*a*).

### 1.4.3 Mathematical models describing the dynamic response

A number of mathematical models describing the dynamic ventilatory response to sustained hypoxia have been developed in different ways depending upon the different hypotheses.

The initial rise and subsequent decline in the ventilatory response to sustained isocapnic hypoxia supports the idea that the dynamic should consist of at least two components. Based on the hypothesis that the decline arises centrally in a way which does not affect the peripheral chemoreflex sensitivity, a model with two parallel components was proposed to describe the ventilatory response in cats (DeGoede *et al.*, 1983) and humans (Ward *et al.*, 1992). In this model, the ventilatory response to prolonged hypoxia was described by one component representing the stimulating effects of hypoxia and another component represents the hypoxic ventilatory decline, the total ventilatory response to hypoxia is represented by the sum of the two components. However, this model failed to describe the asymmetry of the human ventilatory response at the on- and off-transient of the hypoxic stimulus (Boetger Mann *et al.*, 1989).

Based on the hypothesis that HVD results from an alteration of peripheral chemoreflex sensitivity, Painter *et al.* (1993) developed a model to describe the human ventilatory response to both a step into and a step out of hypoxia by allowing the peripheral sensitivity to hypoxia to decline during the sustained exposure to hypoxia. This model was able to describe the features of the ventilatory changes well, in the sense that it fits both the slow decline and asymmetry. However, this model did not appear to describe the period after the relief of hypoxia particularly well, which implies some imperfections with the model.

## 1.5 Aims of this Thesis

The main aim of this thesis is to develop and improve the mathematical models describing the intrinsic breath-to-breath variability in ventilation and also the dynamic ventilatory response to acute and prolonged hypoxia. To achieve this, the following studies were carried out:

1. An investigation of the statistical properties of ventilatory variability to develop an appropriate model for describing the ventilatory behaviour during steady breathing. This model would later be incorporated into dynamic models for describing the ventilatory response to dynamic hypoxic stimuli.

2. An investigation of the fast component of ventilatory response to acute hypoxia in response to periodic hypoxic stimuli; reasonable models which are based on the underlying physiological mechanisms are explored.

3. An investigation of the response to sustained hypoxia; models based on the underlying physiological mechanisms are examined.

# Chapter 2

# Apparatus and Protocols Associated with the Data

大直若屈　大巧若拙

老子・四十五

## 2.1 Introduction

The data analysed in this thesis were collected by Bascom (1991), Clement (1992) and Pandit (1993). The purpose of this chapter is to describe how these data were obtained. In particular it provides a brief description of the experimental apparatus, procedure and the experimental protocols for collecting the data used in the studies presented in subsequent chapters of this thesis. The technique of dynamic end-tidal forcing (DEF) which keeps alveolar gas composition at the levels desired was employed in all of the experiments. The apparatus can basically be divided into the components related to data acquisition and the components related to gas-mixing.

Many of the methods have been described in detail by Khamnei (1990), and are the subject of a number of previous publications (Robbins *et al.*, 1982; Howson *et al.*, 1986; Howson *et al.*, 1987). They have also been reviewed by Bascom (1991), Clement (1992) and Pandit (1993).

## 2.2 Overview of Dynamic End-Tidal Forcing

Dynamic end-tidal forcing employs a computer-controlled system which, by appropriate adjustment of the inspired gases, enables the end-tidal (and hence arterial) partial pressures of the gases to be held at the values desired by the experimenter. When using this technique, the subject's alveolar gas composition is detected and controlled by the system so that it is no longer affected by ventilation. In other words, the "feedback loop" between the ventilation and the blood gases is effectively opened by the system (Fig. 2.1).

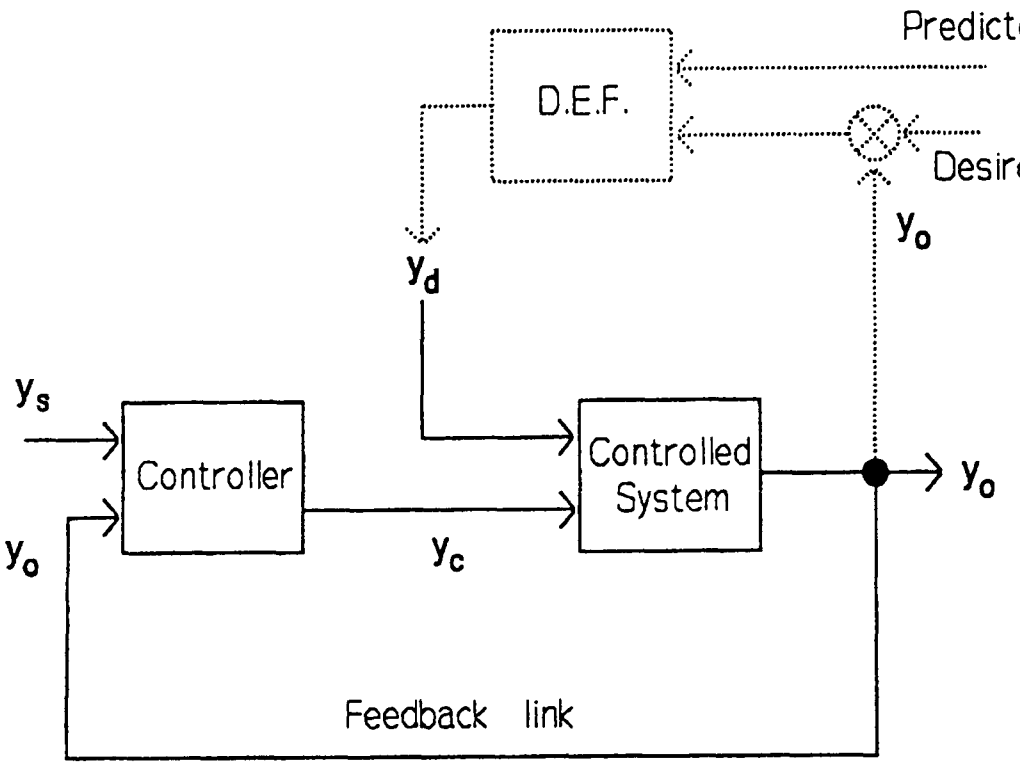


Figure 2.1: Schematic flow diagram of a respiratory chemoreflex loop (solid lines), and the flow diagram representation of the action of the dynamic end-tidal forcing system (D.E.F., dotted lines).

The natural function of a chemoreflex loop is as shown in the lower part of Fig. 2.1 in solid lines. The actual level of arterial gas composition ($y_o$) is detected by the

chemoreceptors (controller) and is compared with the desired level $y_s$. According to difference between the actual gas composition $y_o$ (which could be affected by a disturbance $y_d$) and its desired value $y_s$, ventilation $y_c$ is adjusted, this acts on the controlled system to keep the the value of $y_o$ as close as possible to the value of $y_s$. The function of this chemoreflex loop is to build up a negative feedback to maintain the arterial gas composition steady.

In order to study the properties of the controller in a regulated manner, a dynamic end-tidal forcing system (the upper part of Fig. 2.1 in dotted lines) is used to break the chemoreflex loop. This is achieved by continuous monitoring the arterial blood gas tensions, by sampling end-tidal gas composition, and adjusting them to the desired values.

Experimentally, dynamic end-tidal forcing allows the subject to be exposed to precise stimuli. First and foremost, this is valuable in studying the effects of one or other respiratory gas because the partial pressure of the other respiratory gas can be maintained constant. Thus for studies of hypoxia, the ventilatory response is caused purely by hypoxia, and is not confounded by any resulting hypocapnia. Secondly, because the system can effect very rapid changes in end-tidal partial pressures of the gases, periodical wave stimuli with a reasonable frequency can be generated to study the dynamics of the ventilatory response. In the experiments described in this thesis, the system was used to hold the end-tidal $P_{CO_2}$ constant, while end-tidal $P_{O_2}$ was either kept constant (for steady-state studies) or changed as desired (square waves for studying the peripheral component of ventilatory response to acute hypoxia and step changes for studying the ventilatory decline during sustained hypoxia).

## 2.3 Data Acquisition System

This section describes the components, calibration and operation of the data acquisition system. A schematic representation of the dynamic end-tidal forcing system is shown in Fig. 2.2.

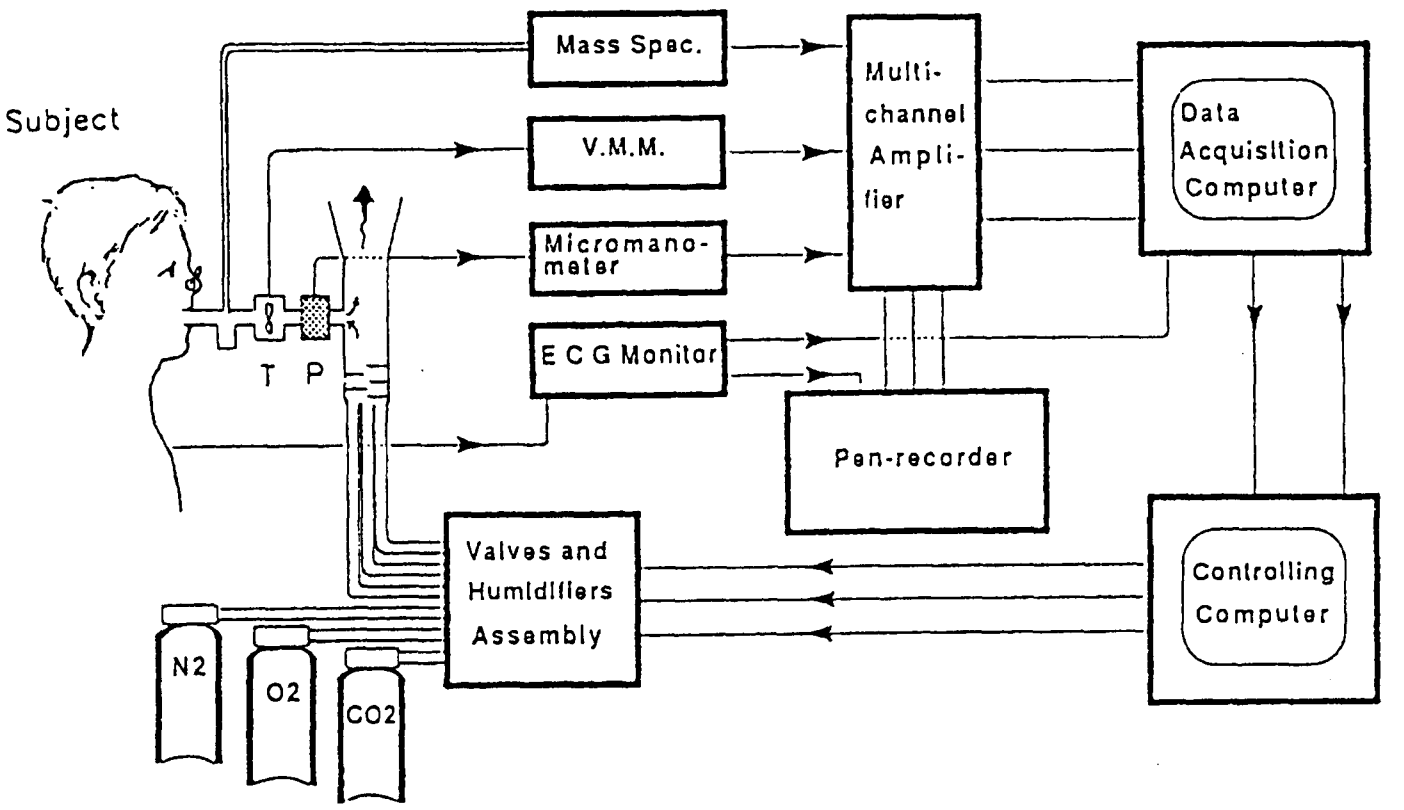


Figure 2.2: Schematic representation of the dynamic end-tidal forcing system. The upper part of the figure shows the elements of the data acquisition system, and the lower part shows the computer-controlled gas mixing system. V.M.M., ventilation measurement module. T, turbine device. P, pneumotachograph. (From Khamnei, 1990.)

### 2.3.1 Apparatus

The principal elements of the data acquisition system are the mouthpiece assembly, the turbine device and associated ventilation measurement module, the pneumotachograph and associated micromanometer, the mass spectrometer, the multi-channel amplifier, the pen recorder and the data acquisition computer.

*Mouthpiece assembly.*

The mouthpiece assembly is the apparatus through which the subject breathes, and forms a T-junction with the chamber through which newly mixed gas flows continuously. The assembly consists of a flexible plastic mouthpiece, a perspex tube with a saliva trap and a port for the sampling catheter from the mass spectrometer, a turbine flow cartridge, and a pneumotachograph. The dead space of the mouthpiece assemble was measured by Khamnei (1990) to be 90 ml. Khamnei also showed that over a flow range of 5 L/min to 100 L/min the mouthpiece assembly had a small, flow-independent resistance (0.1 $mmH_2O \cdot min/L$).

*Turbine volume device.*

Volume flows through the mouthpiece assembly are measured by a turbine device (Cardiokinetics Ltd, U.K.) which consists of a volume cartridge, a photodetector pick-up assembly and an electronic processing module (Howson *et al.*, 1986).

The response of the turbine to different volumes, over a range of 0.5 to 3.0 L, was highly linear as measured by Khamnei (1990). When the frequency of the pump was changed from 10 to 30 cycles/min there was a mean drop in the measured volume of 1.7% suggesting a small degree of frequency dependence. The measured volumes were virtually independent of gas composition, showing a change of less that 0.5% from pure oxygen to pure nitrogen.

On comparing the timings for respiratory phase switches measured by the turbine device with those measured by the pneumotachograph, a delay in turbine reversal times up to 360 msec was detected (Khamnei, 1990). Phase lags such as these make the turbine device inappropriate for determining phase switching times and instantaneous flow.

*Pneumotachograph.*

The pneumotachograph is used to provide a measurement of flow and to sense respiratory timings (from the reversal of airflow). The pneumotachograph normally used is 27 mm in length by 27 mm in diameter (Fleisch, Switzerland), with a measurable resistance to flow (of the order of 3 $mmH_2O \cdot sec/L$) which gives a small pressure drop across the resistance. This pressure drop is linear against flow (Poiseuille's Law), provided that flow is laminar. However, Macfarlane (1985) reported that if flow exceeded 130 L/min when using the small pneumotachograph, flow became turbulent. For this reason, the larger pneumotachograph, with 60 mm in length by 45 mm in diameter (UK distributor, P.K. Morgan, Chatham, Kent), which provided less resistance, was used when high ventilations were expected. This pneumotachograph increased total dead space by 80 ml.

The pressure difference across the pneumotachograph is transduced into an analogue voltage by a fast-responding micromanometer (Validyne Pressure Transducer, Model No. MP45-14-871; Validyne Engineering Corp., California, USA), set to $\pm$ 20 mmHg full deflection.

*Mass spectrometer.*

Gas was sampled from the mouthpiece assembly continuously by a fast responding quadrupole mass spectrometer (Airspec MGA3000, U.K.), at a rate of 20 ml/min via a capillary tube. The mass spectrometer output is updated every 20 msec and returns values for $O_2$, $N_2$, $CO_2$ and Argon. The total output of the four channels of the mass spectrometer is constrained to give a total gas composition of 100%, to prevent drift arising from factors as partial blockade of the sampling catheter. The delay of the mass spectrometer is within a range of 150-200 msec.

*Eight-channel amplifier.*

The analogue voltage outputs from the equipment described above were passed through a laboratory-built eight-channel amplifier. This served to condition each of the analogue signals to a range of ± 5 Volts which is the input range required by the analogue-to-digital converters (Dash-8, Metrabyte; Keithley Instruments Ltd., U.K.) used by the data acquisition computer.

*Pen recorder.*

A second set of outputs from the eight channel amplifier was passed to a hot stylus chart recorder (Lectromed Devices M19, U.K.). The chart recorder displayed the outputs of the $CO_2$ and $O_2$ channels of the mass spectrometer and the inspired and expired volumes from the ventilation measurement module.

*Heart rate monitor.*

A heart rate monitor (Model 302 Rigel Research Ltd., U.K.) provided continuous visual monitoring of the electrocardiogram measured from chest leads placed on the subject. The timing of the QRS complexes was recorded by the data acquisition computer to allow for subsequent analysis of the heart rate. These associated heart rate data were not used in this thesis.

### 2.3.2 Calibration

At the start of each experimental day, the mass spectrometer was calibrated first by using helium, in the complete absence of the analysed gases (the zeroing procedure). Room air and a standard gas (composition approx. 6.5% $CO_2$ and 7.5% $O_2$ in $N_2$) were then used for the sensitivity calibration.

The complete data acquisition system was then calibrated by using a mechanical pump "breathing" at a tidal volume of 1 L and a frequency of 20 cycles/min. Data

were collected for 2-3 min with the mass spectrometer first sensing air and then the standard gas. After the end of the data collection period, the calibration program, CLDATA, was run. The results were written in a *.cal file which contains calibration data for each of the measured variables and the user specified values for standard gas composition, pump volume, room temperature and barometric pressure. This *.cal file was later used by the gas mixing system controlling computer during the experiment and also in the analysis of the data after the experiment.

### 2.3.3 Operation

Data acquisition was performed by the RTDATA program written by P.A. Robbins and K.J. Stratford which ran continuously on the data acquisition computer during an experiment. The program performed a number of functions which included collecting and storing data from the apparatus described above, and detecting the end-expiratory values of $P_{O_2}$ and $P_{CO_2}$.

Data concerning experimental time, gas flow and gas composition were written every 20 msec in a *.raw file. The uncalibrated end-expiratory values of $P_{O_2}$ and $P_{CO_2}$ were passed on to the gas mixing system computer to allow the appropriate changes in inspiratory gas composition to be made.

The input from a manual event marker was received through a digital input/output channel and the experimental times of any event marks were recorded. At the end of the experiment RTDATA wrote a *.pk and a *.hrt file. The *.pk file contains time, volume and gas data associated with the end-inspiratory and end-expiratory point of each breath. The *.hrt file contains a record of the time of each QRS complex during the experiment.

## 2.4 Gas-Mixing System

Accurate breath-by-breath control of end-tidal $P_{CO_2}$ and $P_{O_2}$ was performed by means of a computer-controlled gas-mixing system. The layout of the gas-mixing system is shown schematically in Fig. 2.3. The hardware of the system comprises two main elements, the gas-mixing unit and the controlling computer.

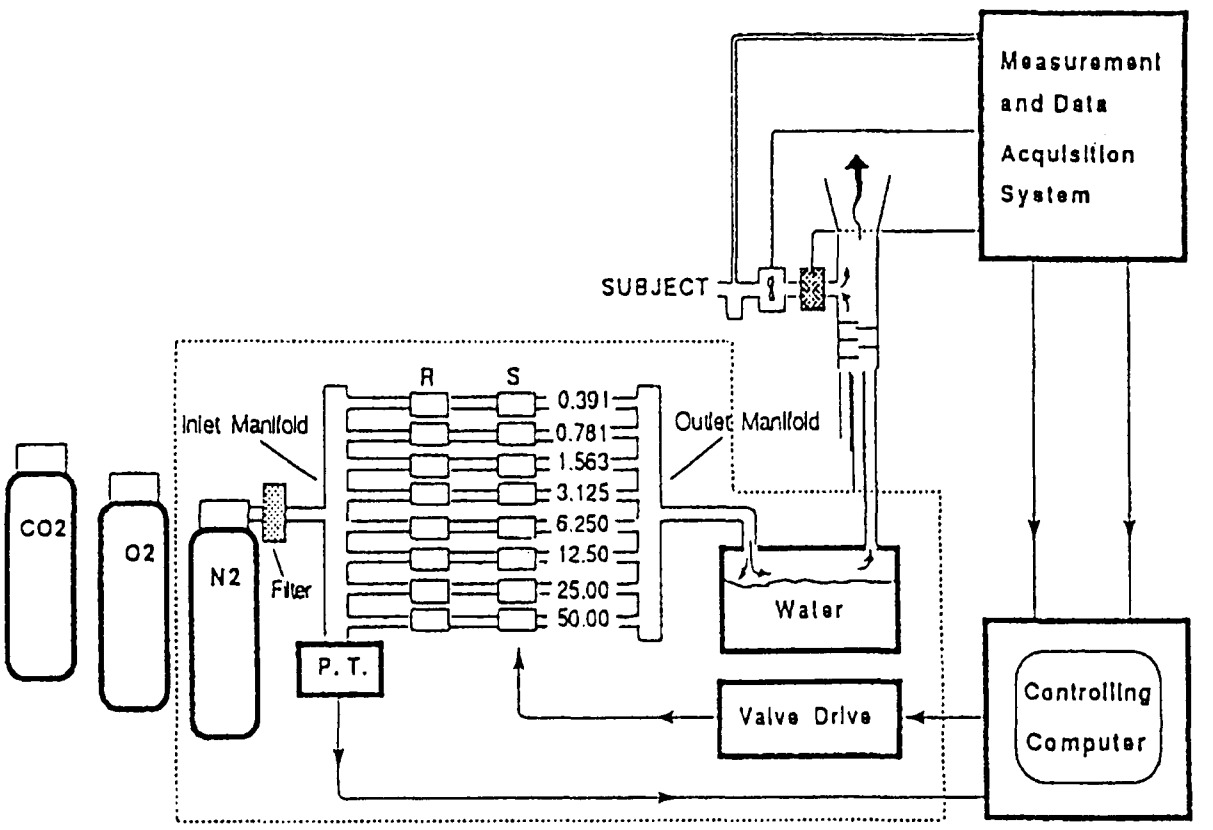


Figure 2.3: Schematic illustration of the layout of the gas mixing system shown completely for one gas species ($N_2$). The flows through each channel (L/min) at the standard supply pressure of 20 p.s.i. are shown. The resistance of each successive channel halves going from top to bottom in the illustration. P.T., pressure transducer. R, flow resistor (needle valve). S, solenoid valve. (From Khamnei, 1990.)

### 2.4.1 Gas-mixing unit

*Gas supply.*

$O_2$, $N_2$ and $CO_2$ are supplied from gas cylinders (British Oxygen Company), $O_2$

and $N_2$ as compressed gas and $CO_2$ as liquid.

*Valve assembly.*

The valve assembly consists of three similar units, one for each of the gases. Each unit consists of a gas filter (LF-3/8-5, Festo Ltd, U.K.) to remove any particles, an inlet manifold incorporating a pressure transducer, eight channels with a needle valve flow resistor (GRO-1/80 and GRO-M5, Festo Ltd., U.K.) for gas flow running in parallel, and an outlet manifold.

*Expansion Bags.*

Anaesthetic bags (M289M, Leymed Ltd, U.K.) were incorporated into the gas circuits down-stream of the outlet manifold, to act as compliant expansion chambers.

*Humidifiers.*

To supply the subject with a fully-humidified inspirate, heated humidifiers are incorporated into the $O_2$ and $N_2$ circuits. The humidifiers are laboratory built perspex boxes (10 L volume) with gas inlet and outlet holes in the top. The boxes are kept about 90% filled with distilled water which is heated to 30°C by a thermostatically controlled 1 kW element (Elmatic Ltd, U.K.).

*Mixing chamber.*

The inspirate is finally mixed when the $O_2$, $N_2$ and $CO_2$ gas circuits converge in the mixing chamber. The mixing chamber is a perspex cylinder with a volume of 0.12 L upstream of the T-junction with the mouthpiece assembly, from which the subject breathes the inspiratory gas. The whole design was aimed to keep the dead space very small and ensure that the gas mixed rapidly and thoroughly.

### 2.4.2 Controlling computer

The gas flow through each of the circuits of the gas mixing unit is controlled by a computer (IBM PC AT) running the DEF program written by P.A. Robbins. The computer controlled the solenoid valves by means of an 8 bit port which communicates with the valve driver box for each gas circuit (Fig. 2.3).

## 2.5 Dynamic End-Tidal Forcing

The process for keeping the alveolar gas composition well controlled to follow the desired levels during an experiment can be divided into two stages. The first is the feedback stage during which the controlling computer decides the inspired gas tensions, according to the information provided by the data acquisition computer. The second is the output stage during which the flow rate for each gas was decided and operation of the solenoid valves was performed. A flow diagram representing this procedure is shown in Fig. 2.4.

*Feedback stage.*

At the end of expiration, the uncalibrated values of end-tidal $P_{O_2}$ and $P_{CO_2}$ measured by the data acquisition computer were passed onto the gas-mixing system controlling computer (running the DEF program) and were converted to real values using the information in the *.cal file. In order to calculate the appropriate inspiratory $P_{O_2}$ and $P_{CO_2}$ a feedforward/feedback procedure is used which takes three factors into account: i) a predicted inspiratory partial pressure based on an estimate of the ventilatory response to the forcing function (feedforward); ii) the difference between the actual and desired end-tidal gas value for the previous breath (proportional feedback); iii) the sum of all previous differences (integral feedback). The calculation of the inspiratory gas partial pressure ($P_I$) can be presented as follows:

$$P_I = P_{I_P} + g_p \cdot (P_{ET_d}^{(n)} - P_{ET_m}^{(n)}) + g_i \cdot \sum_{j=1}^{n} (P_{ET_d}^{(j)} - P_{ET_m}^{(j)})$$

where $P_{I_P}$ is the predicted inspiratory gas tension, $P_{ET_d}$ and $P_{ET_m}$ are the desired and measured end-tidal gas tensions, and $g_p$ and $g_i$ are the proportional and integral feedback gains. The DEF program allows the values of these gains to be varied around a default value during the experiment by means of a potentiometer box. The value of $g_i$ is set to be one-tenth that of $g_p$, empirically. The accuracy with

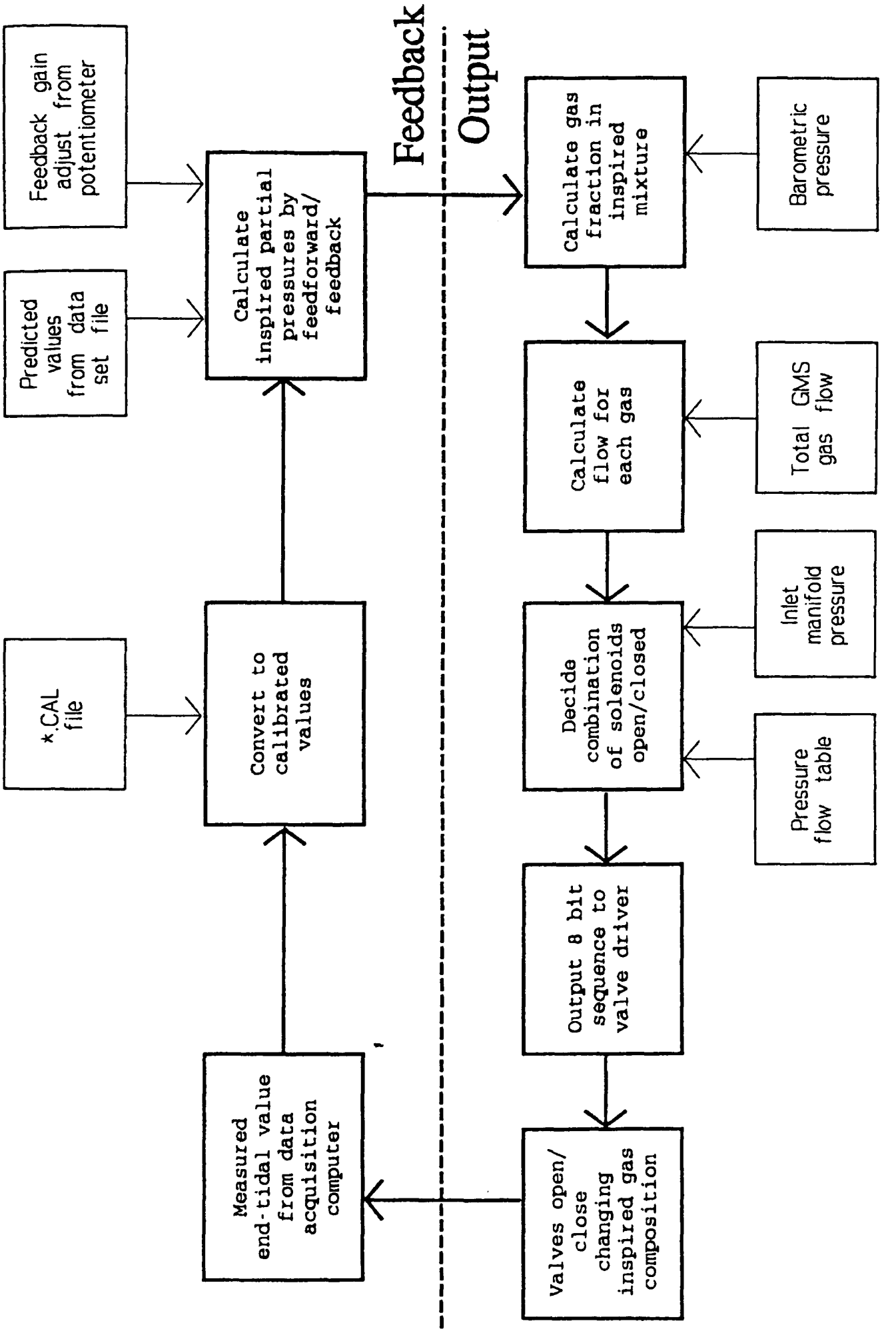


Figure 2.4: Schematic flow diagram illustrating the operation of the D.E.F. system. (From Clement, 1992.)

which the desired forcing function is followed depends on the accuracy of the initial prediction and the values of $g_i$ and $g_p$. The integral control element serves to remove steady-state errors in the prediction.

*Output stage.*

Having decided on the appropriate inspiratory gas partial pressures, the gas mixing system controlling computer calculates the fractions of the total inspirate required to give these gas pressures, which depend on the barometric pressure. It then calculates the flow of each gas required, which depends on the total gas flow specified by the experimenter. The DEF program decides the appropriate combination of valve openings/closings depending on the requested pressure flow for each gas to achieve the desired gas composition.

*Speed of system.*

The inspiratory gas composition is updated (i.e. one complete circuit of the loop in Fig. 2.4 is completed) every second and every time a new end-tidal gas value is detected. The speed of response of the system is limited by dead space, and the delay in detecting the end-tidal gas composition after the end of expiration, which is the longer of either the mass spectrometer delay or the turbine reversal delay. The system is usually sufficiently fast to modify the gas composition of some of the subsequent inspiration following an expiration.

## 2.6 Preliminary Data Analysis

After the end of each experiment the uncalibrated data in the *.raw and *.pk files were converted into meaningful respiratory data using the calibration factors in the *.cal file. A flow diagram showing the preliminary data analysis performed at the end of each experiment is shown in Fig. 2.5.

*BRDATA program.*

The BRDATA program written by P.A. Robbins and K.J. Stratford reads the *.raw, *.pk, *.hrt and *.cal files and writes the results to four files named *.d1, *.d2, *.d3 and *.d4. These files contain a variety of respiratory parameters described breath by breath. The *.d1 file contains inspiratory and expiratory volumes, times and gas tensions, together with breath-by-breath expiratory ventilation calculated as expired volume divided by breath duration measured from the start of successive inspirations. The *.d2 and *.d3 files contain information regarding oscillations in alveolar $P_{CO_2}$ and $P_{O_2}$, and metabolic production and consumption of $CO_2$ and $O_2$, respectively. The *.d4 file contains a record of the times of any marked events. The data used in this thesis are all from *.d1 and *.d4 files. The format for *.d1 and *.d4 files is illustrated in Fig. 2.6.

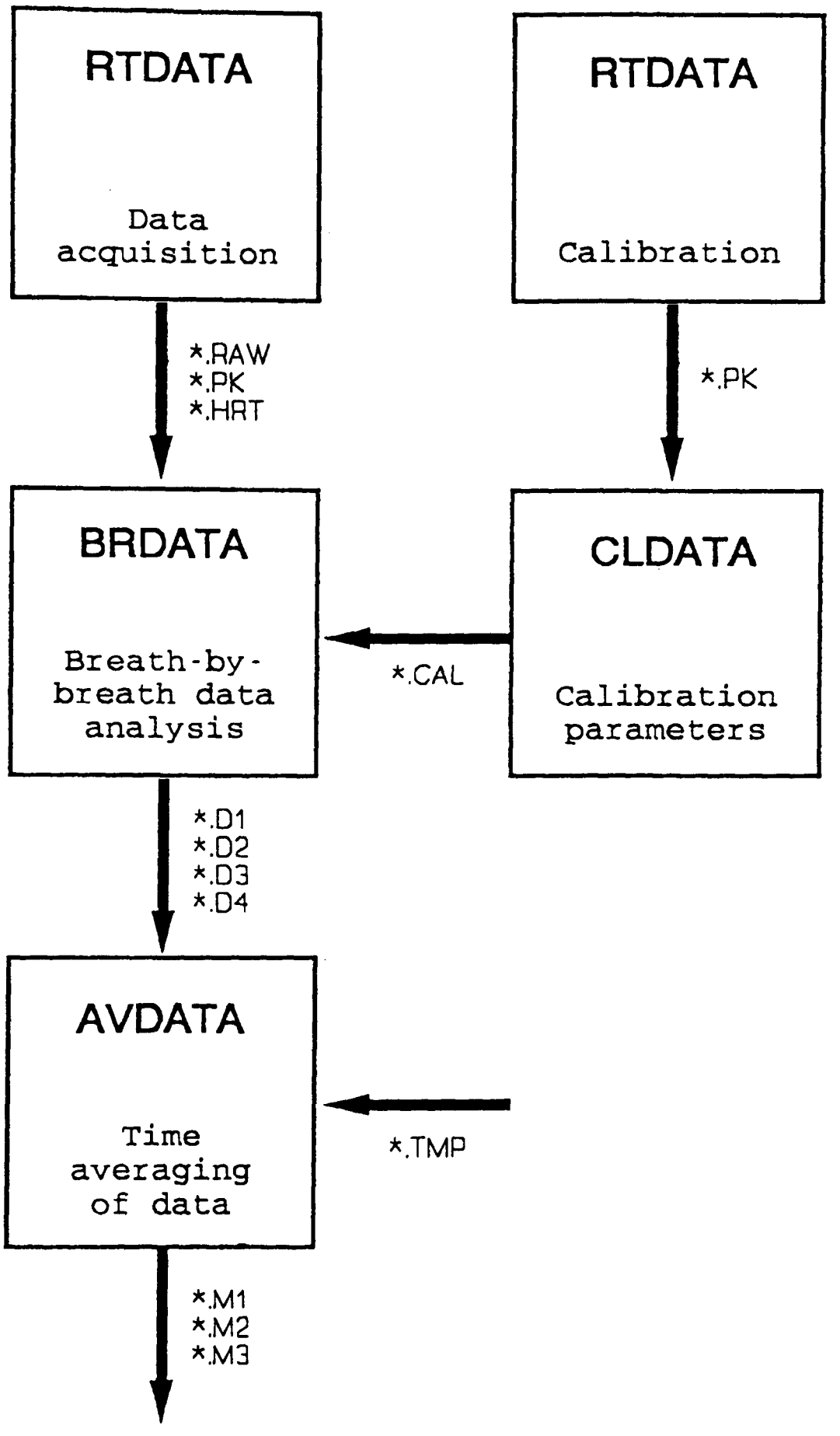


Figure 2.5: Schematic flow diagram showing collection and preliminary analysis of data. (From Bascom, 1991.)

```
Data File written as i7581104.d1
DATE, 29: 3:1991
EXPERIMENTER, idc
SUBJECT NO,  758

EXPERIMENT NO,   11
RUN NO,   4
NO.OF BREATHS,  647
MODE OF THIS EXPERIMENT,   0  1  1  1
INSPIRED GAS TEMPERATURE USED,  23.0
EXPIRED GAS TEMPERATURE USED,  33.2
BRNO  TIME  E12345678  VTI   TI  PIC2  PIO2  VTE   TE  PAC2  PAO2  VENT WRK HRT
   1,   1043,00000000,0.660,1240, 0.6,151.6,0.688,2380,35.9,103.4, 11.4,-50, 87
   2,   4663,00000000,0.707,1520, 0.5,152.3,0.767,3660,36.8,102.4,  8.9,-50, 71
   3,   9843,00000000,0.673,1600, 0.4,152.8,0.771,3680,38.0,100.7,  8.8,-50, 78
   4,  15123,00000000,0.673,2980, 0.5,137.1,0.733,2600,37.9, 97.6,  7.9,-50, 77
   5,  20703,00000000,0.563,1520,40.5,137.0,0.640,2940,41.5, 98.7,  8.6,-50, 67
   6,  25163,00000000,0.591,2200,32.0,121.0,0.684,2440,43.3, 91.9,  8.8,-50, 70
   7,  29803,00000000,0.707,1400, 2.6,150.7,0.771,2740,41.0, 96.1, 11.2,-50, 72
   8,  33943,00000000,0.673,1420,18.9,133.0,0.692,3100,41.0, 95.1,  9.2,-50, 67
   9,  38463,00000000,0.652,1680,34.2,124.0,0.729,2400,43.5, 93.9, 10.7,-50, 65
  10,  42543,00000000,0.632,1440,27.8,128.2,0.894,1840,44.2, 92.8, 16.3,-50, 70
  11,  45823,00000000,0.785,1140,28.1,128.0,0.973,1700,42.9, 94.0, 20.5,-50, 83
  12,  48663,00000000,0.936,1160,30.5,123.2,0.741,1320,42.5, 99.9, 17.9,-50, 86
  13,  51143,00000000,0.921,1160,32.0,123.8,0.890,1460,42.7,100.4, 20.4,-50, 86
  15,  58063,00000000,0.746,1360,29.9,121.8,0.818,2600,43.4, 98.4, 12.4,-50, 74
  16,  62023,00000000,0.873,1520,30.4,125.3,0.955,3100,45.2, 98.6, 12.4,-50, 70
  17,  66643,00000000,0.942,1600,26.5,125.3,0.977,3180,43.5, 97.1, 12.3,-50, 69
  18,  71423,00000000,0.846,1620,28.7,124.7,0.937,2440,43.7, 97.0, 13.8,-50, 75
  20,  81963,00000000,0.919,1380,24.9,128.2,0.998,2400,44.1, 96.5, 15.8,-50, 75


Data File written as i7581104.d4
DATE, 29: 3:1991
EXPERIMENTER, idc
SUBJECT NO,  758
EXPERIMENT NO,   11
RUN NO,   4
NO.OF BREATHS,  647
MODE OF THIS EXPERIMENT,   0  1  1  1
Event Record for All EVENTS in file
 BRNO SWITCH    CODE    ABSTIME  BSTIME
  160      1       1    566403    1760
  160      1       0    568023    3380
```

Figure 2.6: An example for the format of *.d1 file and *.d4 file.

## 2.7 Other Equipment

*Cycle Ergometer.*

A Mijnhardt KEM-3 electromagnetically braked cycle ergometer was used for the exercise studies (Howse *et al.*, 1989). The ergometer was set in the constant power mode, thus ensuring a uniform work rate despite fluctuations in pedal rate.

## 2.8 Subjects

Healthy young subjects were used in the experiments described in this thesis. All subjects gave informed, written consent before each experiment but were unaware of the specific objective of the experiments. In all experiments, subjects breathed through a mouthpiece with the nose occluded, and were distracted with a radio and/or reading material. All the studies presented in this thesis had prior approval of the Central Oxford Research Ethics Committee.

## 2.9 Protocols for Data Collection

Data collected during these previous studies carried out in this laboratory were used in the current thesis:

1. For the study of breath-to-breath ventilatory variability during steady-state breathing, data were taken from the study of Pandit (1993). Two protocols were studied. In the first, the subject was at rest and the end-tidal $P_{CO_2}$ was held constant at 2-5 Torr above the subject's natural resting value. In the second, the subject undertook exercise at 70 W, and the end-tidal $P_{CO_2}$ was held at 2-5 Torr above the subject's natural value during exercise. During both protocols, end-tidal $P_{O_2}$ was held at 100 Torr. The experiments lasted for 43 min.

2. Data for the study of the dynamics of the fast component of ventilatory response to acute hypoxia were taken from Clement (1992). Square wave inputs were generated at a period of 30 sec, with mean upper and lower values of end-tidal $P_{O_2}$ being 69.3 and 46.7 Torr. End-tidal $P_{CO_2}$ was held constant at 2 to 3 Torr above the normal end-tidal value. Experiments lasted for 30 min. Subjects were studied at rest.

3. Data for the study of the ventilatory dynamic response to sustained isocapnic hypoxia were from Bascom (1991). During such experiments, the end-tidal $P_{CO_2}$ was held at 1-2 Torr above the resting value throughout the experimental period. End-tidal $P_{O_2}$ was held at 100 Torr for the first 10 min and at 50 Torr for the next 20 min, then returned to 100 for a 5 min post-hypoxic period and finally reduced to 50 Torr for the last 5 min. Subjects were studied at rest.

# Chapter 3

# Statistical Properties of Breath-to-Breath Variations in Ventilation at Constant End-Tidal $P_{CO_2}$ and $P_{O_2}$ in Humans

千里之行　始于足下

老子・六十四

## 3.1 Introduction

Priban (1963) demonstrated statistically that, in resting human subjects, successive breaths were correlated. Since this study, a number of investigators have used a variety of models to describe the breath-to-breath variation in breathing (Benchetrit and Bertrand, 1975; Jensen, 1987; Ackerson *et al.*, 1989; Dahan *et al.*, 1989; DeGoede and Berkenbosch, 1989; Modarreszadeh *et al.*, 1990; Khatib *et al.*, 1991). These studies cover a wide range of different conditions, including studies of breathing in animals as well as in humans, studies during sleep and anaesthesia as well as during consciousness, and studies in the presence of changing stimulation as well as in the presence of steady stimulation. This makes the results from these studies difficult to compare. Furthermore, many of these studies are somewhat limited in scope. In particular: 1) the investigators often have not examined some of the basic statistical properties of the sequences before applying their models to their data; 2) the investigators often have studied only one model rather than undertaking a comparison across a range of possible models; and 3) the investigators often have not checked the adequacy of the model for describing the correlation once the model had been fitted.

The current study attempts to meet some of the criticisms which can be levelled against these earlier studies. It focuses on steady breathing in conscious humans during both rest and mild exercise under euoxic conditions. The carbon dioxide was slightly elevated compared with air breathing so that the technique of end-tidal forcing could be used to hold end-tidal $P_{CO_2}$ and $P_{O_2}$ as constant as possible. The reason for this was that I wished to concentrate on the statistical properties of the ventilatory controller in the open loop setting, rather than on the properties of the entire closed loop system, which would include the dynamics of the gas stores within the body. Thus, the purpose of the study was to provide a statistical description of

the breath-by-breath ventilatory sequences associated with the respiratory controller in an open loop state in conscious humans.

As well as the description's own intrinsic interest, it has a particular application for studies of the respiratory control system using the end-tidal forcing technique to generate dynamic stimuli in the end-tidal gases. These studies often involve fitting one or more models to the ventilatory sequences obtained, and in order to do this, the model should contain elements to describe both the deterministic and the stochastic parts of the process. Therefore, a particular aim of the current study was to develop a suitable structure for the stochastic part of such models.

## 3.2 Methods

### 3.2.1 Data description

The experimental data came from a previous study from our laboratory (Pandit and Robbins, 1992). Experiments were performed on five subjects with two different protocols each lasting 43 min. In the first protocol (protocol A), the subject was at rest and the end-tidal $P_{CO_2}$ was held constant at 2-5 Torr above the subject's natural resting value. In the second protocol (protocol B), the subject undertook exercise at 70 W, and the end-tidal $P_{CO_2}$ was held at 2-5 Torr above the subject's natural value during exercise. During both protocols, end-tidal $P_{O_2}$ was held at 100 Torr. Each protocol was repeated six times for each subject.

Ventilatory data during steady-state breathing were used for model fitting and statistical analysis. Data collected during the first 50 breaths for protocol A and the first 300 breaths for protocol B were discarded to remove any initial transients in the response.

The mean value for ventilation together with any linear trend were removed from the data before any statistical analysis (except the testing of homogeneity between individual data sets) and model fitting was undertaken.

### 3.2.2 Model independent statistical analysis

*Homogeneity between data sets.*

A $\chi^2$-test (Armitage and Berry, 1987) was used to test for homogeneity of the ventilatory data. The test was applied to groups of six data sets, which consisted of the individual repeats of the same protocol within each subject. The test statistic, $G$, was calculated as

$$G = \sum_i w_i (\overline{\dot{V}}_{E_i} - \overline{\dot{V}}_E)^2 \tag{3.1}$$

where $\overline{\dot{V}}_{E_i}$ is the average ventilation for the $i^{th}$ data set, $\overline{\dot{V}}_E$ is the overall weighted mean ventilation for all data sets ($\sum_i w_i \overline{\dot{V}}_{E_i} / \sum_i w_i$), and $w_i$ is the reciprocal of the variance for the $i^{th}$ data set. On the null hypothesis of homogeneity $G$ is distributed as $\chi^2_5$. High values of $G$ are evidence against homogeneity.

*Normality of the data.*

For each data set, a quantile-quantile plot was constructed of the data against the standard normal distribution (Chambers *et al.*, 1983). If the data have a normal distribution, then the plot will be approximately a straight line.

A plot with a "U" shape indicates the data distribution is skewed while an "S" shape implies that one distribution has longer tails than the other distribution.

*Specific periodicities.*

Spectral analysis was used to investigate whether there were any specific periodicities in the data. For each data set a smoothed periodogram was calculated using a modified Daniell Window. The modified Daniell Window was obtained by combining three Daniell Windows of lengths of 3, 5 and 7. The ratio of the estimated spectral density $\hat{h}(\omega)$ over its real value $h(\omega)$ approximately follows a $\chi^2$ distribution such that $\{\hat{h}(\omega)/h(\omega)\} \sim \{a\chi^2_v\}$ with both values of $a$ and $v$ determined by the window and the length of the original data set (Priestley, 1981*a*). This enables the 95% confidence intervals for the spectral density to be calculated.

Truncating each data set from the same subject and the same protocol to the same length ensures that the estimated spectral density $\hat{h}(\omega)$ over its real value $h(\omega)$ will follow a $\chi^2$ distribution with the same degrees of freedom $v$ for each of the data sets (since this depends entirely upon the structure of the window and the length of the data set). Thus, the average value for the six estimated spectral densities (for the same subject and the same protocol) over its real value will also follow a $\chi^2$

distribution with the degrees of freedom being simply six times that of the original data sets ($6v$). This enables the 95% confidence intervals for the mean spectral density to be calculated in a similar way to that used for the spectral densities from the individual data sets.

*Evolutionary spectral analysis.*

Evolutionary spectral analysis is a technique for assessing whether there are changes occurring in the power spectrum of a series over time (Priestley and Rao, 1969; Priestley, 1981*b*). The principle is to apply a double window in both time and frequency domains to calculate values for evolutionary spectral density corresponding to the selected times and frequencies. First, the estimate $(U_t)$ for the spectrum for a central frequency of angular velocity $\omega_0$ is calculated using:

$$U_t = \sum_{u=-\infty}^{\infty} g_u X_{t-u} e^{-\omega_0 (t-u)} \tag{3.2}$$

where $\{X_t\}$ is the data sequence to be analysed and $g_u$ is a Bartlett window given by

$$g_u = \begin{cases} 1/(2\sqrt{h\pi}) & |u| \leq h \\ 0 & \text{otherwise} \end{cases} \tag{3.3}$$

where $h$ was chosen at 7 (See equations *11.2.57, 11.2.52* of Priestley, 1981*b*). This choice of $h$ gives a bandwidth in the frequency domain of $(\pi/h)/(2\pi) = 1/14$. So the spacings between the selected central frequencies were chosen as 3/40 (giving central frequencies of 1/40, 4/40, 7/40, 10/40, 13/40, 16/40 and 19/40). From this, estimates of the spectrum $(V_t)$ for the selected central time points are calculated using:

$$V_t = \sum_{v=-\infty}^{\infty} w_{T',v} |U_{t-v}|^2 \tag{3.4}$$

where the weight function $w_{T',t}$ (corresponding to a Daniell window) is given by

$$w_{T',t} = \begin{cases} 1/T' & -T'/2 \leq t \leq T'/2 \\ 0 & \text{otherwise} \end{cases} \tag{3.5}$$

and $T'$ was chosen as 100 (See equations *11.2.58, 11.2.53* of Priestley, 1981*b*). $V_t$ is an (approximately) unbiased estimate of the (weighted) average value of the power spectrum at the frequency $\omega_0$ in the neighbourhood of the time instant $t$ (Priestley, 1981*b*). A two-way analysis of variance on the logarithmic values of the spectral density using factors of time and frequency is then applied to test whether there is significant variation in the spectral density with time.

An example of this form of analysis is shown in tables 3.1 and 3.2 for subject 797 at rest. The values for logarithmic spectral densities for selected time and frequency points are listed in table 3.1 while the results of variance analysis are listed in table 3.2. The first step is to test the "interaction + residual" term ($\chi^2$ = (sum of squares)/$\sigma^2$; in this study $\sigma^2 = 4h/3T' = (4 \times 7)/(3 \times 100) = 7/75$ (see Priestley and Rao, 1969), where $h$ and $T'$, selected to be 7 and 100 respectively, are the parameters for the windows of the frequency and time domains). If the interaction is not significant, we conclude that the sequence is a uniformly modulated process, and proceed to examine the "between times" term. The sequence is accepted as having a constant power spectrum provided the "between times" term is not significant.

Using the particular windows described above and data which had been simulated to correspond closely in structure and length to the experimental data, we found that the analysis was oversensitive. Based on these simulation results, we used a value of $\chi^2$ corresponding to $p$-value of 0.0025 as significant for this test (see Discussion). In the example in table 3.2, the value of $\chi^2$ for "interaction + residual" results in a $p$-value of 0.0074, which implies that the sequence analysed can be accepted as uniformly modulated. However, the value of $\chi^2$ for "between times" is high, which results in a $p$-value close to zero and means that the sequence cannot be accepted as having a constant power spectrum.

All the statistical calculations were done by S-plus statistical software (Statistical

Table 3.1: Example of evolutionary spectral densities (log) for subject 797 at rest.

| Central breath | Central frequency (Hz) | | | | | | |
|---|---|---|---|---|---|---|---|
| number | 1/40 | 4/40 | 7/40 | 10/40 | 13/40 | 16/40 | 19/40 |
| 60 | -0.28 | -0.64 | -1.43 | -1.69 | -2.18 | -1.93 | -2.06 |
| 160 | -0.29 | -1.00 | -0.74 | -0.88 | -1.32 | -1.13 | -2.03 |
| 260 | -0.03 | -0.99 | -1.15 | -0.93 | -2.08 | -2.32 | -2.02 |
| 360 | -0.57 | -0.36 | -0.05 | -0.76 | -1.19 | -1.16 | -0.84 |
| 460 | 0.88 | 0.10 | -0.76 | -0.48 | -0.97 | -1.44 | -2.06 |
| 560 | 0.28 | -1.20 | -1.66 | -1.49 | -1.69 | -1.74 | -1.42 |

Table 3.2: Analysis of variance for the evolutionary spectral densities in table 3.1.

| Item | Degrees of freedom | Sum of squares | $\chi^2 =$ (sum of squares/$\sigma^2$) |
|---|---|---|---|
| Between times | 5 | 3.95 | 42.27 |
| Between frequencies | 6 | 13.81 | 147.97 |
| Interaction + residual | 30 | 4.86 | 52.12 |
| Total | 41 | 22.62 | 242.36 |

Sciences U.K. Ltd; Oxford, U.K.).

### 3.2.3 Model dependent statistical analysis

Two simple linear time-independent approaches to modelling the sequences were employed. The first is the simple autoregressive moving average ($ARMA$) model. The second is a simple model in state-space form. Both of these models have a time-independent structure. Both of the models assume there is no exogenous input. These assumptions are explored further in both the Results and Discussion sections.

*Simple $ARMA$ model fitting.*

The general form for an autoregressive moving average ($ARMA$) model is:

$$y(t) - a_1 y(t-1) - \cdots - a_p y(t-p) = \epsilon(t) - c_1 \epsilon(t-1) - \cdots - c_q \epsilon(t-q) \quad (3.6)$$

In this study three different low order models were applied to the data: $AR_1$ (single $a_1$ coefficient), $AR_2$ ($a_1$ and $a_2$ coefficients) and $AR_1MA_1$ ($a_1$ and $c_1$ coefficients). Parameters for each data set for each model were estimated using a maximum likelihood technique. A "portmanteau" test, introduced by Box and Jenkins (1976), was used to test the whiteness of the residuals (*i.e.* whether the model describes the correlation within the data sequence satisfactorily), where the test statistic, $Q$, is defined as

$$Q = n \sum_{k=1}^{K} \hat{\gamma}_k^2 \sim \chi^2_{K-p-q} \quad (3.7)$$

where $n$ is the number of observations used to compute the likelihood; $\hat{\gamma}_k$ is the estimated autocorrelation value for the sequence of residuals with lag of $k$; $K$ is an integer, the exact choice of which is arbitrary (we used $10+p+q$ in this study); and $p$ and $q$ are the numbers of autoregressive and moving average coefficients respectively.

The coefficients of $ARMA$ models were estimated using S-plus statistical software.

*State-space model fitting.*

As an alternative to specifying the noise processes in terms of an $ARMA$ model, the noise processes can also be modelled in state-space form:

$$x(t+1) = fx(t) + v(t) \tag{3.8}$$

$$y(t) = x(t) + w(t) \tag{3.9}$$

where $x(t)$ is the system state at time $t$; $y(t)$ is the observation at time $t$; $f$ is the system gain; $v(t)$ and $w(t)$ are mutually independent white Gaussian noise processes with means of zero and constant variances of $R_v$ and $R_w$ respectively. This state-space model can be reduced to $AR_1MA_1$ form (see Appendix and Ljung, 1987).

In this state-space form, provided the system parameter $f$, $R_v$ and $R_w$ are all known, the system state and variance can be predicted from the measurement $y(t)$ through a Kalman filter as follows (Anderson and Moore, 1979):

$$\hat{x}(t+1 \mid t) = f\hat{x}(t \mid t) \tag{3.10}$$

$$P(t+1 \mid t) = fP(t \mid t)f + R_v \tag{3.11}$$

and the update of state and variance are given by

$$\hat{x}(t+1 \mid t+1) = \hat{x}(t+1 \mid t) + W(t+1)(y(t+1) - \hat{x}(t+1 \mid t)) \tag{3.12}$$

$$\begin{aligned} P(t+1 \mid t+1) &= (1 - W(t+1))P(t+1 \mid t)(1 - W(t+1)) \\ &\quad + W(t+1)R_w W(t+1) \end{aligned} \tag{3.13}$$

where

$$W(t+1) = P(t+1 \mid t)[P(t+1 \mid t) + R_w]^{-1} \tag{3.14}$$

is the Kalman gain at time $t+1$.

However, in the present study, both $R_v$ and $R_w$ are unknown and they can not be identified separately using the scalar observation $y(t)$. Therefore, we define

$P' = P/R_w$. The procedure for prediction and update then becomes:

$$\hat{x}(t+1 \mid t) = f\hat{x}(t \mid t) \tag{3.15}$$

$$P'(t+1 \mid t) = fP'(t \mid t)f + R_v/R_w \tag{3.16}$$

$$\hat{x}(t+1 \mid t+1) = \hat{x}(t+1 \mid t) + W(t+1)(y(t+1) - \hat{x}(t+1 \mid t)) \tag{3.17}$$

$$\begin{aligned} P'(t+1 \mid t+1) &= (1 - W(t+1))P'(t+1 \mid t)(1 - W(t+1)) \\ &\quad + W(t+1)W(t+1) \end{aligned} \tag{3.18}$$

where

$$W(t+1) = P'(t+1 \mid t)[P'(t+1 \mid t) + 1]^{-1} \tag{3.19}$$

The initial values for $x(0|0)$ and $P'(1|0)$ were set arbitrarily at 0 and $R_v/R_w$ respectively. The initial transient lasts for only a few steps of iteration.

By minimizing the prediction error $\sum_t (y(t) - \hat{x}(t \mid t-1))^2$, the system parameter $f$ along with the ratio $R_v/R_w$ can be estimated. The sequences obtained using the Kalman filter for $v(t)$ and $w(t)$ ($\hat{v}(t) = \hat{x}(t+1 \mid t+1) - f\hat{x}(t \mid t)$ and $\hat{w}(t) = y(t) - \hat{x}(t \mid t)$) are such that one is simply a scalar multiple of the other. It should be noted that this procedure provides a maximum likelihood estimate for the parameters, and is different from the common procedure of using an extended Kalman filter to estimate parameters on line (Ljung, 1987).

The parameters of the state-space model were estimated using a least-squares method provided in the Numerical Algorithms Group Fortran library (NAG; Oxford, UK), subroutine E04FDF.

## 3.3 Results

### 3.3.1 Model independent statistical analysis

*Homogeneity between individual data sets.*

The mean ($\pm$ S.D.) values for ventilation and the $\chi^2$ values for the homogeneity tests for the data sets from each protocol for each subject are listed in table 3.3. The $\chi^2$ values are all extremely large when compared with $\chi^2_{5,0.05}(= 11.070)$. Consequently the null hypothesis that the data sets are homogeneous for same subject and the same protocol should be rejected.

*Normality of the data.*

Quantile-quantile plots (qq-plot) against the standard normal distribution were used to assess the distribution of the data within each data set (after the mean value and linear trend had been removed). Fig. 3.1 gives an example of the qq-plot from one subject in one protocol (subject 797, at rest). From Fig. 3.1, it can be seen that the six qq-plots from the single subject and protocol are quite similar.

This was generally true for all subjects and protocols, and consequently the data from all data sets for a single subject and protocol have been combined to produce a single qq-plot against standard normal distribution. The shapes of these were similar to those of the individual qq-plot. These qq-plots for the combined data are shown in Fig. 3.2. In general, the data from the resting studies were reasonably symmetrically distributed, although the data clearly have more pronounced tails than the normal distribution. The data from the exercising studies generally appeared to be somewhat skewed with a larger tail formed from the lower values.

*Specific periodicities.*

The smoothed periodicities for the six data sets for one subject and protocol

Table 3.3: Mean ventilation (l/min) and linear trend term (l/min/min) during rest and exercise for each subject.

| Subject | | No. of data sets | Ventilation (mean±S.D.) | Linear trend (mean±S.D.) | $\chi^2$ value |
|---|---|---|---|---|---|
| 797 | Rest | 6 | 13.58±2.227 | 0.033±0.0565 | 5686 |
| | Exer | 6 | 40.30±2.443 | 0.064±0.1040 | 1265 |
| 799 | Rest | 6 | 8.73±0.996 | 0.007±0.0310 | 878 |
| | Exer | 6 | 32.91±4.354 | 0.107±0.1264 | 4393 |
| 800 | Rest | 6 | 13.93±1.409 | 0.024±0.0534 | 1586 |
| | Exer | 6 | 47.39±4.328 | 0.158±0.2423 | 5197 |
| 807 | Rest | 6 | 33.31±1.676 | -0.014±0.0342 | 361 |
| | Exer | 6 | 57.15±5.298 | 0.194±0.2283 | 2731 |
| 811 | Rest | 6 | 12.63±1.900 | -0.020±0.0615 | 3519 |
| | Exer | 6 | 52.56±6.646 | 0.051±0.1461 | 7159 |

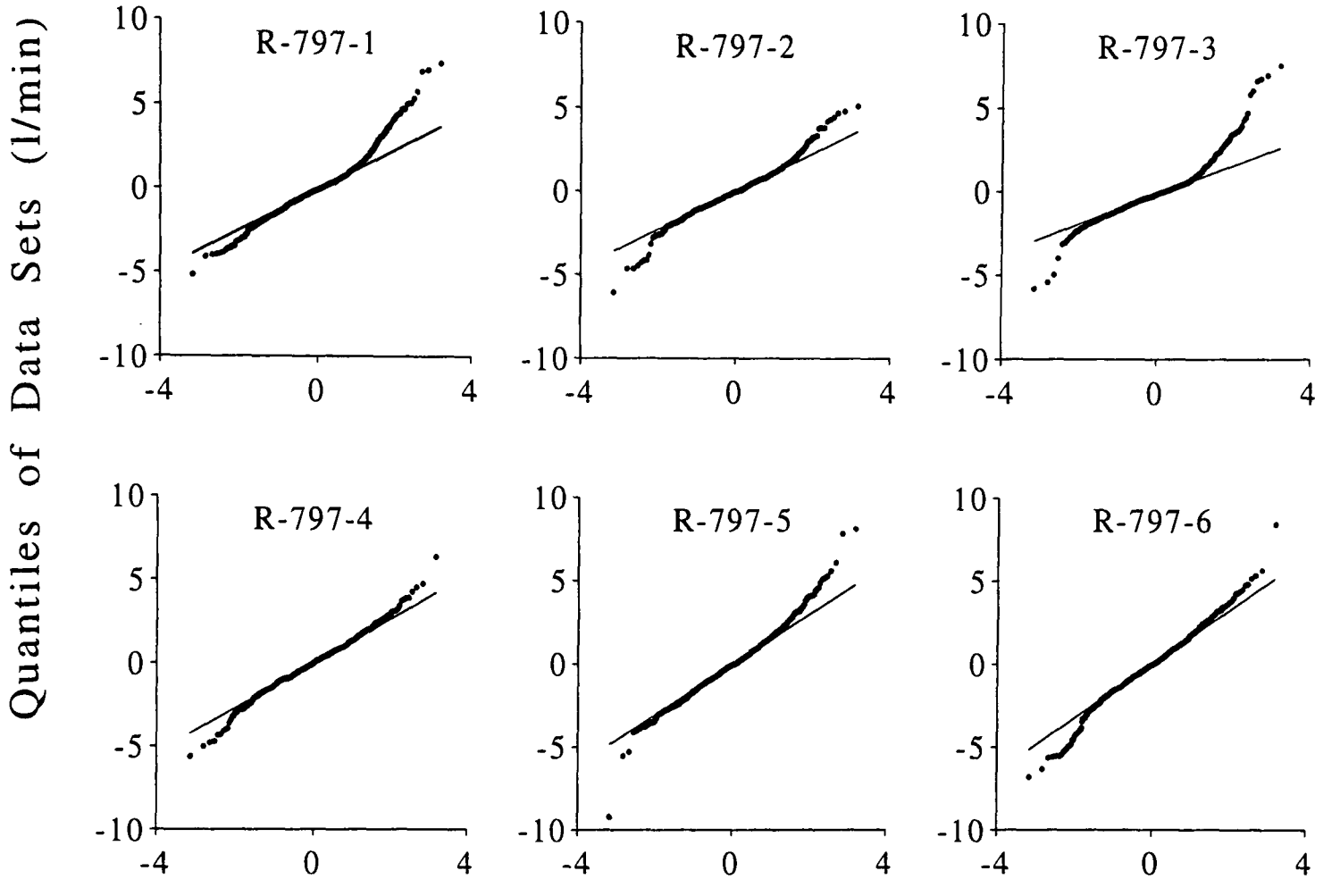


Figure 3.1: Quantile-quantile plot against standard normal distribution for subject 797 during rest.

(subject 811, exercise) are shown in Fig. 3.3. These show that the power is concentrated in the low frequencies, suggesting the presence of correlation within the data sets. No particular peaks are apparent that are consistent across the six data sets. Furthermore, in general a smooth decline in power can be traced within the 95% confidence intervals. These findings were generally true for all the individual data sets, and following this observation the periodograms were averaged to produce a single periodogram for each subject and protocol. The results of this are shown in

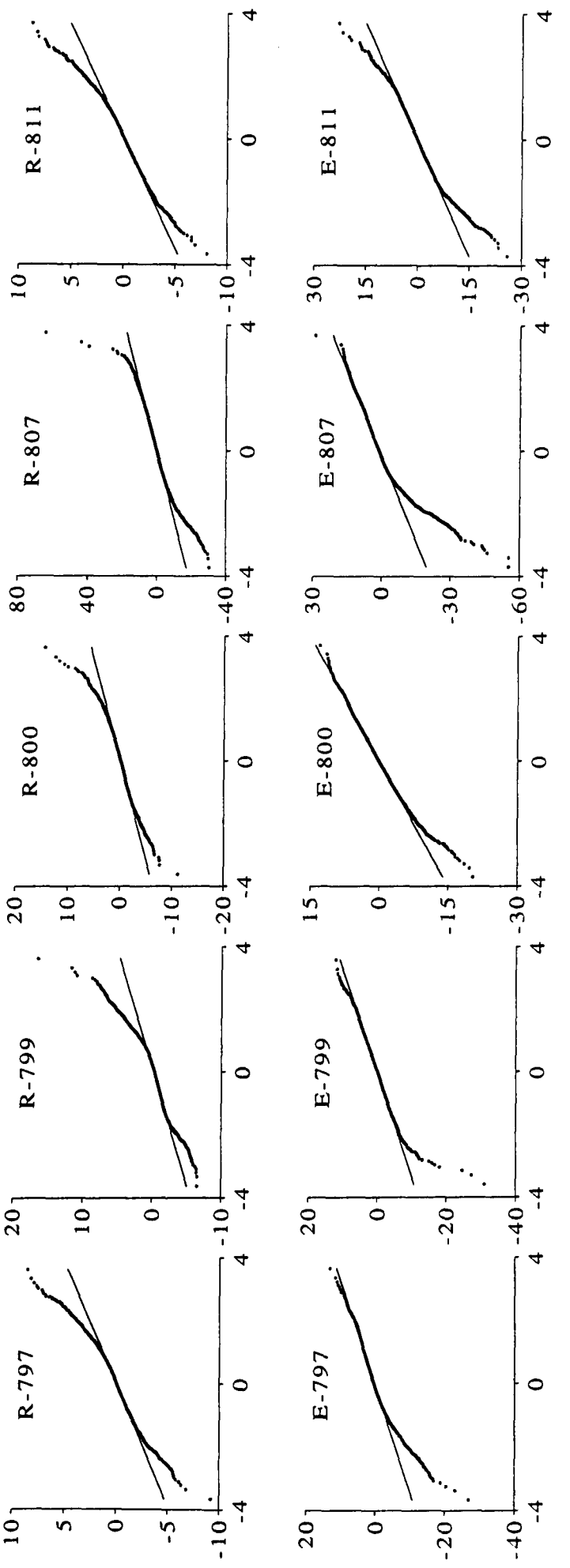


Figure 3.2: Quantile-quantile plot of combined data against standard normal distribution for each subject under each protocol.

Fig. 3.4. Again smooth lines for the power can be traced within the 95% confidence intervals, suggesting the absence of marked specific periodicities within the data.

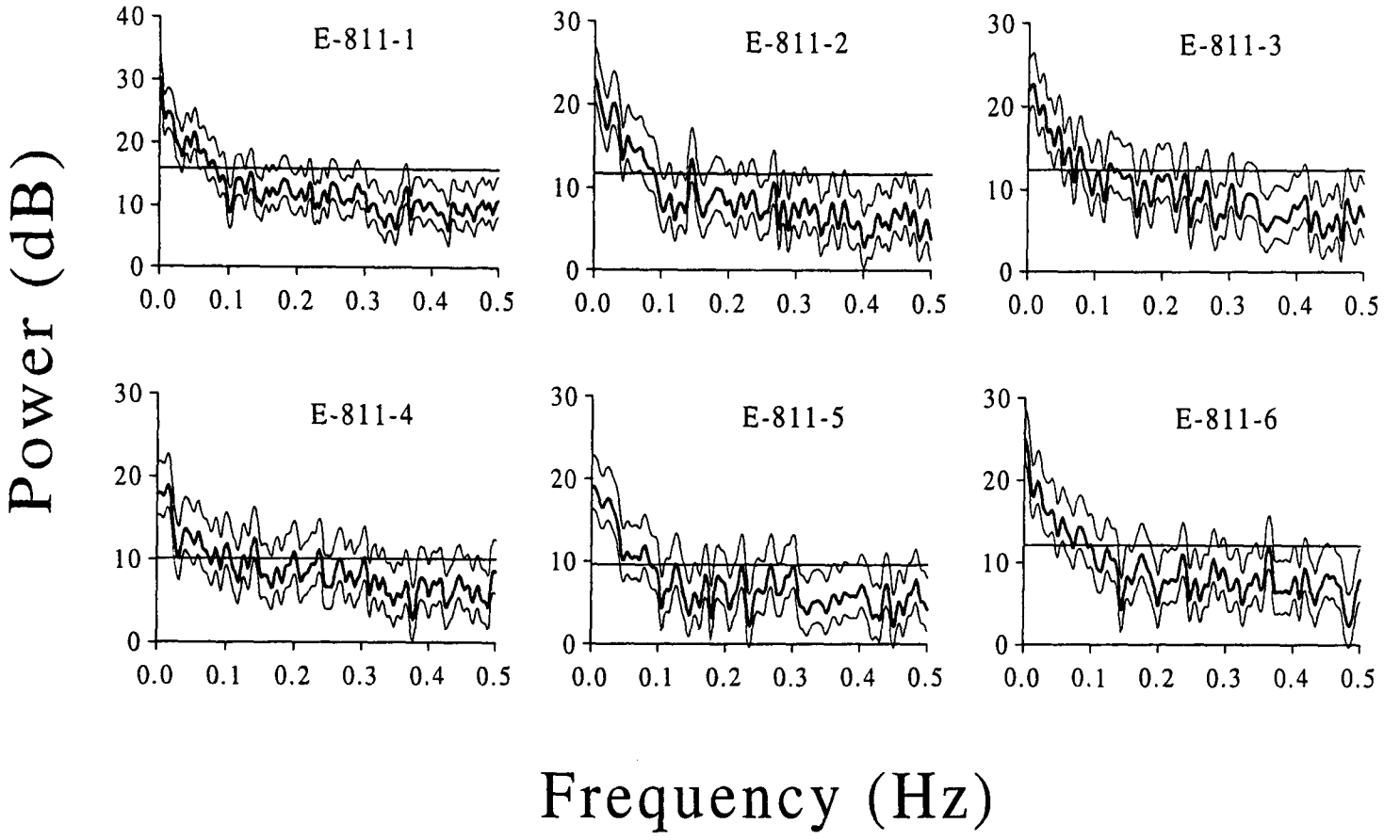


Figure 3.3: Power spectra for individual data sets for subject 811, exercise. Central thick line, power spectrum calculated by smoothed periodogram; fine lines 95% confidence intervals; horizontal line, mean power level.

*Evolutionary spectral analysis.*

Evolutionary spectral analysis was used to determine whether there were changes occurring over time in the power spectrum. The results are shown in table 3.4. Examining the values for the "interaction + residual" term, shows that 24 of these 30 data sets for rest can be accepted as uniformly modulated, but only 7 could be accepted as having a constant power spectrum over time. For exercise, 26 out of the 30 data sets could be treated as uniformly modulated, but only 6 as having a constant power spectrum.

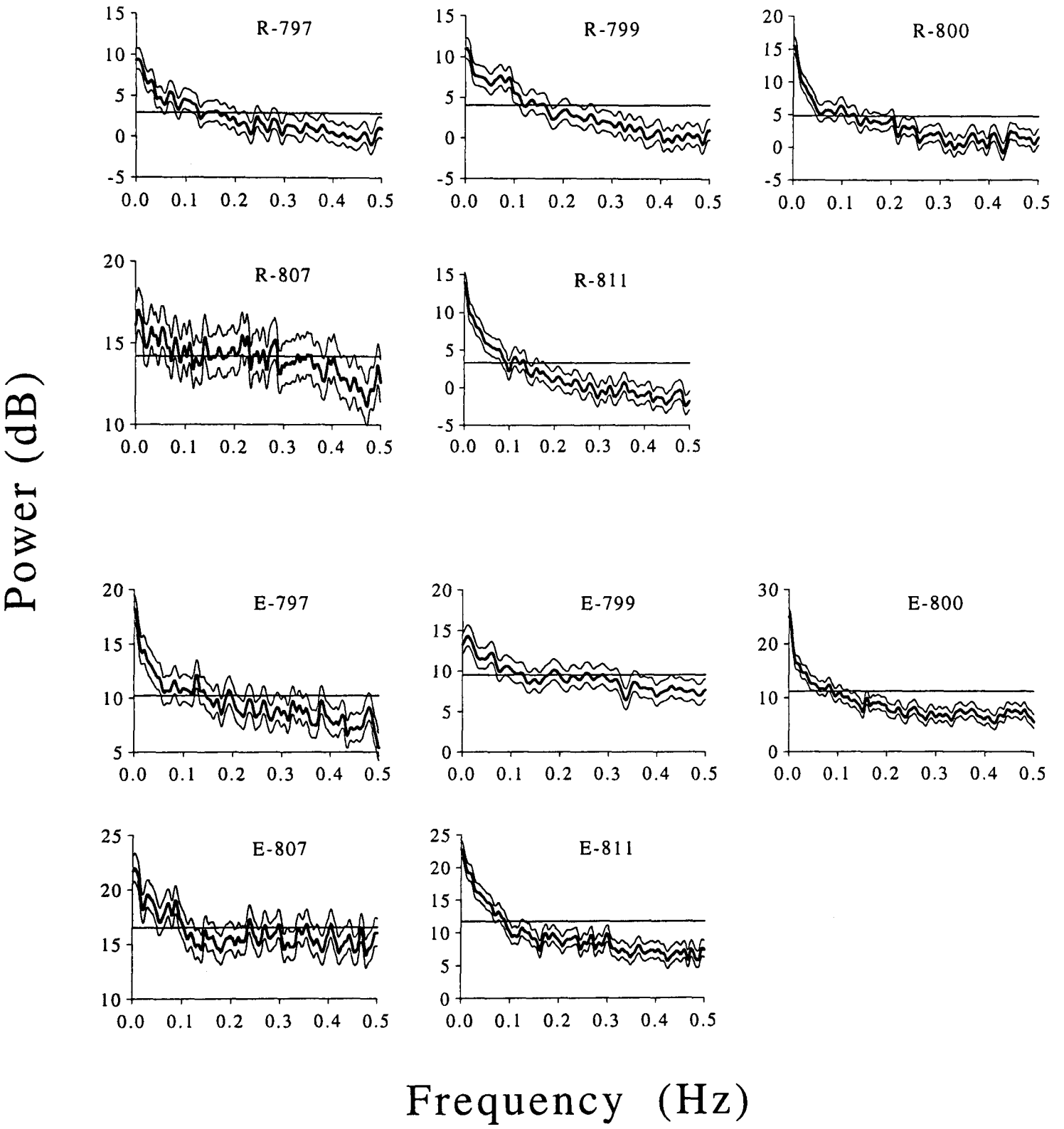


Figure 3.4: Averaged power spectra for each subject, each protocol. The upper panel is for Protocol A (rest) and the lower panel is for Protocol B (exercise). Central dark solid line, power spectrum calculated by smoothed periodogram; fine lines, 95% confidence intervals; horizontal line, mean power level.

Table 3.4: Results from evolutionary spectral analysis on experimental data.

| Subject | Protocol | Total number of data sets | Constant power | Uniformly modulated |
|---|---|---|---|---|
| 797 | Rest | 6 | 0 | 5 |
| | Exer | 6 | 1 | 5 |
| 799 | Rest | 6 | 2 | 5 |
| | Exer | 6 | 2 | 6 |
| 800 | Rest | 6 | 3 | 4 |
| | Exer | 6 | 0 | 5 |
| 807 | Rest | 6 | 0 | 6 |
| | Exer | 6 | 0 | 4 |
| 811 | Rest | 6 | 2 | 4 |
| | Exer | 6 | 3 | 6 |

### 3.3.2 Model dependent statistical analysis

The results from the evolutionary spectral analysis suggest that simple linear time-invariant models are unlikely to describe the data fully. Nevertheless, we start with these models to investigate what aspects of the data the models fail to fit, and also to determine whether there are aspects of the data that these models can describe well despite inadequacies elsewhere.

*Simple ARMA model fitting.*

Three kinds of low order time-series models were applied to each individual data set. They were $AR_1$, a single autoregressive term; $AR_2$, two autoregressive terms; and $AR_1MA_1$, a single autoregressive term together with a moving average term. The result of each model fitting was tested by assessing the whiteness of the residuals using a portmanteau test. The numbers of data sets with white residuals for each subject and protocol are listed in table 3.5. The $AR_1MA_1$ model is the most satisfactory model for both protocols. This model described 22 of the 30 resting data sets and 24 of 30 exercise data sets with overall white residuals.

Examples of the autocorrelation functions of the original data sequences and the residuals after different model fittings for two typical runs are plotted in Fig. 3.5. The upper panel shows an example where only the $AR_1MA_1$ model is satisfactory in the sense that the residual sequence is white, and the lower panel shows another example which was not satisfactorily described by any of the three different models. It should be noted that all the three models are successful in removing a considerable degree of the correlation present in the original data sequence, and that even when the models fail to fit, the autocorrelation functions are not too far from white when compared with the original data sequence.

The mean values and standard deviations for each coefficient of the three fitted

Table 3.5: Number of data sets accepted as white before and after fitting time series models.

| Subject | | No. of | No. of white | No. of white residuals after $ARMA$ model fitting | | |
|---|---|---|---|---|---|---|
| | | data sets | data sets | $AR_1$ | $AR_2$ | $AR_1MA_1$ |
| 797 | Rest | 6 | 0 | 1 | 4 | 6 |
| | Exer | 6 | 0 | 1 | 2 | 5 |
| 799 | Rest | 6 | 0 | 4 | 5 | 5 |
| | Exer | 6 | 0 | 4 | 5 | 5 |
| 800 | Rest | 6 | 0 | 0 | 3 | 2 |
| | Exer | 6 | 0 | 0 | 1 | 4 |
| 807 | Rest | 6 | 1 | 5 | 5 | 5 |
| | Exer | 6 | 0 | 0 | 2 | 4 |
| 811 | Rest | 6 | 0 | 0 | 3 | 4 |
| | Exer | 6 | 0 | 0 | 1 | 6 |

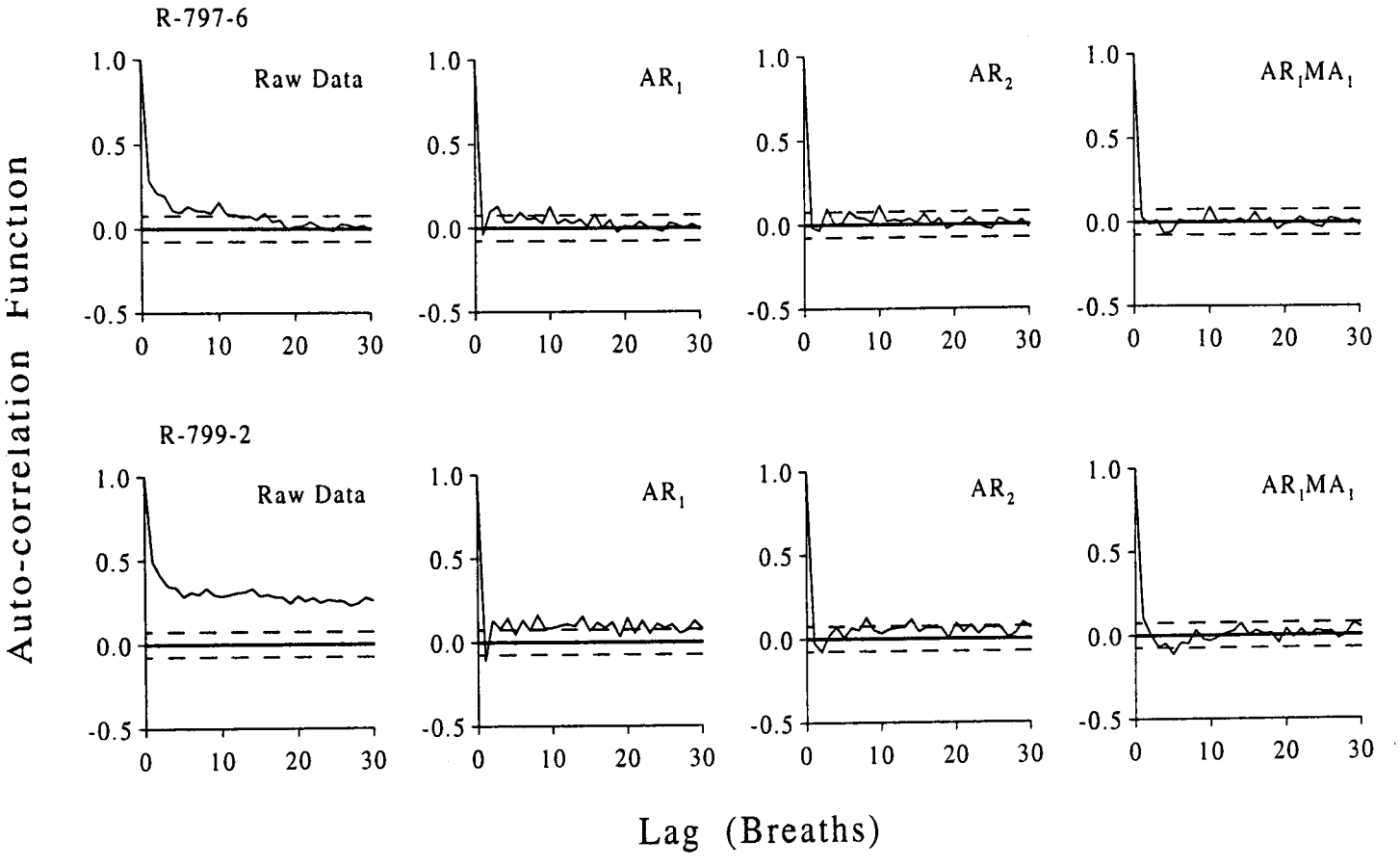


Figure 3.5: Autocorrelation functions of the original data sequences and the residuals after different model fittings for two typical data sets. Upper panel, only $AR_1MA_1$ model is adequate; lower panel, none of the three models is adequate. Solid lines, autocorrelation functions; dashed lines, 95% confidence intervals.

models for each subject and protocol are listed in table 3.6. In general these coefficients are not too different between protocols and subjects, although the values for subject 807 at rest are unusual. The autocorrelation function for this subject at rest appeared much closer to white than in all other subjects and protocols.

The residuals of the $AR_1MA_1$ model were tested using evolutionary spectral analysis to determine whether their power spectra were constant. The results are shown in table 3.7. The findings were very similar to those before any model had been fitted. This suggests that the model does not describe this feature of the data.

*State-space model fitting.*

As an alternative to the approach of using $ARMA$ models, one state-space model

Table 3.6: Coefficients (mean±S.D.) for time series models fitted to the experimental data.

| Subject | | $AR_1$ | $AR_2$ | | $AR_1MA_1$ | |
|---|---|---|---|---|---|---|
| | | $a_1$ | $a_1$ | $a_2$ | $a_1$ | $c_1$ |
| 797 | Rest | 0.32±0.077 | 0.29±0.075 | 0.10±0.052 | 0.67±0.172 | 0.41±0.229 |
| | Exer | 0.32±0.081 | 0.30±0.084 | 0.08±0.093 | 0.68±0.198 | 0.42±0.297 |
| 799 | Rest | 0.42±0.069 | 0.39±0.048 | 0.08±0.112 | 0.56±0.292 | 0.20±0.345 |
| | Exer | 0.25±0.066 | 0.24±0.058 | 0.05±0.041 | 0.62±0.156 | 0.41±0.189 |
| 800 | Rest | 0.48±0.070 | 0.40±0.075 | 0.17±0.048 | 0.80±0.058 | 0.45±0.122 |
| | Exer | 0.58±0.052 | 0.44±0.039 | 0.24±0.058 | 0.89±0.061 | 0.53±0.115 |
| 807 | Rest | 0.12±0.057 | 0.12±0.057 | -0.02±0.032 | -0.13±0.529 | -0.25±0.495 |
| | Exer | 0.21±0.082 | 0.19±0.070 | 0.11±0.041 | 0.80±0.090 | 0.65±0.130 |
| 811 | Rest | 0.54±0.086 | 0.47±0.089 | 0.14±0.057 | 0.77±0.097 | 0.34±0.154 |
| | Exer | 0.60±0.072 | 0.50±0.060 | 0.18±0.051 | 0.84±0.046 | 0.39±0.098 |

Table 3.7: Results from evolutionary spectral analysis on the residuals sequences from the $AR_1MA_1$ model.

| Subject | Protocol | Total number of data sets | Constant power | Uniformly modulated |
|---|---|---|---|---|
| 797 | Rest | 6 | 0 | 5 |
| | Exer | 6 | 1 | 5 |
| 799 | Rest | 6 | 1 | 6 |
| | Exer | 6 | 2 | 6 |
| 800 | Rest | 6 | 2 | 4 |
| | Exer | 6 | 2 | 6 |
| 807 | Rest | 6 | 0 | 6 |
| | Exer | 6 | 0 | 5 |
| 811 | Rest | 6 | 1 | 6 |
| | Exer | 6 | 3 | 6 |

of the noise processes was investigated.

The residuals were tested for whiteness in the same manner as for the residuals from the $ARMA$ model. Overall 22 out of 30 resting data sets were white and 26 out of 30 exercise data sets were white. The results are listed in table 3.8. This is broadly similar to the findings with the $AR_1MA_1$ model.

The parameters (mean $\pm$ S.D.) of state-space model for each subject and protocol are listed in table 3.9. Theoretically, the state-space model specified reduces to an $AR_1MA_1$ model with certain restrictions on the values of the $a_1$ and $c_1$ coefficients of the $AR_1MA_1$ model (Harvey, 1989; Ljung, 1987; and Appendix). This means that the values for $a_1$ and $c_1$ coefficients can be calculated from the state-space model, and these are also given in table 3.9. In most cases, these parameter values were similar to those obtained from the $AR_1MA_1$ model fitting (table 3.6).

Finally the residuals were tested using evolutionary spectral analysis to determine if the power spectrum was constant. The results are shown in table 3.10 and are very similar to those obtained from the original data sequences showing that the fitting of the model has not affected this feature of the sequences.

*Changes in ventilatory variance.*

The residuals from the $ARMA$ and state-space models are mostly overall white, but evolutionary spectral analysis shows that the residual sequence does not have a constant power spectrum throughout. This result, coupled with the finding that many of the sequences may be classified as uniformly modulated by evolutionary spectral analysis, suggests that the variance of the sequence may be slowly changing.

Assuming that the mean value of the data sequence remains constant (equal to zero) and that the only factor causing the variation in power spectrum is a changing

Table 3.8: Number of data sets accepted as white before and after fitting state-space model.

| Subject | | No. of data sets | No. of white data sets | No. of white residuals after model fitting |
|---|---|---|---|---|
| 797 | Rest | 6 | 0 | 6 |
| | Exer | 6 | 0 | 5 |
| 799 | Rest | 6 | 0 | 3 |
| | Exer | 6 | 0 | 4 |
| 800 | Rest | 6 | 0 | 6 |
| | Exer | 6 | 0 | 5 |
| 807 | Rest | 6 | 1 | 3 |
| | Exer | 6 | 0 | 6 |
| 811 | Rest | 6 | 0 | 4 |
| | Exer | 6 | 0 | 6 |

Table 3.9: Parameters (mean±S.D.) for the state-space model with the noise processes.

| Subject | | $f$ | $R_v/R_w$ | $W$ | $a_1$ | $c_1$ |
|---|---|---|---|---|---|---|
| 797 | Rest | 0.67±0.165 | 1.23±2.021 | 0.43±0.231 | 0.67±0.165 | 0.41±0.220 |
| | Exer | 0.75±0.135 | 0.37±0.299 | 0.32±0.146 | 0.75±0.135 | 0.52±0.193 |
| 799 | Rest | 0.73±0.167 | 0.99±0.828 | 0.49±0.211 | 0.73±0.167 | 0.40±0.256 |
| | Exer | 0.76±0.192 | 0.42±0.360 | 0.34±0.173 | 0.76±0.192 | 0.50±0.188 |
| 800 | Rest | 0.81±0.058 | 0.59±0.377 | 0.44±0.121 | 0.81±0.058 | 0.45±0.125 |
| | Exer | 0.89±0.061 | 0.40±0.229 | 0.40±0.092 | 0.89±0.061 | 0.53±0.115 |
| 807 | Rest | 0.49±0.272 | 0.72±0.819 | 0.38±0.276 | 0.49±0.272 | 0.34±0.304 |
| | Exer | 0.81±0.088 | 0.14±0.130 | 0.19±0.094 | 0.81±0.088 | 0.66±0.133 |
| 811 | Rest | 0.77±0.095 | 1.23±0.956 | 0.56±0.148 | 0.77±0.095 | 0.34±0.152 |
| | Exer | 0.84±0.046 | 0.85±0.448 | 0.53±0.103 | 0.84±0.046 | 0.40±0.099 |

Table 3.10: Results from evolutionary spectral analysis on the residuals sequences from the state-space model.

| Subject | Protocol | Total number of data sets | Constant power | Uniformly modulated |
|---|---|---|---|---|
| 797 | Rest | 6 | 0 | 5 |
| | Exer | 6 | 1 | 5 |
| 799 | Rest | 6 | 1 | 6 |
| | Exer | 6 | 2 | 6 |
| 800 | Rest | 6 | 3 | 6 |
| | Exer | 6 | 1 | 5 |
| 807 | Rest | 6 | 0 | 6 |
| | Exer | 6 | 1 | 4 |
| 811 | Rest | 6 | 0 | 6 |
| | Exer | 6 | 3 | 6 |

variance, the "uniformly-modulated" sequence $X(t)$ can be written as

$$X(t) = C(t)X_0(t) \tag{3.20}$$

where $X_0(t)$ is a time-invariant process and $C(t)$ is the modulating function. We chose to try to construct a modulating function $C(t)$ using an autoregressive estimate of the variance as follows

$$C^2(t) = 0.95C^2(t-1) + 0.05y^2(t) \tag{3.21}$$

where $y(t)$ is the observation of the present time $t$. Examples for $C(t)$ for each subject for both the rest and exercise protocols are shown in Fig. 3.6. Based on the average values for breath durations, this function may be considered to have a time constant of 66 sec for the data obtained at rest and 47 sec for the data obtained during exercise.

Demodulating the original sequence by $C(t)$, we obtain the "demodulated" sequence. Evolutionary spectral analysis on this demodulated sequence was then used to determine whether the variation in power spectrum had been removed by demodulation. The results are shown in table 3.11.

The number of data sets which had a constant power spectrum rose from 7 and 6 before demodulation to 24 and 26 following demodulation for resting data and exercising data respectively. It is possible that these figures could rise further with a different choice of demodulation function. Finally, it is worth noting that similar results are obtained if demodulation is applied to the residuals from the state-space model instead of the original data sequences (table 3.12).

*Suitability of models.*

Both the $ARMA$ models and the state-space model used above are linear time-invariant models. However, the results from evolutionary spectral analysis show

Table 3.11: Results from evolutionary spectral analysis on the demodulated sequences of experimental data.

| Subject | Protocol | Total number of data sets | Constant power | Uniformly modulated |
|---|---|---|---|---|
| 797 | Rest | 6 | 5 | 5 |
| | Exer | 6 | 5 | 5 |
| 799 | Rest | 6 | 5 | 5 |
| | Exer | 6 | 6 | 6 |
| 800 | Rest | 6 | 5 | 5 |
| | Exer | 6 | 4 | 5 |
| 807 | Rest | 6 | 5 | 6 |
| | Exer | 6 | 5 | 5 |
| 811 | Rest | 6 | 4 | 6 |
| | Exer | 6 | 6 | 6 |

Table 3.12: Results from evolutionary spectral analysis on the demodulated residuals sequences from the state-space model.

| Subject | Protocol | Total number of data sets | Constant power | Uniformly modulated |
|---|---|---|---|---|
| 797 | Rest | 6 | 6 | 6 |
| | Exer | 6 | 5 | 5 |
| 799 | Rest | 6 | 5 | 5 |
| | Exer | 6 | 6 | 6 |
| 800 | Rest | 6 | 5 | 5 |
| | Exer | 6 | 4 | 4 |
| 807 | Rest | 6 | 5 | 6 |
| | Exer | 6 | 6 | 6 |
| 811 | Rest | 6 | 5 | 6 |
| | Exer | 6 | 6 | 6 |

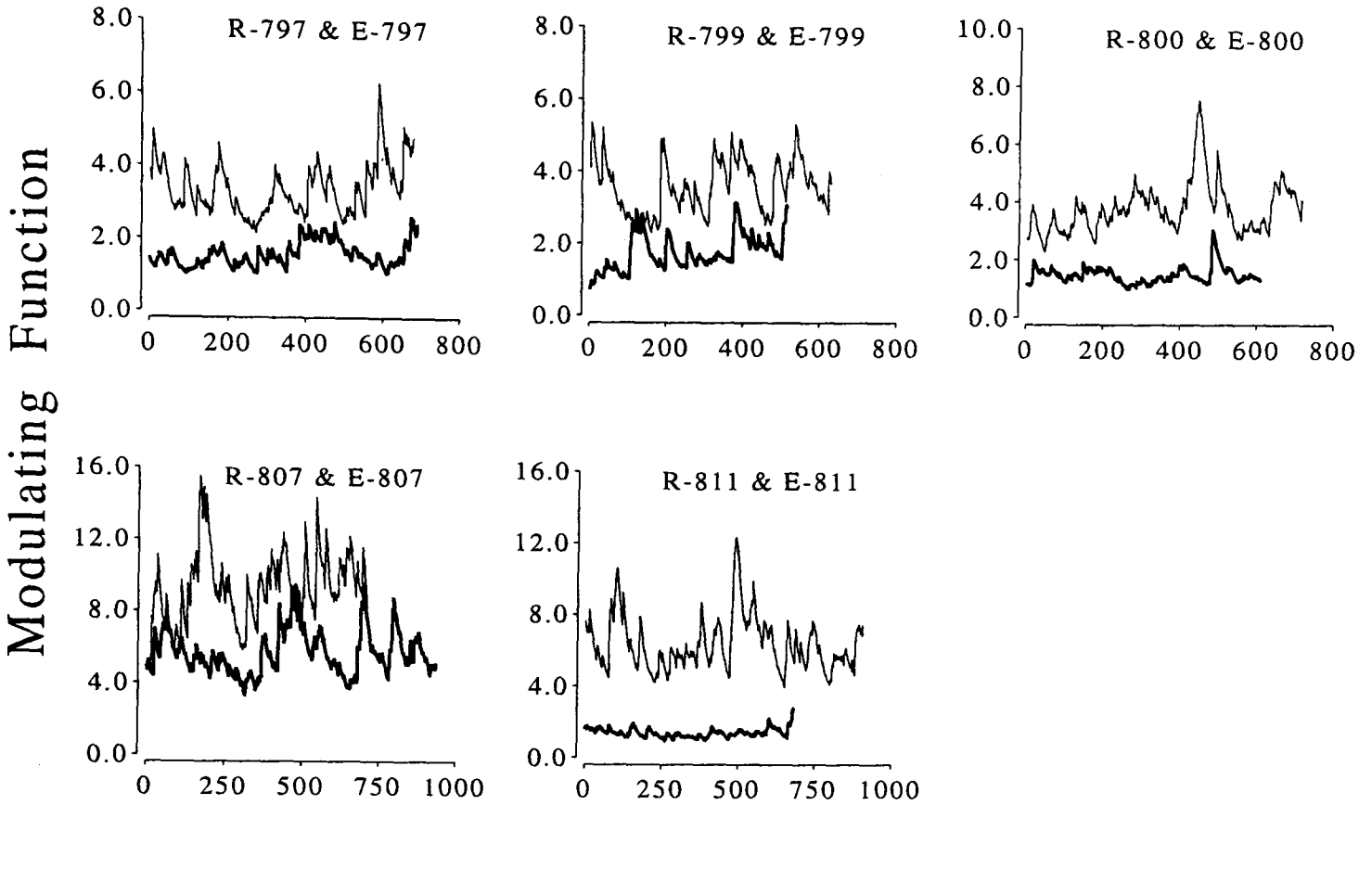


Figure 3.6: Examples of the autoregressive estimate of variance $C(t)$ for each subject for both rest and exercise protocols. Thick lines, rest; fine lines, exercise.

that in most sequences the power spectrum is varying, and this may suggest that the process underlying the generation of the sequence is non-stationary and/or non-linear. This variation is clearly not described by these models. The question thus arises as to whether these models are at all useful for describing the data sequences.

One approach to answering this question is to apply the models to the data after demodulation which removes, or at least attenuates, the variation in the power spectrum from the sequence. There was little difference between the number of residual data sets accepted as white prior to demodulation compared with after demodulation (table 3.13).

Also, the coefficients from the $ARMA$ model fitting on the demodulated data

Table 3.13: Number of data sets accepted as white before and after fitting time series models to demodulated data.

| Subject | | No. of | White | ARMA residuals | | | State-space |
|---|---|---|---|---|---|---|---|
| | | data sets | data sets | $AR_1$ | $AR_2$ | $AR_1MA_1$ | residuals |
| 797 | Rest | 6 | 0 | 3(1) | 4(4) | 5(6) | 6(6) |
| | Exer | 6 | 0 | 1(1) | 3(2) | 5(5) | 5(5) |
| 799 | Rest | 6 | 0 | 4(4) | 5(5) | 5(5) | 3(3) |
| | Exer | 6 | 0 | 2(4) | 3(5) | 5(5) | 4(4) |
| 800 | Rest | 6 | 0 | 0(0) | 2(3) | 3(2) | 6(6) |
| | Exer | 6 | 0 | 0(0) | 1(1) | 1(4) | 5(5) |
| 807 | Rest | 6 | 1 | 3(5) | 4(5) | 5(5) | 2(3) |
| | Exer | 6 | 0 | 2(0) | 2(2) | 5(4) | 6(6) |
| 811 | Rest | 6 | 0 | 1(0) | 3(3) | 4(4) | 4(4) |
| | Exer | 6 | 0 | 0(0) | 2(1) | 6(6) | 6(6) |

Number in brackets indicate the number of residual data sets accepted as white after fitting the models to the original data.

Table 3.14: Coefficients (mean±S.D.) for time series models fitted to demodulated data sets.

| Subject | | $AR_1$ | $AR_2$ | | $AR_1MA_1$ | |
|---|---|---|---|---|---|---|
| | | $a_1$ | $a_1$ | $a_2$ | $a_1$ | $c_1$ |
| 797 | Rest | 0.32±0.074 | 0.29±0.069 | 0.08±0.043 | 0.63±0.155 | 0.36±0.187 |
| | Exer | 0.33±0.081 | 0.31±0.085 | 0.08±0.074 | 0.66±0.195 | 0.38±0.281 |
| 799 | Rest | 0.40±0.085 | 0.36±0.074 | 0.08±0.085 | 0.58±0.198 | 0.23±0.213 |
| | Exer | 0.26±0.062 | 0.24±0.055 | 0.05±0.048 | 0.61±0.179 | 0.39±0.218 |
| 800 | Rest | 0.45±0.033 | 0.39±0.041 | 0.15±0.046 | 0.78±0.070 | 0.43±0.114 |
| | Exer | 0.54±0.038 | 0.41±0.040 | 0.23±0.043 | 0.87±0.050 | 0.53±0.103 |
| 807 | Rest | 0.14±0.039 | 0.13±0.036 | 0.01±0.034 | 0.13±0.461 | 0.00±0.446 |
| | Exer | 0.25±0.085 | 0.22±0.075 | 0.11±0.049 | 0.78±0.105 | 0.59±0.154 |
| 811 | Rest | 0.52±0.086 | 0.45±0.087 | 0.13±0.041 | 0.76±0.094 | 0.35±0.161 |
| | Exer | 0.55±0.078 | 0.46±0.060 | 0.16±0.034 | 0.82±0.046 | 0.41±0.081 |

(table 3.14) are similar to the values obtained prior to demodulation (table 3.6). Analysis of variance performed on the $AR_1MA_1$ model coefficients revealed no significant differences between the values obtained with the modulated and demodulated data.

These findings suggest that the autocorrelation in the sequence can usefully be described by a simple model despite the presence of a slowly varying variance. The state-space model is equivalent to the $AR_1MA_1$ model with certain restrictions, and similar results for whiteness were obtained before and after demodulation (table 3.13).

## 3.4 Discussion

The major findings of this study are: 1) Both a simple $ARMA$ model and a simple linear time invariant state-space model for the breath-to-breath correlations present in the ventilatory data gathered using an end-tidal forcing system to hold end-tidal gas tensions constant can produce residuals which in the majority of cases are overall white. 2) Neither the simple $ARMA$ models nor the simple linear time invariant state-space model fully describe the data because the power spectra associated with the residuals sequences vary with time. 3) In a sizable proportion of cases this variation in power spectrum can be explained by a process of uniform modulation of the variance of the ventilatory data or residuals. 4) One chosen modulating function was shown to be effective in reducing these data sequences to ones with constant power spectra in the majority of cases.

### 3.4.1 General comments on the statistical results

*Heterogeneity of the data.*

The heterogeneity of responses to repeats of the same protocol in the same subject seen with our data is something that has been widely recognised by physiologists, and similar findings for the mean level of ventilation in response to a given stimulus have been previously reported from our laboratory (Clement and Robbins, 1993*b*). The finding that single data sets are, more often than not, non-stationary, has not been generally recognised.

*Non-normality of the data.*

The distribution of breath-by-breath ventilation was found to be non-normal. Much statistical theory relys on individual measurements being normally distributed, and thus in a strict sense such theory should not be applied to those data. However, it is also true that this theory is often robust, in the sense of that it deals with

many data in a satisfactory manner even though the data do not completely meet the assumption of normality (Bellville *et al.*, 1988). In this study, where the prime departure from normality was an increased spread in the tails of the distribution (although there was some degree of skewness in the exercise data), it was felt that these departures from normality were not likely to have serious statistical consequences.

### 3.4.2 Comparison with previous studies

In general it is quite difficult to draw direct comparisons between the results from our study and results from previous studies. First, by using data gathered with the end-tidal forcing technique, our study has concentrated on the properties of the respiratory controller whereas most other studies have examined breath-by-breath variations when the chemical feedback loop is intact. Such a feedback loop might be expected to affect the correlational structure very significantly. Secondly, studies have varied in terms of the background level of stimulation employed (if any), the species employed and whether the study was conducted awake, asleep or under anaesthesia.

*Specific periodicities.*

In our study, the results from spectral analysis failed to reveal any sustained specific periodicities in the data. In conscious humans, by displaying the spectral densities for sequential subsets of the original data series, Jensen (1987) failed to find any peaks or troughs that were persistently present throughout the length of the series. This is also in keeping with a study of human subjects during stage 2 sleep (Modarreszadeh *et al.*, 1990). These results support the absence of specific periodic components in the data series. However, in the current study the results of evolutionary spectral analysis generally show the power spectrum is not constant, and thus none of the above studies can exclude the presence of brief periods of

periodicity which are not present throughout the data sequence.

*Evolutionary spectral analysis.*

Most studies have not considered whether the data sequence retains a constant power spectrum throughout. In conscious humans, Jensen (1987) calculated power spectra for sequential subsets of ventilatory data sequences, but did not test whether they differed significantly from one another. Ackerson *et al.* (1989) commented that data sequences were often "non-stationary" when assessed using a "likelihood ratio test", but did not provide any results to compare with those in this study. Nevertheless, in their study Ackerson *et al.* developed an adaptive time-series model for describing non-stationary ventilatory variations. This model has many similarities to the modulation model proposed in the current study.

*$ARMA$ models.*

The results from our study suggest that out of $AR_1$, $AR_2$ and $AR_1MA_1$ model structures, the $AR_1MA_1$ structure was the most satisfactory for describing the breath-by-breath correlation in the data sequence. We have not found another study which has investigated the $AR_1MA_1$ structure for ventilatory sequences. Jensen (1987) reports values in humans for coefficients from multivariate $AR_1$ and $AR_2$ models for tidal volume, inspired time and expired time pooled from a range of different experimental conditions. All coefficients for the lagged effects of each variable on itself are positive. Modarreszadeh *et al.* (1990) examined an $AR_2$ model for describing ventilatory variability in sleeping humans. They found that the $AR_1$ coefficient was significantly positive, but that the $AR_2$ coefficient did not differ significantly from zero.

In the anaesthetized cat, Benchetrit and Bertrand (1975) used an "isolated respiratory centre" preparation in order to examine the statistical properties of the

phrenic nerve output. This was done so as to circumvent the influence of the chemical feedback system rather as has been attempted with the end-tidal forcing system in our current study. The study employed a multivariate $AR_1$ structure and found a positive autocorrelation coefficient suggesting that there was indeed breath-to-breath correlation arising within the respiratory controller. The first order model structure was not always adequate.

Khatib *et al.* (1991) used an $AR_1$ model structure to compare the correlation between tidal volumes in anaesthetised spontaneously breathing rats, with the correlation between the integrated phrenic neurogram in anaesthetised vagotomised artificially ventilated rats. In hyperoxia and hypercapnia, they found positive autoregressive coefficients for the tidal volume data in the spontaneously breathing rats, but not for the integrated phrenic neurogram in the artificially ventilated rats. From these results, they conclude that the autocorrelation in tidal volume arises from the presence of noise within the chemical feedback system rather than as a function of the respiratory controller. They suggest the difference between their results and those of Benchetrit and Bertrand (1975) could either be due to species differences or due to Benchetrit and Bertrand failing to eliminate experiments in which there was non-stationarity. The results from our study in conscious humans accord much more closely with Benchetrit and Bertrand than with those of Khatib *et al.*

*State-space models.*

We are unaware of any studies in which a state-space formulation has been used for the noise processes in the absence of additional deterministic input stimuli. However, there have been studies of different noise models in experiments involving step changes in end-tidal $P_{CO_2}$ in both anaesthetized cats and conscious humans (Dahan *et al.*, 1989; DeGoede *et al.*, 1989). These studies do not report any of

the parameter values associated with the stochastic part of the model, but the example autocorrelation functions suggest that both a "process" and a "parallel" noise model lead to a considerable whitening of the residuals when compared with the "measurement only" noise model.

*The effects of exercise.*

We are unaware of any previous studies which have provided a comparison of these models between the states of rest and exercise. In general, the results from the two states were surprisingly similar given the differences in the mean ventilations, the associated differences in respiratory cycle durations and the somewhat different "mental state" that may exist between rest and exercise. Inspection of tables 3.6 and 3.9 suggests that there may be some increase in the degree of auto-correlation observed in exercise compared with rest, but this did not reach significance when the values of the coefficients were compared for the $AR_1MA_1$ and state-space models.

### 3.4.3 Evolutionary spectral analysis, stationarity, time- and state-dependent models

*Evolutionary spectral analysis.*

Evolutionary spectral analysis is a means of assessing whether the power spectrum of a data sequence is constant by estimating the power spectrum at certain specified points in time. This has been applied as a test of whether the underlying data sequence is stationary (Priestley and Rao, 1969; Priestley, 1981*b*). This section discusses the utility of evolutionary spectral analysis for this purpose, together with what may be inferred about the underlying model structure from this analysis. It also considers the reliability of the analysis for the particular form and length of data sequence that has been used in this study.

A series is (weakly) stationary if the first and second moments are constant over

time (i.e. $E(x) = \mu$ and $Var(x) = \sigma^2$). If there are multiple independent realisations of a time series, then stationarity may be tested for by estimating the mean and variance at each point in the sequence. However, in other cases multiple realisations may not exist, as is the case with our data. In this case, it is necessary to test for stationarity by sampling the series at intervals which are sufficiently far apart for the samples to be considered independent. Evolutionary spectral analysis is one method based on this approach. This leaves the question of how far apart do the samples have to be in order to be sufficiently far apart. The problem is that very slow variations in the structure of a time series may occur (especially with non-linear series) despite the fact that the series is actually still stationary. Thus it is safer to interpret results from evolutionary spectral analysis in terms of whether there is long-term variation in a sequence than whether the process is truly stationary or not. Indeed, the autoregressive model used to estimate the slowly changing variance in this study is a time invariant model despite the fact that it is being used to descibe "non-stationary" behaviour detected by evolutionary spectral analysis.

There is an interesting form of "duality" between the ideas of non-stationarity and non-linearity (Priestley, 1991). A general stationary state-dependent model may be written as:

$$X_t + \sum_{u=1}^{k} \phi_u(\mathbf{x}_{t-1}) X_{t-u} = \mu(\mathbf{x}_{t-1}) + e_t + \sum_{u=1}^{k} \psi_u(\mathbf{x}_{t-1}) e_{t-u} \tag{3.22}$$

where $X_t$ is the state at time $t$, $e_t$ is a white sequence, $\mathbf{x}_t$ denotes the "state vector", $\mathbf{x}_t = (e_{t-l-1}, \ldots, e_t, X_{t-k+1}, \ldots, X_t)'$, $\phi_u$ and $\psi_u$ are $AR$ and $MA$ coefficients respectively, and $\mu$ is local mean.

This form is a stationary non-linear model. However, for a single realisation, it is also possible to think of the state dependent coefficients ($\phi_u(\mathbf{x}_t)$, $\psi_u(\mathbf{x}_t)$) as time dependent coefficients ($\phi_u(t)$, $\psi_u(t)$) via the definitions $\phi_u(t) \triangleq \phi_u(\mathbf{x}_t)$ and $\psi_u(t) \triangleq \psi_u(\mathbf{x}_t)$. In this formulation the model may be thought of as a linear non-

stationary model (Priestley, 1991). This duality illustrates clearly the difficulty of distinguishing between linear non-stationary models and stationary non-linear models when there is only a single realisation of the data sequence.

The success, or otherwise, of using evolutionary spectral analysis to classify time series must depend on the type and length of the actual sequences used together with the particular forms of window chosen. In order to explore this further, sixty sets of $AR_1MA_1$ data sets were generated, each set matching one of the real data sets for $AR_1$ and $MA_1$ coefficients and for record length. Evolutionary spectral analysis was then undertaken on these sequences. Using a signifcance level of $p < 0.05$ for the $\chi^2$-test, over 20% of the sequences were incorrectly classified as arising from a process generating sequences without a constant power spectrum. However, modulating each of the sequences with a modulating function which was the same as that which had been determined for the matching experimental data sequence and then repeating the evolutionary spectral analysis on the modulated sequences, generally resulted in levels of significance for the $\chi^2$-test that were very much higher than for the unmodulated sequences. Using a value for $\chi^2$ corresponding to $p < 0.0025$ resulted in only 4 of the 60 stationary data sets being misclassified as not having constant power, but only 7 of the 60 modulated data sets were classified as being of constant power. Furthermore, it must be remembered that in a number of cases the modulating function may have been very "mild". The results from this simulation determined the choice of significance level used for the $\chi^2$-test in this study.

*Adequacy of simple linear time invariant models.*

A major result of this study is that the correlation between breaths can be modelled by simple linear time invariant $ARMA$ or state-space models, but that there remains a longer-term variation in the variance of the sequence. One question which naturally arises is, to what extent can we separate these two features of

the sequence, and, in particular, to what degree may a longer-term variation in ventilatory variance affect the estimation of the coefficients describing the shorter-term correlational structure? A partial answer to this question is found in the Results section, where the coefficients of the $AR_1MA_1$ model were estimated both before and after demodulation. No significant differences were found. However, it might be argued that this result arises because both the modulation and the autoregressive coefficients were estimated from the same data sequence.

In order to overcome this objection, a simulation study was performed. A set of ten data sequences were constructed with a known underlying $AR_1MA_1$ structure with the coefficient values equal to the mean values for each subject and protocol. First, the coefficients were estimated from these simulated data using the same technique as used for the real data sequences. Secondly the simulated data sequences were modulated using a randomly selected modulating function, one from each subject and protocol. Then the coefficients were re-estimated using these modulated sequences. Finally, the values estimated from both the original and modulated sequences were compared. Comparing the parameter values between the modulated and unmodulated data sets revealed an average deviation for the $a_1$ coefficient of $0.8 \pm 8.35\%$ (mean $\pm$ S.D.) and for the $c_1$ coefficient of $5.9 \pm 20.08\%$. Analysis of variance revealed no significant differences for either coefficient. These results support the notion that the shorter term correlations in the data sequence can be estimated in the presence of the slower variations in the variance of the sequence.

### 3.4.4 Influence of $CO_2$ on data sequences

A major intent of this study was to examine the open-loop characteristics of the respiratory controller with chemical levels of stimulation held constant. However, the experimental technique of dynamic end-tidal forcing is imperfect, and small fluctuations in end-tidal $P_{CO_2}$ and end-tidal $P_{O_2}$ remain. Since all experiments

were conducted at a mean end-tidal $P_{O_2}$ of 100 Torr, it is most unlikely that the variations in end-tidal $P_{O_2}$ will have any effect on the ventilatory sequence because the respiratory controller's sensitivity to changes in end-tidal $P_{O_2}$ around this mean level will be extremely low (Cunningham *et al.*, 1986). The same may not necessarily be true for $P_{CO_2}$, since the ventilatory sensitivity to changes in $P_{CO_2}$ is much higher, and indeed cross-correlation analysis reveals a significant effect of $P_{ET_{CO_2}}$ on $\dot{V}_E$ in 30 out of 60 data sets ("portmanteau" test for cross-correlation). Thus, one question that arises is whether my results reflect the combined properties of the human respiratory system coupled to our dynamic end-tidal forcing apparatus rather than simply the open-loop properties of the respiratory controller.

In order to try to answer this question, a multivariate time series approach has been adopted. This is necessary because not only may the end-tidal $P_{CO_2}$ affect the ventilation, but the breath-by-breath fluctuations in ventilation will affect end-tidal $P_{CO_2}$. Many different model structures are possible using multivariate analysis, and in order to make progress it was decided to focus on one simple model which has some structural basis in terms of the known properties of both the physiological and the dynamic end-tidal forcing systems.

The end-tidal $P_{CO_2}$ ($P_{ET_{CO_2}}$) of a breath is determined (assuming $CO_2$ delivery to the lungs via the blood remains constant) by: 1) the end-tidal $P_{CO_2}$ ($P_{ET_{CO_2}}$) of the previous breath, 2) the inspired $P_{CO_2}$ of the current breath and, 3) the ventilation of the current breath. Thus we may write:

$$P_{ET_{CO_2}}(n) = g(P_{ET_{CO_2}}(n-1), P_{I_{CO_2}}(n), \dot{V}_E(n)) \tag{3.23}$$

The end-tidal forcing system uses a prediction-correction scheme with the correction based on an integral-proportional controller structure. We may write for this:

$$P_{I_{CO_2}}(n) \;=\; P_{I_{CO_2}.p} + g_p(P_{ET_{CO_2}.d} - P_{ET_{CO_2}.m}(n-1))$$

$$+ \quad g_i \sum_{j=1}^{n-1} (P_{ET_{CO_2}.d} - P_{ET_{CO_2}.m}(j)) \tag{3.24}$$

where $P_{I.p}$ is the predicted inspired gas tension, $P_{ET.d}$ and $P_{ET.m}$ are the desired and measured end-tidal gas tensions, and $g_p$ and $g_i$ are the proportional and integral feedback gains.

In our experiments, $P_{ET_{CO_2}.d}$ is constant and after a period of time the integral term should be relatively constant. Thus $P_{I_{CO_2}}(n)$ is really just a linear function of $P_{ET_{CO_2}.m}(n-1)$. Hence we may write equation (3.23) as:

$$P_{ET_{CO_2}}(n) = g'(P_{ET_{CO_2}}(n-1), \dot{V}_E(n)) \tag{3.25}$$

For small fluctuations in $P_{ET_{CO_2}}$, we linearise around the means and write:

$$\begin{aligned} P_{ET_{CO_2}}(n) \quad - \quad & P_{ET_{CO_2}.mean} \\ = \quad & \alpha(P_{ET_{CO_2}}(n-1) - P_{ET_{CO_2}.mean}) + \beta(\dot{V}_E(n) - \dot{V}_{E.mean}) \end{aligned} \tag{3.26}$$

This now gives a simple expression for the way ventilation may affect $CO_2$ in our system.

The end-tidal $P_{CO_2}$ may affect ventilation either through the peripheral chemoreceptors or through the central chemoreceptors or both. A reasonable estimate for the median lag to the peripheral chemoreceptors is 2 breaths (Clement and Robbins, 1993*b*). Estimates for the lag for the central chemoreceptors vary, but a value of 3-4 breaths might be reasonable (Dahan *et al.*, 1990). In order to keep the model simple, we chose to use a lag of two breaths which should model a peripheral response and still be capable of modelling at least some of any central response that is present. Combining this with our $AR_1MA_1$ model for ventilation and the model derived above for end-tidal $P_{CO_2}$ gives an entire multivariate model of the form:

$$\dot{V}_E(n) = a_{11}\dot{V}_E(n-1) + a_{12}P_{ET_{CO_2}}(n-2) + \epsilon_1(n) - c_{11}\epsilon_1(n-1) \tag{3.27}$$

$$P_{ET_{CO_2}}(n) = a_{21}\dot{V}_E(n) + a_{22}P_{ET_{CO_2}}(n-1) + \epsilon_2(n) - c_{21}\epsilon_2(n-1) \tag{3.28}$$

This model was fitted to our data using the NAG library routine G13DCF with and without the coefficient $a_{12}$ being fixed at zero to examine the effects of either incorporating or not incorporating the effects of end-tidal $P_{CO_2}$ on ventilation. The exclusion of the effects of end-tidal $P_{CO_2}$ on ventilation reduced the average value of coefficient $a_{11}$ by 7%, and reduced the average value of coefficient $c_{11}$ by 14%. Both these changes were significant using analysis of variance. Thus we conclude that ignoring the variations in $P_{ET_{CO_2}}$ causes a modest underestimation of the degree of correlation associated with the respiratory controller.

After fitting the multivariate model, the cross-correlations between the residuals for ventilation and the end-tidal $P_{CO_2}$ were calculated. There was no significant effect of $P_{CO_2}$ on $\dot{V}_E$ in 51 out of 60 data sets, confirming that the effect of fluctuations in end-tidal $P_{CO_2}$ on $\dot{V}_E$ had been modelled satisfactorily for most data sequences.

### 3.4.5 Generalisation of state-space model to incorporate a time- and state- dependent form

The results have shown that the degree of variation in ventilatory variance observed with a constant level of stimulation is such that it does not affect the fitting of the correlational structure unduly. However, it is not clear whether this would still be the case when the level of stimulation is varying because in this case the variation in ventilatory variance is likely to be substantially greater (*e.g.* compare variances for rest and exercise in Fig. 3.6). In this sense, the results of the current study might be seen as rather limited when applying models to situations in which the level of stimulation is varying (*i.e.* there is a deterministic input present, rather than the purely stochastic processes considered in the current study).

As an alternative to the linear time invariant state-space model, a more general state-space model can be written as follows:

$$x(t+1) \quad = \quad fx(t) + \xi(t) \tag{3.29}$$

$$y(t) = x(t) + \eta(t) \tag{3.30}$$

where $\xi(t)$ and $\eta(t)$ are noise processes with state- and time-dependent variances:

$$R_\xi = g(x(t), t)R_v \tag{3.31}$$

$$R_\eta = g(x(t), t)R_w \tag{3.32}$$

$R_v$ and $R_w$ have the same definition as before.

This model allows the variances to vary with amplitude of ventilation and with time through the function $g(x(t), t)$. This is known as a heteroscedastic form (Harvey, 1989). The advantage is that provided $g(x(t), t)$ is fully determined at time $t$, then the same Kalman filter can be used to estimate the coefficients much as before, since the term in $g$ drops out while estimating the ratio of the variances. The only differences are that the prediction and update equations for the variance $P$ should be defined using $R_\xi$ and $R_\eta$ instead of $R_v$ and $R_w$:

$$P(t+1 \mid t) = fP(t \mid t)f + R_\xi \tag{3.33}$$

$$\begin{aligned} P(t+1 \mid t+1) = {} & (1 - W(t+1))P(t+1 \mid t)(1 - W(t+1)) \\ & + W(t+1)R_\eta W(t+1) \end{aligned} \tag{3.34}$$

where

$$W(t+1) = P(t+1 \mid t)[P(t+1 \mid t) + R_\eta]^{-1} \tag{3.35}$$

is the Kalman gain at time $t+1$, and that $P'$ is defined as $P' = P/R_\eta$ for the estimating procedure. The ratio $R_\xi/R_\eta$ equals the ratio $R_v/R_w$ and may be estimated in the estimation procedure.

The question now remains, is this heteroscedastic form likely to be an adequate model for ventilatory variability? Two possible limitations are: 1) the same function $g$ is used to modulate variances of both noise sequences, and 2) the function $g$ has

to be fully determined (*i.e* non-stochastic) at time $t$. For the scalar output of ventilation, the first of these limitations is unimportant as $\xi(t)$ and $\eta(t)$ are not separately identifiable, and the sequences $\hat{\xi}(t)$ and $\hat{\eta}(t)$ are scalar multiples of each other. Consequently, the same function $\phi(t)$ may be constructed to modulate both $v(t)$ and $w(t)$ to produce $\xi(t)$ and $\eta(t)$.

The importance of the second of these limitations is less clear theoretically. However, if $g(t)$ is varying sufficiently slowly with respect to the observations, then a good estimation of $g(t)$ may be obtained from prior observations. The observation in this study that many sequences were uniformly modulated combined with the practical construction of the demodulation function $C(t)$ for the residual sequences suggests that such a function does exist (or at least a good approximation).

For use in parameter estimation, the heteroscedastic noise model is no more complicated than the ordinary form, since the algorithms associated with each are the same. Thus for a parallel noise structure, the heteroscedastic noise model can be combined with deterministic models in the same way as an ordinary noise model. The deterministic and stochastic components are simply added together. Because the algorithms are the same for both the ordinary and heteroscedastic models, parameter estimates obtained using these models will be the same in each case. The important point is that the heteroscedastic model provides the necessary theoretical extension to deal with noise processes which are not of constant power, but which are nevertheless uniformly modulated.

In summary, the heteroscedastic structure allows the variation in ventilatory variance to be introduced into the model in a general way, without specifying the precise form that it takes. Although this does not contribute further to understanding the origins of the variation in ventilatory variance, it does provide a useful means to incorporate this feature into overall models of ventilatory control and still provide

a structure that is amenable to parameter estimation.

## 3.5 Appendix: Relationship Between State-Space Form and $AR_1MA_1$ Form

The first section of this appendix derives the appropriate $ARMA$ representation of the state-space model employed in this study. The second section derives the relations between the parameters of the state-space model and those of the $ARMA$ model.

### 3.5.1 $ARMA$ representation of state-space model

The state-space model with noise processes and zero input employed in this study may be written as:

$$x(t+1) = fx(t) + v(t) \tag{3.36}$$

$$y(t) = x(t) + w(t) \tag{3.37}$$

where $v(t)$ and $w(t)$ are mutually independent white Gaussian noise processes with means of zero and constant variances of $R_v$ and $R_w$ respectively.

From equation (3.37), we may write:

$$y(t) - a_1y(t-1) = x(t) + w(t) - a_1(x(t-1) + w(t-1)) \tag{3.38}$$

Substituting for $x(t)$ using equation (36) yields:

$$\begin{aligned} y(t) - a_1y(t-1) &= fx(t-1) + v(t-1) + w(t) - a_1(x(t-1) + w(t-1)) \\ &= (f - a_1)x(t-1) + v(t-1) + w(t) - a_1w(t-1) \end{aligned} \tag{3.39}$$

If $a_1$ is chosen to be equal to $f$, the term in $x(t-1)$ drops out, and the equation may be written as:

$$y(t) - a_1y(t-1) = v(t-1) + w(t) - a_1w(t-1) \tag{3.40}$$

The right hand side of equation (3.40) is a combination of a $MA_0$ process and a $MA_1$ process which by a general result is a $MA$ process. Since the noise sequences

$v(t)$ and $w(t)$ are mutually independent white, the autocorrelation function of this $MA$ process has the "cut-off" property that $\gamma_k = 0$ for all $k > 1$, the combination of these two processes builds up a $MA_1$ process (Kendall and Stuart, 1969). So equation (3.40) can be re-written as:

$$y(t) - a_1 y(t-1) = \epsilon(t) - c_1 \epsilon(t-1) \tag{3.41}$$

which is an $AR_1MA_1$ process.

### 3.5.2 Relationship between parameters of $AR_1MA_1$ and state-space model

Define $z(t)$ as:

$$z(t) = y(t) - a_1 y(t-1) \tag{3.42}$$

From equation (3.40), we have

$$\begin{aligned} z(t) &= y(t) - a_1 y(t-1) \\ &= v(t-1) + w(t) - f w(t-1) \end{aligned} \tag{3.43}$$

Squaring both sides and taking expected values yields

$$E[z(t)]^2 = E[v(t-1) + w(t) - f w(t-1)]^2 \tag{3.44}$$

Since $v$, $w$ are mutually independent white noise processes, it yields

$$R_z = R_v + (1 + f^2) R_w \tag{3.45}$$

where $R_z$ represents the variance of sequence $z$.

Also, from equations (3.41) and (3.42)

$$\begin{aligned} z(t) &= y(t) - a_1 y(t-1) \\ &= \epsilon(t) - c_1 \epsilon(t-1) \end{aligned} \tag{3.46}$$

Squaring and taking expected value of equation (3.46), yields

$$E[z(t)]^2 = E[\epsilon(t) - c_1\epsilon(t-1)]^2 \tag{3.47}$$

and so, since $\epsilon(t)$ is white,

$$R_z = (1 + c_1^2)R_\epsilon \tag{3.48}$$

where $R_\epsilon$ is the variance of sequence $\epsilon$.

Equating (3.45) and (3.48) and eliminating $R_z$, we get

$$R_v + (1 + f^2)R_w = (1 + c_1^2)R_\epsilon \tag{3.49}$$

In addition to the above result, we may also calculate $E[z(t)z(t-1)]$. From equation (3.43) we obtain

$$E[z(t)z(t-1)] = E[(v(t-1) - fw(t) + w(t-1))(v(t-2) - fw(t-1) + w(t-2))] \tag{3.50}$$

Since $v$, $w$ are mutually independent white sequences, it yields

$$E[z(t)z(t-1)] = -fR_w \tag{3.51}$$

Also, from equation (3.46), we can write

$$E[z(t)z(t-1)] = E[(\epsilon(t) - c_1\epsilon(t-1))(\epsilon(t-1) - c_1\epsilon(t-2))] \tag{3.52}$$

Since $\epsilon$ is white, then

$$E[z(t)z(t-1)] = -c_1 R_\epsilon \tag{3.53}$$

Equating (3.51) and (3.53) and eliminating $E[z(t)z(t-1)]$ yields

$$fR_w = c_1 R_\epsilon \tag{3.54}$$

Combining (3.49) and (3.54), eliminating $R_\epsilon$ we obtain

$$\frac{1 + c_1^2}{R_v + (1 + f^2)R_w} = \frac{c_1}{fR_w} \tag{3.55}$$

Equation (3.55) is quadratic in $c_1$. Solving equation (3.55) yields

$$c_1 = \frac{R_v + (1+f^2)R_w \pm \sqrt{[R_v + (1+f^2)R_w]^2 - 4f^2R_w^2}}{2fR_w} \tag{3.56}$$

By inspection, one value for $\mid c_1 \mid$ is greater than 1 and another value is less than 1. We require the latter. Thus in summary, the relationship between the parameters of the $ARMA$ model and the state-space model is given by:

$$a_1 = f \tag{3.57}$$

$$c_1 = \frac{R_v + (1+f^2)R_w - \sqrt{[R_v + (1+f^2)R_w]^2 - 4f^2R_w^2}}{2fR_w} \tag{3.58}$$

Notice that in this solution, there is a constraint on the sign of the coefficients in that both $a_1$ and $c_1$ should have the same sign as $f$. Consequently, the state-space model represents only a subset of the models that can be represented in $AR_1MA_1$ form. The coefficients obtained from our study for the $AR_1MA_1$ model are mostly, but not always, within these constraints.

# Chapter 4

# An Extended Model of the Ventilatory Response to Sustained Isocapnic Hypoxia in Humans

图难于其易　为大作于细

老子 · 六十三

## 4.1 Introduction

The ventilatory response to sustained hypoxia is biphasic: there is an initial rapid increase in ventilation which is then followed by a slow decline (Easton *et al.*, 1986; Weil and Zwillich, 1976). This slow decline is known variously as hypoxic ventilatory decline or depression (HVD) or hypoxic ventilatory "roll-off".

In anaesthetised animals, HVD may be independent of the peripheral chemoreflex sensitivity since: 1) in anaesthetised cats, the peripheral chemoreflex sensitivity to $CO_2$ is unchanged during HVD induced by central hypoxia (VanBeek *et al.*, 1984); 2) in anaesthetised cats, the rapid ventilatory response at the onset and relief of hypoxia is almost symmetric (Berkenbosch and DeGoede, 1986); and 3) respiratory depression during hypoxia has been a consistent finding in anaesthetised animals which have undergone peripheral chemodenervation (Neubauer *et al.*, 1990).

In conscious humans, however, HVD may arise predominantly through an alteration of peripheral chemoreflex sensitivity. The evidence for this is: 1) the rapid ventilatory response at the relief of sustained hypoxia is much smaller than the rapid response at the onset of the period of hypoxia (Easton *et al.*, 1986; Easton and Anthonison, 1988*b*; Khamnei and Robbins, 1990); 2) the re-introduction of hypoxia after a brief relief from sustained hypoxia will cause a ventilatory response with a smaller magnitude compared with the first exposure to hypoxia (Bascom *et al.*, 1992, Easton *et al.*, 1988*a*); and 3) brief exposures to additional hypoxia during the development of HVD elicit progressively smaller ventilatory responses as the HVD develops (Bascom *et al.*, 1990).

On the basis of the above findings, Painter *et al.* (1993) developed a mathematical model to describe HVD during sustained hypoxia in humans in which HVD arises as the result of a progressive decline in peripheral chemoreflex sensitivity. The ventilatory response to sustained hypoxia and the asymmetric magnitudes of

the ventilatory on- and off-transients at the onset and relief of hypoxia are both described well by this model. However, as noted by Painter *et al.*, this model fails to describe the ventilatory behaviour after the step out of hypoxia very well in cases where there may be some undershoot and subsequent recovery of the ventilatory response. One possible cause of the undershoot and recovery sometimes observed at the relief of hypoxia might be the existence of an additional component of HVD in conscious humans, which is independent of peripheral chemoreflex sensitivity as has been described in the studies relating to anaesthetised animals.

The purpose of the current study was to explore an extension of the model of Painter *et al.* which has an additional component for HVD that is not related to the peripheral chemoreflex sensitivity. In particular, we wished to determine 1) whether the addition of this component would improve the fit of the model to the data at the relief of hypoxia; and 2) what proportion of HVD would be attributed to the component that is independent of the peripheral chemoreflex sensitivity.

In the original model of Painter *et al.*, the parameter estimation was performed with a simple least-squares fitting technique (this corresponds to a measurement-only noise model). With respiratory data, use of this technique generally results in residuals which are correlated, and this can make statistical comparisons between different models difficult. In order to overcome this, a parallel noise structure was used in conjunction with the deterministic models to remove this correlation. The noise model was fitted using a Kalman filter algorithm.

## 4.2 Methods

### 4.2.1 Data

Data were taken from a previous study carried out in our laboratory (Bascom *et al.*, 1992). Each experiment lasted 40 min. End-tidal $P_{O_2}$ ($P_{ET_{O_2}}$) was held at 100 mmHg for the first 10 min, at 50 mmHg for the next 20 min, at 100 mmHg for the next 5 min and at 50 mmHg for the final 5 min. End-tidal $P_{CO_2}$ was kept constant throughout the experiment at 1-2 mmHg above the subject's natural value. Minute ventilation was measured breath by breath. Data were available from six subjects, with 3-6 repeats of the protocol on each subject.

Both the strength of the stimulus ($P_{ET_{O_2}}$=50mmHg) and background end-tidal $P_{CO_2}$ ($P_{ET_{CO_2}}$) were the same as for the data used by Painter *et al.* (1993). However, the data differ in the sense that the protocol used to generate the data modelled in the current study was prolonged to allow for the re-introduction of hypoxia to provide a second on-transient. In the data modelled by Painter *et al.*, there was no second on-transient. This second on-transient may help to discriminate between a component of HVD that arises through modulation of peripheral chemoreflex sensitivity and a component which does not act via such a mechanism.

### 4.2.2 Models

*Model of Painter et al.*

The model of Painter *et al.* can be written in the form:

$$\dot{V}_E = \dot{V}_c + \dot{V}_p \tag{4.1}$$

$$d\dot{V}_p/dt = (1/T_p)(g_p(1 - S(t - d_p) + k_p) - \dot{V}_p) \tag{4.2}$$

$$dg_p/dt = (1/T_h)(g_{100} - g_h(1 - S(t - d_p)) - g_p) \tag{4.3}$$

where $\dot{V}_c$ and $\dot{V}_p$ represent the central and peripheral chemoreflex contributions to

ventilation respectively. In equation (4.2): $T_p$ denotes the time constant for the rapid peripheral chemoreflex response; $(1 - S)$ is the hypoxic stimulus, where $S$ represents the arterial oxygen saturation as used by Painter *et al.* (1993) as

$$S = 1 - 1.89e^{-0.05P_{ETO_2}} \tag{4.4}$$

$d_p$ is the peripheral time delay; $k_p$ is a non-negative peripheral offset; and $g_p$ represents the peripheral chemo-sensitivity to hypoxia, which is a variable determined by a 1st-order dynamic process described by equation (4.3). In equation (4.3): $T_h$ denotes the time constant associated with the development of HVD; $g_{100}$ denotes the steady-state chemoreflex sensitivity in hyperoxia when $S = 1.0$; and $g_h$ denotes the ratio of the sensitivity decrease to the decrease in the arterial oxygen saturation $S$. Both $g_{100}$ and $g_h$ are constrained to be positive.

In the original formulation, Painter *et al.* used a parameter $k_h$, whereas in the current formulation the parameter $g_{100}$ has been used. The relationship between these two parameters is given by:

$$g_{100} = g_h + k_h \tag{4.5}$$

There were two reasons for prefering the revised parametrization of the Painter model. First, $g_{100}$, the hypoxic sensitivity following exposure to hyperoxia, is a more intuitive parameter than $k_h$ in a physiological sense. Secondly, $g_h$ and $k_h$ appeared to be highly correlated in the study of Painter *et al.*, whereas there appeared to be much less correlation between $g_h$ and $g_h + k_h$ ($g_{100}$, see their table 1).

Assuming both saturation $S$ and gain $g_p$ remain constant throughout the breath, these differential equations can be solved to provide a set of difference equations which can be written as:

$$(g_p)_{n+1} = g_{100} - g_h(1 - S(t_n - d_p))$$

$$-(g_{100} - g_h(1 - S(t_n - d_p)) - (g_p)_n)e^{-(t_{n+1}-t_n)/T_h} \tag{4.6}$$

$$\begin{aligned}(\dot{V}_p)_{n+1} &= (g_p)_n(1 - S(t_n - d_p) + k_p) \\ &\quad -((g_p)_n(1 - S(t_n - d_p) + k_p) - (\dot{V}_p)_n)e^{-(t_{n+1}-t_n)/T_p} \qquad (4.7)\end{aligned}$$

$$(\dot{V}_E)_n = (\dot{V}_c)_n + (\dot{V}_p)_n \tag{4.8}$$

where $t_n$ refers to the time of the $n^{th}$ breath.

*An extended model.*

The original model of Painter *et al.* describes the whole of the hypoxic ventilatory decline as arising from a modulation of peripheral reflex sensitivity. The object of the extended model is to introduce a component of HVD ($\dot{V}_d$) which may be independent of the peripheral chemoreflex. This model can be written as:

$$\dot{V}_E = \dot{V}_c + \dot{V}_p + \dot{V}_d \tag{4.9}$$

where

$$d\dot{V}_d/dt = (1/T_d)(g_d(1 - S(t - d_p)) - \dot{V}_d) \tag{4.10}$$

where $\dot{V}_c$ and $\dot{V}_p$ have the same meaning as previously; $g_d$ is a non-positive gain term, which is constant, independent of the oxygen saturation $S$; and $T_d$ is a time constant. Again, assuming the saturation remains constant throughout a breath, a difference equation for the new component can be written as:

$$\begin{aligned}(\dot{V}_d)_{n+1} &= g_d(1 - S(t_n - d_p)) \\ &\quad -(g_d(1 - S(t_n - d_p)) - (\dot{V}_d)_n)e^{-(t_{n+1}-t_n)/T_d} \qquad (4.11)\end{aligned}$$

The time delay for this component is assumed to be the same as for the sensitivity related component ($d_p$).

### 4.2.3 Fitting technique

*Simple least-squares parameter estimations.*

The approach to estimating parameter values adopted by Painter *et al.* was to use a simple least-squares fitting technique. With this technique, the objective function to be minimised is

$$\sum_{n}(\dot{V}_{E.meas}(n) - \dot{V}_{E.det}(n))^2 \tag{4.12}$$

where $\dot{V}_{E.meas}$ denotes the measured value and $\dot{V}_{E.det}$ is the deterministic output from the model. This fitting procedure was initially used for Painter's model in order to examine the effects of incorporating a more complicated noise model (see below).

*Parameter estimation using a Kalman filter.*

One problem associated with estimating the parameters of the deterministic models is that successive breaths are not independent (Priban, 1963). Based on a previous study of breathing during steady levels of stimulation (see Chap. 3), the stochastic behaviour was modelled using a parallel noise process of the form:

$$x(n+1) = fx(n) + v(n) \tag{4.13}$$

$$y(n) = x(n) + w(n) \tag{4.14}$$

where $x(n)$ and $y(n)$ are the system state and observation for the parallel noise component at the $n^{th}$ breath; $f$ is the system gain; and $v(n)$ and $w(n)$ are mutually independent white Gaussian noise processes with means of zero and a constant variance ratio of $R_v/R_w$. Thus the model output ($\dot{V}_{E.out}$) for the ventilatory response to the stimulus can be written as the sum of the deterministic component ($\dot{V}_{E.det}$) and the stochastic component ($x$):

$$\dot{V}_{E.out}(n) = \dot{V}_{E.det}(n) + x(n) \tag{4.15}$$

In order to estimate the stochastic component $x(n)$, a Kalman filter algorithm was employed. The prediction and update values for the system state of the noise component were calculated as follows:

$$\hat{x}(n+1 \mid n) = f\hat{x}(n \mid n) \tag{4.16}$$

$$\hat{x}(n+1 \mid n+1) = \hat{x}(n+1 \mid n) + K(n+1)(y(n+1) - \hat{x}(n+1 \mid n)) \tag{4.17}$$

and the prediction and update of a modified variance (see Chap. 3) are given by

$$P'(n+1 \mid n) = fP'(n \mid n)f + R_v/R_w \tag{4.18}$$

$$P'(n+1 \mid n+1) = (1 - K(n+1))P'(n+1 \mid n)(1 - K(n+1)) + K(n+1)K(n+1) \tag{4.19}$$

where

$$K(n+1) = P'(n+1 \mid n)[P'(n+1 \mid n) + 1]^{-1} \tag{4.20}$$

is the Kalman gain at the $(n+1)^{th}$ breath.

The physiological parameters of the deterministic model ($\dot{V}_c$, $g_{100}$, $g_h$, $k_p$, $T_p$, $T_h$, $g_d$, $T_d$) along with the two parameters of the stochastic model ($f, R_v/R_w$) can now be estimated by minimising the sum of the squared prediction errors of the model which is given by

$$\sum_n (\dot{V}_{E.meas}(n) - (\dot{V}_{E.det}(n) + \hat{x}(n \mid n-1)))^2 \tag{4.21}$$

where $\dot{V}_{E.meas}$ denotes the measured value.

*Minimisation process.*

The simple least-squares objective function (eq. 4.12) and the objective function for the Kalman filter (eq. 4.21) were minimised using a standard Numerical

Algorithms Group (NAG; Oxford, UK) subroutine (E04FDF) that finds an unconstrained minimum of a sum of squared residuals. The fitting procedure was repeated over a range of fixed values for $d_p$ for each data set. The value for $d_p$ corresponding with the lowest sum of squared error was regarded as the optimal value for $d_p$ for the data set.

In the study from which the data are taken (Bascom *et al.*, 1992), the authors report that the speed of the initial ventilatory response to the rapid changes of $P_{ET_{O_2}}$ appeared to be different at the different stages in the protocol. Thus, instead of fitting a single value for the fast time constant $T_p$, separate values for the time constant were fitted for the onset, relief and the second on-transient of the hypoxic stimulus ($T_{p_1}$, $T_{p_2}$ and $T_{p_3}$ respectively).

*Goodness of fit.*

The improvement of the fit with the extended model as compared with the original model was assessed using an F-ratio test on the sum of squared prediction errors (Armitage and Berry, 1987). The $F$ statistic is given by

$$F = \frac{(RSS_1 - RSS_2)/(df_1 - df_2)}{RSS_2/df_2} \sim F(df_1 - df_2, df_2) \tag{4.22}$$

where $RSS_1$ and $df_1$ refer to the residual sum of squares and the degrees of freedom for the original model, and $RSS_2$ and $df_2$ refer to the residual sum of squares and the degrees of freedom for the extended model. Tests were conducted on a subject-by-subject basis, and so the sum of squares and degrees of freedom were accumulated across the individual repeats of the protocol and fits of the model on each individual subject.

*Parameter values for each subject.*

Overall parameter values for each subject for each model were obtained using a technique employed by Swanson and Bellville in their study of modelling the

ventilatory responses to $CO_2$ (Swanson and Bellville, 1975). First, an idealized stimulus of 5 min euoxia ($P_{ET_{O_2}} = 100$ mmHg), 20 min hypoxia ($P_{ET_{O_2}} = 50$ mmHg), 5 min euoxia ($P_{ET_{O_2}} = 100$ mmHg) and finally 5 min hypoxia ($P_{ET_{O_2}} = 50$ mmHg) was used to generate model ventilatory responses from each individual parameter set associated with each individual experimental repeat of the protocol (the time duration for each breath was idealised as 3 sec). For each subject, this gave between three and six sets of calculated responses to the idealized stimulus (one response corresponding to each individual parameter set obtained from a single experimental record). The responses were then averaged to give the average responses for that subject to the idealized stimulus. Following this, a single set of parameters was estimated from the average response to this idealized stimulus (no noise model is necessary, as there is no noise). This set of parameters is taken as the overall estimate for that particular subject and model.

### 4.2.4 Sensitivity analysis

To determine whether the parameters of the model were theoretically identifiable, a sensitivity analysis was undertaken.

Model data were generated for the input function associated with the protocol. The more complex extended model was used with a set of physiologically reasonable parameter values (actually the parameter values determined for subject 758) and a breath duration of 3 sec. The model parameters were then estimated repeatedly for the data set, with the exception that one of the parameters would be fixed, in turn, to the value used to generate the data and then to values ranging from 80% to 120% of this value (except for $k_p$, where a range of 0.0 to 0.02 was used since its value is close to zero). The sum of squared residuals could then be plotted against the value of the fixed parameter. If the parameter is not identifiable, then the plot should be flat, whereas if the value of the parameter affects the fit, then the plot should have

a definite minimum (zero) at the parameter value used to generate the data.

## 4.3 Results

### 4.3.1 Sensitivity analysis

The results for the sensitivity analysis are shown in Fig. 4.1. For all parameters, a minimum (zero) for the sum of squared residuals can be observed at the parameter value used to generate the data set. This indicates that all the parameters are theoretically identifiable in the model with the input function used to generate the data. However, the sensitivity of the sum of squared residuals to variations in parameter value vary considerably for the different parameters, and in some cases the sensitivity plots are quite asymmetric. The importance or otherwise of these features is difficult to gauge.

### 4.3.2 Fitting technique

The effect on the residuals of incorporating the noise model in the Kalman filter technique is illustrated in Fig. 4.2. A large degree of autocorrelation is seen in the residuals from the simple least-squares fitting process, which appears to have been almost totally removed by incorporating the parallel noise structure. Results from the portmanteau test demostrated that all 31 sets of residuals from the simple least-squares fitting algorithm were significantly non-white with $p$-values close to zero, whereas only 5 out of 31 sets of residuals from the model using a Kalman filter algorithm were found to be non-white. These 5 sets of non-white residuals were still much less correlated than the ones from the simple least-squares fitting technique.

Average parameter values from both the simple least-squares fitting technique and the Kalman filter algorithm are shown for Painter's model in table 4.1. In general, the parameter estimates from the two techniques appear quite similar. However, for the time constants associated with the rapid on-transients ($T_{p_1}$, $T_{p_3}$), the Kalman filter algorithm consistently yielded lower values for the time constants than

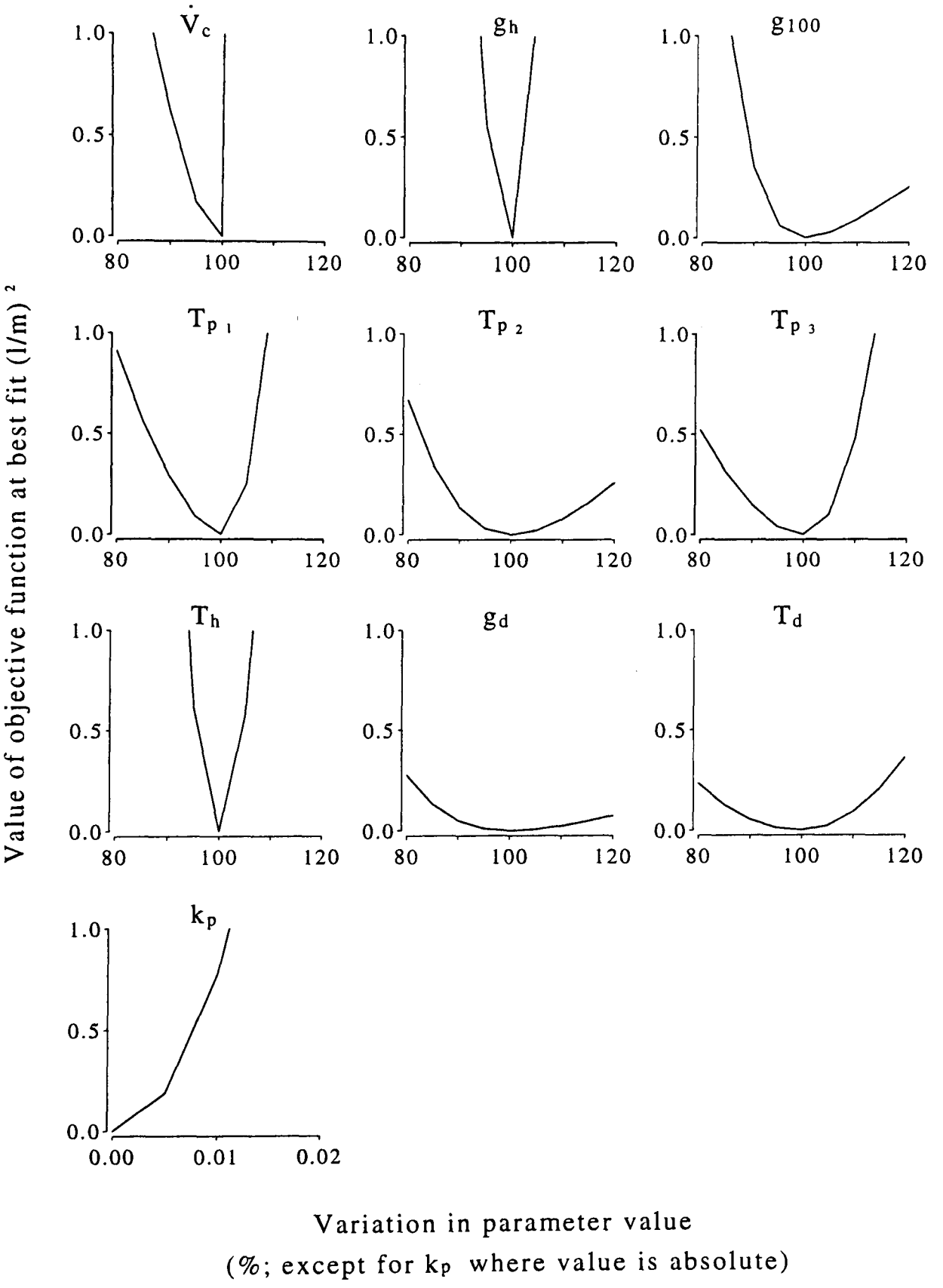


Figure 4.1: Sensitivity analysis for the parameters of the extended model. Abscissa is the percentage variations in the parameter value from that used to generate the model response (except for $k_p$, where the range of real values is shown). Ordinate is the sum of squared residuals.

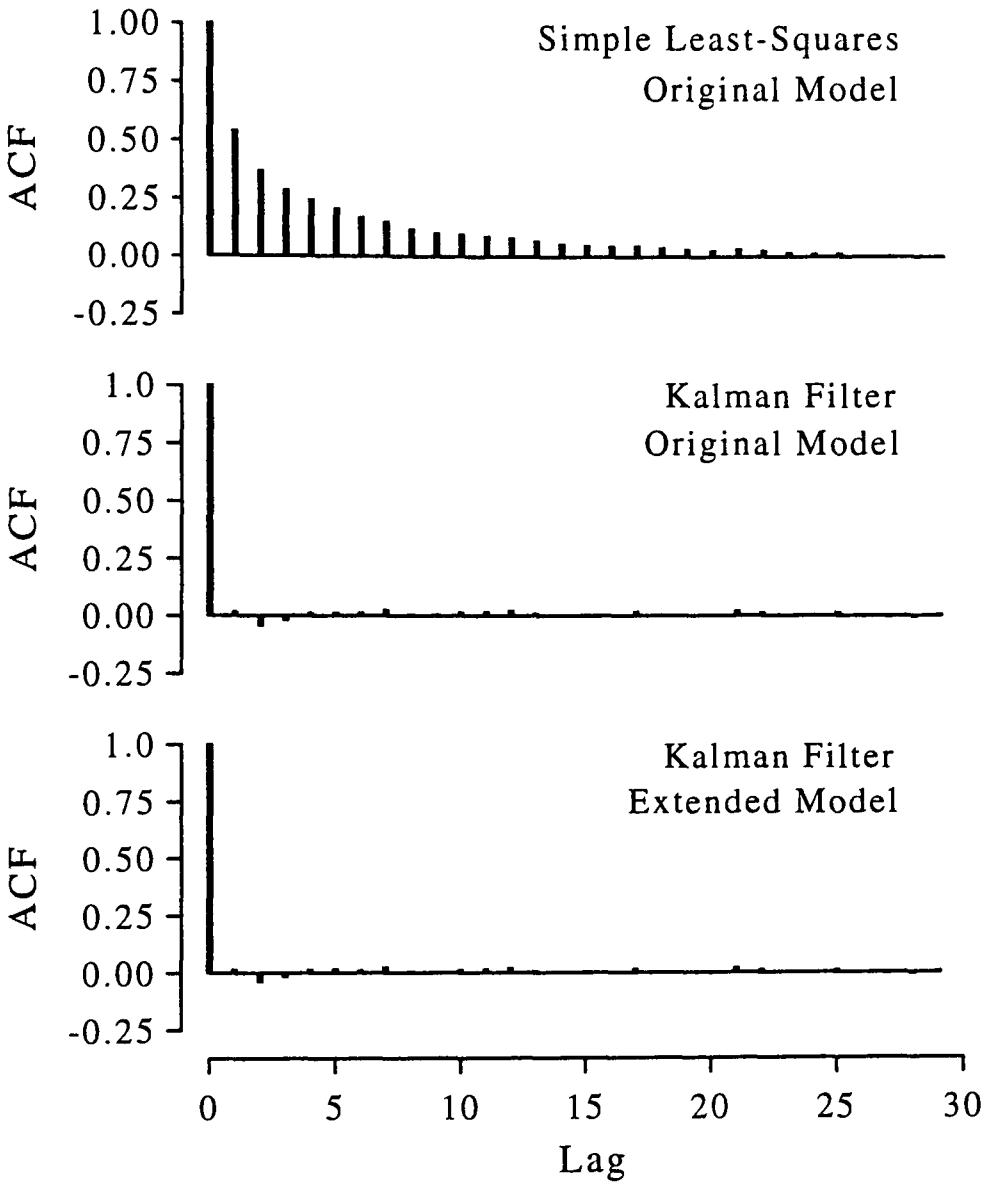


Figure 4.2: Autocorrelation functions (ACF) for the residuals from the original model of Painter *et al.* fitted with a simple least-squares fitting technique (upper panel), the model of Painter *et al.* fitted using a Kalman filter (middle panel) and the extended model (lower panel). Values are averages across entire data set.

did the simple least-squares fitting procedure. For the time constant for the hypoxic ventilatory decline ($T_h$), the reverse was true with the values from the Kalman filter algorithm being consistently higher than from the simple least-squares fitting procedure. Consistent effects across all the six subjects are significant at the level $P < 0.05$ (sign test), and suggest some element of bias in estimating these values with a simple least-squares fitting routine.

Table 4.1: Parameter values estimated for each subject for Painter's model using least-squares fitting technique and Kalman filter algorithm.

| | Subject | $\dot{V}_c$ l/min | $g_{100}$ l/min | $g_h$ l/min | $k_p$ | $T_{p_1}$ sec | $T_{p_2}$ sec | $T_{p_3}$ sec | $T_h$ sec | $d_p$ sec |
|---|---|---|---|---|---|---|---|---|---|---|
| *Least* | 743 | 12.7 | 139 | 295 | 0.06 | 48.1 | 5.3 | 33.9 | 205 | 0 |
| *squares* | 758 | 8.8 | 79 | 272 | 0.05 | 51.2 | 3.2 | 56.8 | 296 | 0 |
| | 766 | 6.6 | 92 | 433 | 0.01 | 24.7 | 4.7 | 11.5 | 759 | 0 |
| | 796 | 14.7 | 59 | 244 | 0.06 | 17.9 | 1.6 | 3.9 | 299 | 1 |
| | 818 | 18.7 | 257 | 1436 | 0.02 | 8.9 | 6.7 | 33.4 | 344 | 0 |
| | 824 | 15.0 | 222 | 804 | 0.02 | 27.1 | 30.9 | 19.5 | 312 | 0 |
| *Kalman* | 743 | 14.4 | 136 | 273 | 0.04 | 31.2 | 4.8 | 26.7 | 273 | 0 |
| *filter* | 758 | 10.2 | 84 | 335 | 0.03 | 46.8 | 3.9 | 56.3 | 315 | 0 |
| | 766 | 6.5 | 88 | 407 | 0.01 | 15.6 | 5.7 | 5.8 | 832 | 0 |
| | 796 | 12.7 | 50 | 165 | 0.11 | 2.5 | 1.2 | 0.8 | 380 | 3 |
| | 818 | 18.3 | 249 | 1006 | 0.03 | 6.3 | 4.1 | 18.7 | 392 | 2 |
| | 824 | 16.0 | 210 | 729 | 0.01 | 12.3 | 16.3 | 12.1 | 359 | 0 |

### 4.3.3 Model comparison

Fig. 4.3 shows one example of the respiratory data together with the model fits for the two models. (Model fits for Painter's model using the simple least-squares fitting procedure are not shown as the appearence was essentially identical to the appearence of the results for the deterministic component using the Kalman filter algorithm.) The left panel shows the fit for the original model developed by Painter *et al.* (1993), and the right panel shows the fit for the extended model which incorporates the additional component of HVD which is independent of chemoreflex sensitivity. The lower panels (which show the deterministic component of the model output) illustrate clearly for this particular data set that the simpler model of Painter *et al.* can describe most of the experimental record reasonably well, but that the model does not reflect the transient undershoot in ventilation at the relief of the stimulus particularly well. The introduction of the extra chemoreflex insensitive component of the extended model greatly improves the fit to this part of the record.

Fig. 4.4 shows average data and model fits for each subject for the model of Painter *et al.* and Fig. 4.5 shows average data and model fits for each subject for the extended model. These were calculated from the individual data sets and model fits by interpolating the data every 3 seconds, and then averaging across all the individual responses for each subject. The average of the residuals sequences for each subject was calculated in the same way, and the 95% confidence intervals (calculated as $\pm 1.96$ S.E.) were plotted in the figures along with the averaged ventilatory output. For much of the response, the outputs of the two models are very similar. However, for the two subjects (758, 796) that show the greatest undershoot and recovery at the relief of hypoxia, the extended model appears to describe this process more accurately than does the original model of Painter *et al.*

F-ratio tests on the sum of squared prediction errors revealed that, for these two

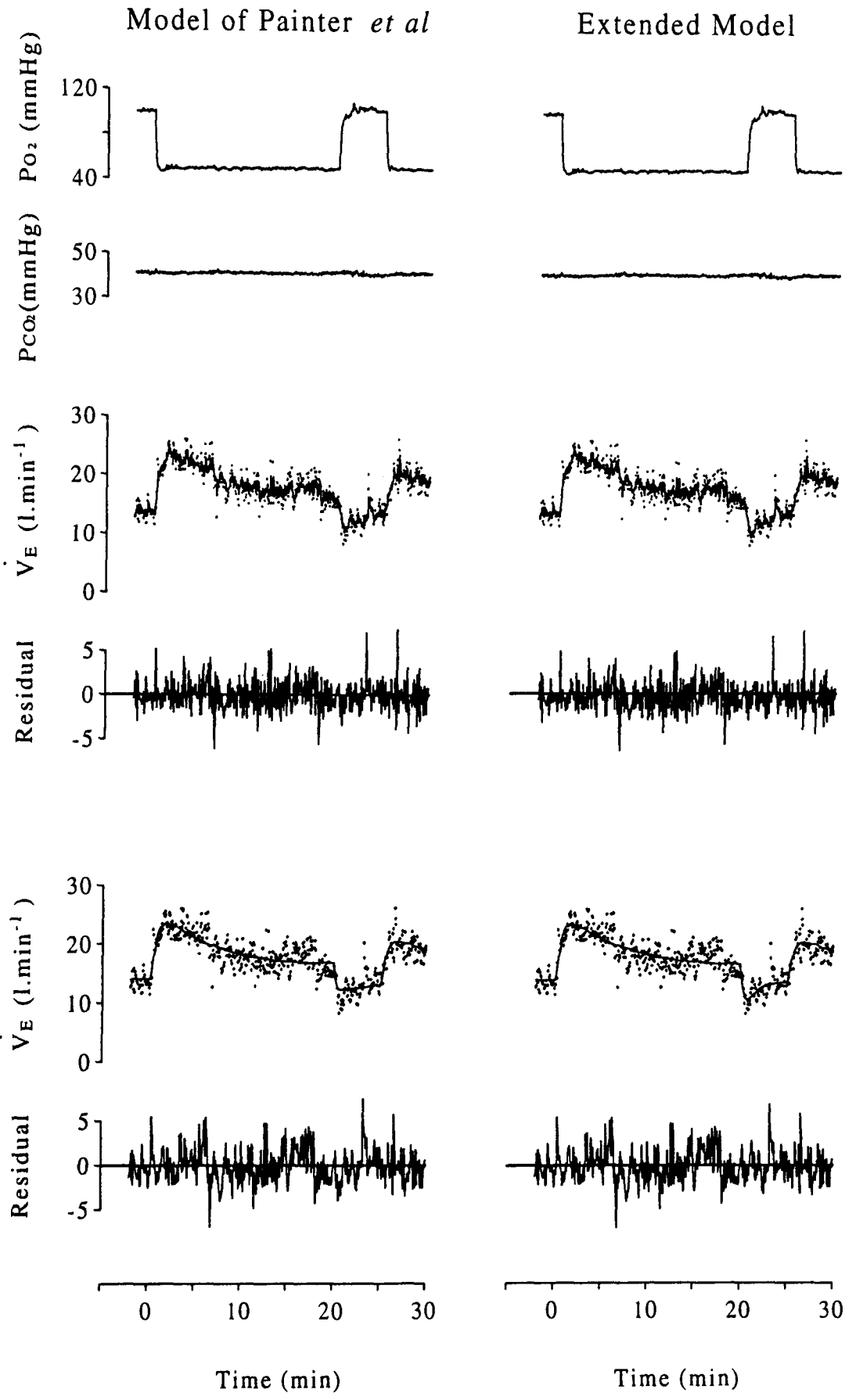


Figure 4.3: A comparison between the original model and the extended model fitted to one set of experimental observations. Left panels are for the model of Painter *et al.*; right panels are for the extended model. Upper two panels show the experimental input ($P_{ET_{O_2}}$ and $P_{ET_{CO_2}}$); middle two panels illustrate the model prediction and residuals with a Kalman filter (solid lines for the model outputs and dots for the experimental observations); lower two panels illustrate the deterministic component of the model and associated residuals (solid lines for calculated values and dots for the experimental observations).

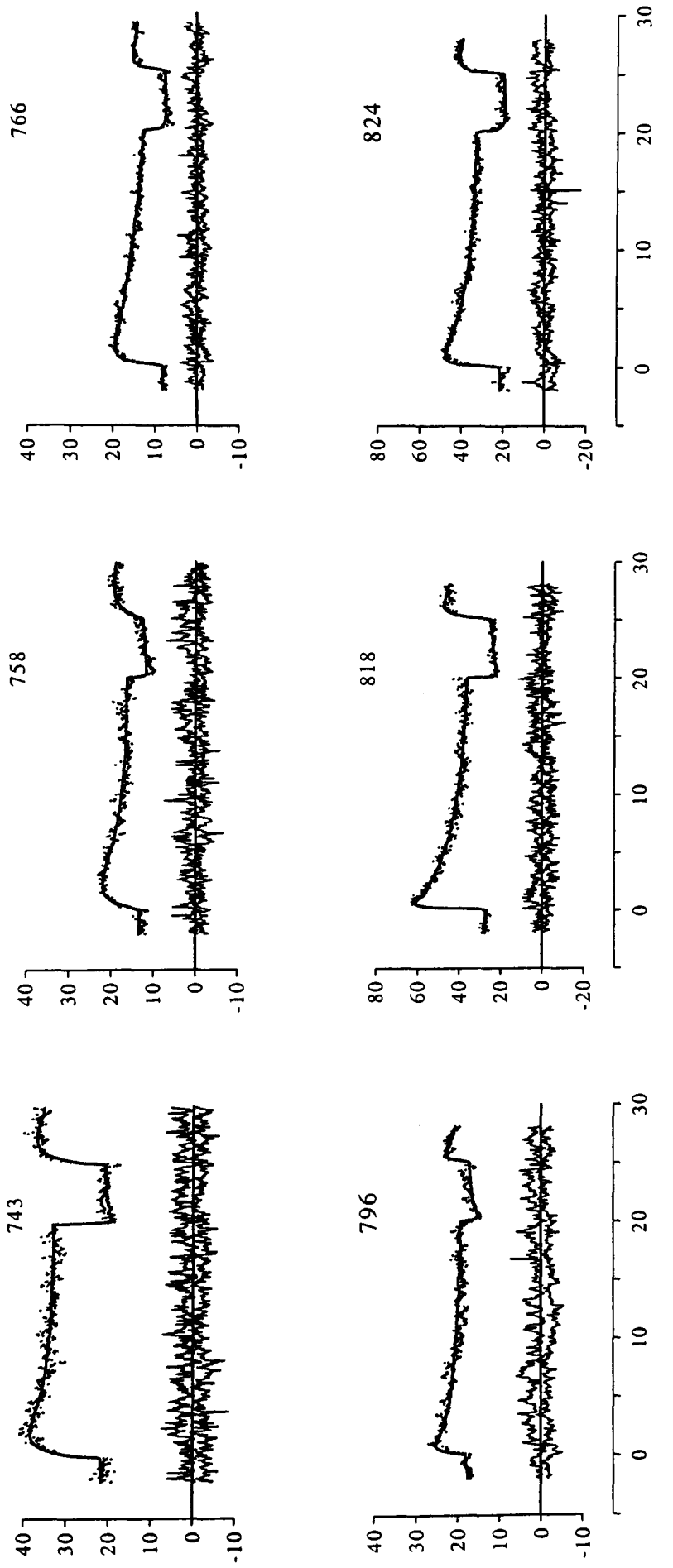


Figure 4.4: Ventilatory response and model fit for the original m
over 3 sec intervals). Upper section for each subject shows the a
ministic component of the model response (solid lines); lower sec
intervals for the associated residuals.

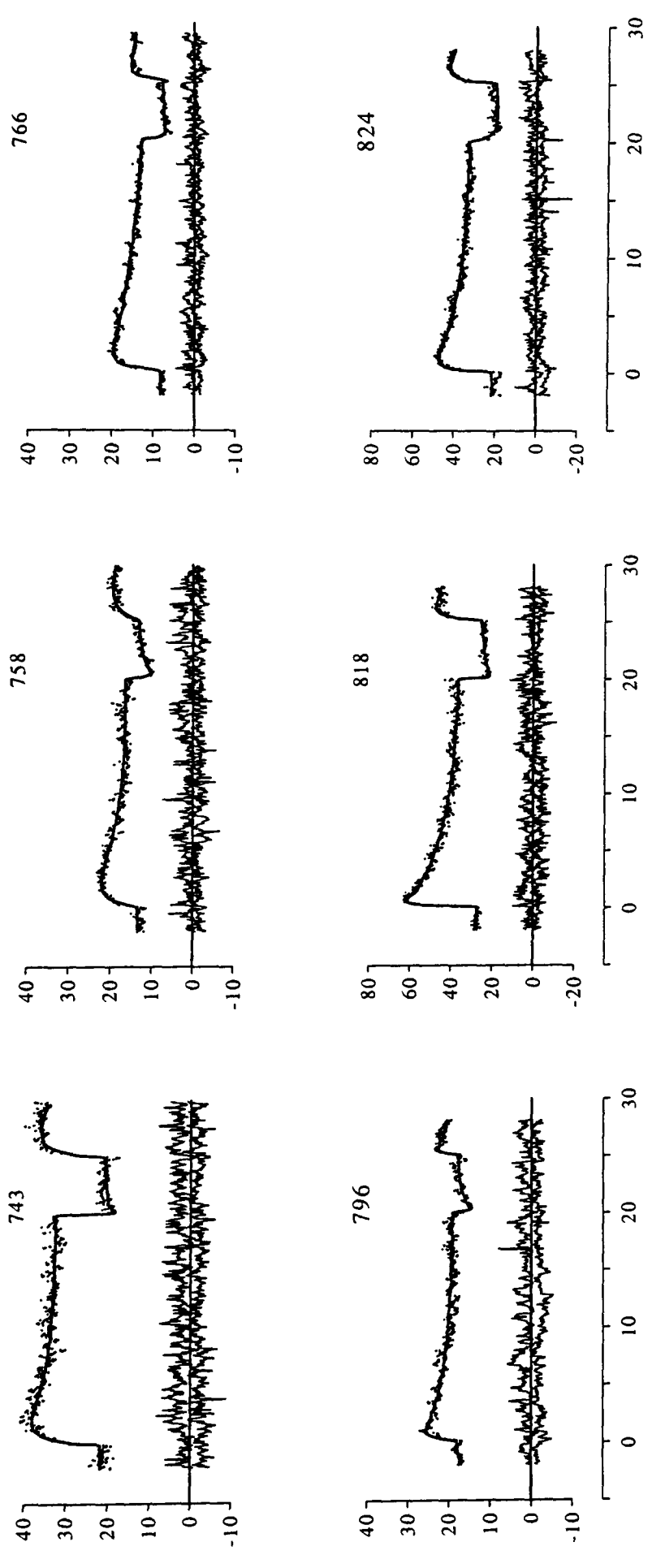


Figure 4.5: Ventilatory response and model fit for the extended model for all subjects (averaged over 3 sec intervals). Upper section for each subject shows the averaged experimental data (dots) and the deterministic component of the model response (lines); lower section for each subject shows the 95% confidence intervals for the associated residuals.

subjects (758, 796), the extended model fitted significantly better than the original model of Painter *et al.* For all other subjects, no significant improvement in the sum of squared prediction errors was detected. A whiteness test (Portmanteau test) on the prediction errors showed that 26 out of 31 sequences could be accepted as white for the model of Painter *et al.* and 28 out of 31 sequences could be accepted as white for the extended model. Thus fitting a stochastic component to the data makes the use of an F-ratio test possible without the complications of trying to correct the degrees of freedom for correlation present within the residuals.

Overall parameter values for each subject for the original model and the extended model using the Kalman filter algorithm are shown in table 4.2. The time constants for the rapid ventilatory response to the onset and the relief of hypoxia ($T_{p_1}$, $T_{p_2}$ and $T_{p_3}$) are faster than the time constant for the slow change in the peripheral chemoreflex sensitivity ($T_h$). In most cases, the time constant for the rapid ventilatory response at the relief of hypoxia ($T_{p_2}$) appears faster than those for the rapid ventilatory response at the onset of hypoxia ($T_{p_1}$ and $T_{p_3}$). However, this effect does not reach statistical significance overall.

In the extended model, some effect was attributed to the extra component of the model by the fitting process in 5 out of 6 subjects. The values estimated for both $g_d$ and $T_d$ were quite variable between the different subjects. Table 4.3 shows the percentage contributions to HVD of the component acting via modulation of the peripheral chemoreflex sensitivity ($\dot{V}_p$) and the component that is independent of the peripheral chemoreflex ($\dot{V}_d$) for each subject. These figures were obtained from the steady-state expressions for $g_p$, $\dot{V}_p$ and $\dot{V}_d$ that can be obtained by setting the derivatives in equations (4.2), (4.3) and (4.10) to zero. After an acute step to an end-tidal $P_{O_2}$ of 50 mmHg from a sustained level of 100 mmHg, the values for $\dot{V}_p$ and $\dot{V}_d$ can be approximated by assuming that the values for $g_p$ and $\dot{V}_d$ are

Table 4.2: Parameter values estimated for each subject for both models.

| | Sub. | $\dot{V}_c$ l/m | $g_{100}$ l/m | $g_h$ l/m | $k_p$ | $T_{p_1}$ sec | $T_{p_2}$ sec | $T_{p_3}$ sec | $T_h$ sec | $g_d$ l/m | $T_d$ sec | $d_p$ sec |
|---|---|---|---|---|---|---|---|---|---|---|---|---|
| *Ori.* | 743 | 14.4 | 136 | 273 | 0.04 | 31.2 | 4.8 | 26.7 | 273 | | | 0 |
| *model* | 758 | 10.2 | 84 | 335 | 0.03 | 46.8 | 3.9 | 56.3 | 315 | | | 0 |
| | 766 | 6.5 | 88 | 407 | 0.01 | 15.6 | 5.7 | 5.8 | 832 | | | 0 |
| | 796 | 12.7 | 50 | 165 | 0.11 | 2.5 | 1.2 | 0.8 | 380 | | | 3 |
| | 818 | 18.3 | 249 | 1006 | 0.03 | 6.3 | 4.1 | 18.7 | 392 | | | 2 |
| | 824 | 16.0 | 210 | 729 | 0.01 | 12.3 | 16.3 | 12.1 | 359 | | | 0 |
| *Ext.* | 743 | 20.2 | 136 | 281 | 0.0 | 27.8 | 4.1 | 23.5 | 328 | -12.4 | 300 | 0 |
| *model* | 758 | 12.5 | 135 | 352 | 0.0 | 46.1 | 15.0 | 53.3 | 324 | -55.4 | 52 | 0 |
| | 766 | 7.2 | 91 | 431 | 0.0 | 20.4 | 5.4 | 6.9 | 869 | -4.5 | 232 | 0 |
| | 796 | 16.7 | 102 | 252 | 0.0 | 11.5 | 1.9 | 5.4 | 499 | -53.1 | 22 | 3 |
| | 818 | 18.5 | 248 | 1009 | 0.03 | 6.2 | 2.8 | 18.7 | 395 | 0.0 | — | 2 |
| | 824 | 19.0 | 213 | 723 | 0.0 | 16.1 | 32.6 | 12.9 | 319 | -16.9 | 738 | 0 |

unchanged from their steady state pre-hypoxic levels, but that the value for $\dot{V}_p$ is that associated with the hypoxic level of saturation. After a sustained period of end-tidal $P_{O_2}$ equal to 50 mmHg, the values for $g_p$, $\dot{V}_p$ and $\dot{V}_d$ can be obtained using the hypoxic value for saturation in all the equations. The falls in $\dot{V}_p$ and $\dot{V}_d$ can be calculated from the differences between the acute hypoxic and the sustained hypoxic values in each case. The averaged contributions calculated across all the six subjects were 73.8% for the component acting via the peripheral chemoreflex and 26.2% for the peripheral chemoreflex insensitive component.

Comparing parameter values between the models, one striking feature is that a positive value for $k_p$ was estimated for the model of Painter *et al.* for all 6 subjects whereas a positive value for $k_p$ was estimated for only 1 out of 6 subjects for the extended model. Physiologically, $k_p$ represents the component of peripheral chemoreflex drive that is present in high oxygen, and this suggests that the model of Painter *et al.* attributes a higher proportion of the total ventilation to peripheral chemoreflex drive in euoxia than does the extended model. This is confirmed by inspection of table 4.3, where the contributions of each component to ventilation have been calculated for both models in euoxia. The mean contribution to ventilation by the peripheral chemoreflex drive is significantly lower in the extended model compared with the model of Painter *et al.* ($P$ <0.05, paired Student's t-test) and there is a corresponding increase in the central component of ventilation in the extended model compared with the model of Painter *et al.* The reduction of total ventilation by $\dot{V}_d$ is small in euoxia as would be expected by the fact that the saturation is close to 1.

Table 4.3: Ventilations in euoxia and the percentage of HVD attributed to each component for both models.

| | Subject | Ventilation (l/min) | | | | Decline (%) | |
|---|---|---|---|---|---|---|---|
| | | $\dot{V}_c$ | $\dot{V}_p$ | $\dot{V}_d$ | $\dot{V}_E$ | $\dot{V}_p$ | $\dot{V}_d$ |
| *Original* | 743 | 14.4 | 7.0 | | 21.4 | 100 | 0 |
| *model* | 758 | 10.2 | 3.4 | | 13.6 | 100 | 0 |
| | 766 | 6.5 | 1.9 | | 8.4 | 100 | 0 |
| | 796 | 12.7 | 5.9 | | 18.6 | 100 | 0 |
| | 818 | 18.3 | 10.1 | | 28.4 | 100 | 0 |
| | 824 | 16.0 | 4.6 | | 20.6 | 100 | 0 |
| *Extended* | 743 | 20.2 | 1.7 | -0.2 | 21.8 | 76 | 24 |
| *model* | 758 | 12.5 | 1.7 | -0.7 | 13.5 | 48 | 52 |
| | 766 | 7.2 | 1.1 | -0.1 | 8.3 | 93 | 7 |
| | 796 | 16.7 | 1.3 | -0.7 | 17.3 | 40 | 60 |
| | 818 | 18.5 | 10.1 | 0.0 | 28.6 | 100 | 0 |
| | 824 | 19.0 | 2.6 | -0.2 | 21.4 | 86 | 14 |

## 4.4 Discussion

### 4.4.1 Fitting technique

In the study by Painter *et al.* (1993) no model of the noise structure was employed, whereas in the current study both a simple least-squares fitting procedure and a simple state-space model for a parallel noise process were explored. A suitable noise model allows the inherent correlation between successive breaths to be included in the model, and results in residuals that are overall white or close to white. This is useful when comparing the overall quality of fit between different models. This approach has been adopted by others for modelling the ventilatory response to carbon dioxide (DeGoede and Berkenbosch, 1989). The ability of the particular state-space model chosen to describe ventilatory variability has been demonstrated previously (see Chap. 3), and this result is supported by the observation that 26-28 out of 31 sets of residuals could be accepted as white on the basis of a Portmanteau test in the current study, whereas all the residuals sequences from the simple-least squares fitting technique were highly correlated.

### 4.4.2 Model comparison

Comparisons between the models may be drawn in a number of ways. First, the question may be asked whether the extended model produces any statistically significant improvement in the fit as compared with the original model of Painter *et al.* This can be determined both by examining the overall sum of squared residuals, and also by inspection of the confidence intervals for the ensemble averaged residuals over the time course of the protocol. Secondly, some physiological judgement may be exercised in terms of whether the estimated parameter values are likely to be consistent with other known features of the respiratory system.

In statistical terms, only two subjects (758, 796) showed a significant reduction

in the total sum of squared residuals with the extended model as compared with the model of Painter *et al.* These two subjects consistently showed an apparent undershoot and then recovery of ventilation at the relief of hypoxia in all the individual experimental repeats of the protocol. In other subjects, an undershoot followed by recovery was either not observed or appeared inconsistently in some but not all of the repeats. Inspection of the plots of the model fit and ensemble averaged residuals over time shows that it is during the period following the relief from hypoxia that the models are most distinct. We conclude that the use of the extended model may significantly improve the fit in some subjects who show a reasonable degree of undershoot and recovery of ventilation following the relief of hypoxia, but that this is not the case for all subjects.

The two subjects in whom the fit of the extended model was a significant improvement over the model of Painter *et al.* had the two largest magnitudes for the gain term ($g_d$) of the additional chemoreflex-independent component. In these two subjects, slightly over 50% of HVD (mean 56%) was attributed to the peripheral chemoreflex independent component. In the other four subjects, the value was very much smaller with a mean value of 11%. Again, this emphasises the importance of inter-subject differences.

For the two subjects with a substantial contribution to ventilation from the peripheral chemoreflex independent compartment, the time constants associated with this compartment were rather fast (22 s and 50 s), and are consistent with the comments of Bascom *et al.* (1992) that the baseline ventilation appears to recover more quickly than does the peripheral chemoreflex sensitivity. These values do not really correlate well with the sorts of values previously obtained for the development of HVD in anaesthetised animals (onset of HVD 149.7 $\pm$ 8.5 s (mean $\pm$ S.E.); offset of HVD 105.5 $\pm$ 10.1 s, (Ward *et al.*, 1990)). Thus, on the basis of data from

these two subjects, it would appear that this peripheral chemoreflex insensitive component cannot really be equated simply with a chemoreflex insensitive form of HVD observed in anaesthetised animals as postulated in the introduction. However, for the other three subjects in whom some component of the ventilatory response was attributed to the peripheral chemoreflex independent term, the time constants were all somewhat longer than those associated with HVD in anaesthetised animals. Overall, I feel that it would be unwarranted to draw any very firm conclusions from these values.

One notable feature that differs between the two models is the parameter estimates determined for $k_p$. In the original model of Painter *et al.*, values for $k_p$ were all positive, whereas in the extended model the value for $k_p$ was zero in five out of six subjects. Physiologically, $k_p$ is a parameter relating to the contribution of the peripheral chemoreflex to ventilation in hyperoxia when the arterial blood is fully saturated. There is a substantially greater contribution of the peripheral chemoreflex to overall ventilation in the model of Painter *et al.* as compared with the extended model. We consider that the positive values for $k_p$ in the model of Painter *et al.* may be necessary to fit the slightly lower level of euoxic ventilation seen following the relief of hypoxia when compared with the original baseline ventilation. In the extended model, this feature of the data can be modelled via the additional term $\dot{V}_d$. Which of these approaches in a physiological sense is correct is difficult to determine. While there is some evidence to suggest that the peripheral chemoreflex is inactivated by hyperoxia in humans (Miller *et al.*, 1974; see also Dahan, 1990), in which case the extended model might represent the physiology better, it is also possible that positive values of $k_p$ might simply represent some non-linearity of the response of the peripheral chemoreflex to saturation in this range.

# Chapter 5

# Dynamics of the Fast Component of the Ventilatory Response to Cyclic Hypoxia in Humans

知止可以不殆

老子・三十二

## 5.1 Introduction

To study the behaviour of the ventilatory response to acute changes in alveolar oxygen tension, a simple first order model was examined by Clement and Robbins (1993*a*). Using a least-square fitting technique, the proposed model was fitted to ventilatory data collected during square wave stimulation by hypoxia under isocapnic conditions. The results revealed that this simple proportional model fails to describe some of the features that are present in the experimental observations. In particular the ventilatory response to the cyclic onset and relief of brief periods of isocapnic hypoxia appears asymmetric in two aspects: 1) the on-transient dynamics are faster than the off-transient dynamics, and 2) an overshoot may appear in the latter part of the ventilatory response to the hypoxic on-transient. This led to a suggestion that, to describe these features of the ventilatory response to cyclic acute hypoxia, an additional rate-sensitive element might need to be incorporated into the simple proportional model.

Following this suggestion, an extended model incorporating a non-linear rate-sensitive component was explored briefly in data from one subject by Medina-Alvarez (1993), using a least-square fitting technique. The results suggested that such an extended model does improve the model description of the data, in the sense that the extended model can describe the difference in speed between the on- and off-transient, and also describe the overshoot that appears in the averaged data.

However, all the model fitting carried out by these research workers was based on a least-square fitting procedure, and, with such a procedure, the noise structure existing in the ventilatory behaviour is not considered — it is assumed white. This assumption does not hold for these data, and the residuals sequences from both studies have been shown to be correlated (Clement and Robbins, 1993*a*; Medina-Alvarez, 1993). The presence of such correlation introduces two potential problems, first the

parameter estimates may be biased and, secondly, the statistical comparisons of the goodness of fit become harder to make.

The purpose of the current study is to examine the data collected by Clement and Robbins to explore: 1) the influence that the presence of correlated noise has on the parameter values with this particular input; 2) to use the Kalman filter technique to fit both the extended model as well as the simple model, so that the residuals from both model fits are uncorrelated and a statistical comparison between the two models may be drawn more easily; and 3) to examine further the extended model to see if it can give a full description of the ventilatory response during cyclic hypoxia.

## 5.2 Methods

### 5.2.1 Data

The experimental data came from a previous study from our laboratory (Clement and Robbins, 1993*a*). Experiments were performed on 5 young healthy subjects during rest, with 4-5 repeats on each subject, and resulted in 24 sets of experimental data in total. End-tidal $P_{CO_2}$ was kept constant at 2-3 Torr above the normal end-tidal value for each subject. A square wave input of hypoxia was given as a stimulus at a period of 30 sec, with the mean upper and lower values of end-tidal $P_{O_2}$ being 69.3 and 46.7 Torr. Each experiment lasted for 30 min.

To illustrate the ventilatory behaviour under such an input, Fig. 5.1 gives an example of an experimental record, including the cyclic hypoxic input and the ventilatory response to it. The ventilation appears to have a slow drift in the baseline over the experimental period and there are occasional big breaths occuring during the cyclic hypoxia. These features of variability seem unlikely to be directly related to the cyclic input of hypoxia. Fig. 5.2 gives an overview of the entire data set showing the cyclic hypoxia and the ventilatory output for each individual experiment as an average for a single 30 sec period.

### 5.2.2 Smoothing

To remove the baseline drift which is not directly dependent on the cyclic hypoxic input (Fig. 5.1), a smoothing technique was applied to the data before any other numerical analysis was performed.

A smoother is a tool for summarising the trend of a certain measurement and it produces an estimate of the trend that is less variable than measurement itself. Since it does not assume a rigid parametric form, it is often referred to as a tool for nonparametric regression (Hastie and Tibshirani, 1990). Generally, a smoother

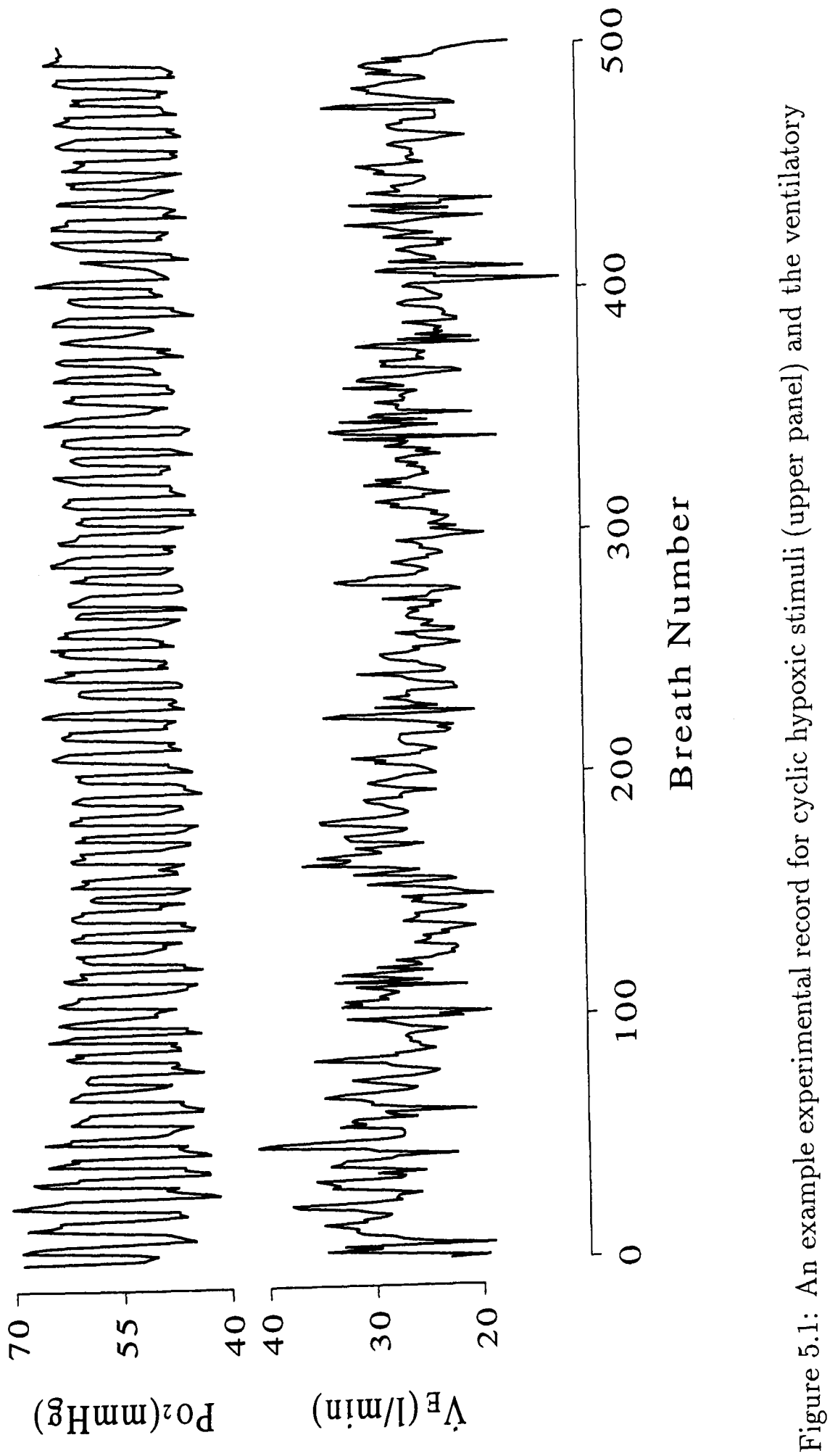


Figure 5.1: An example experimental record for cyclic hypoxic stimuli (upper panel) and the ventilatory response (lower panel).

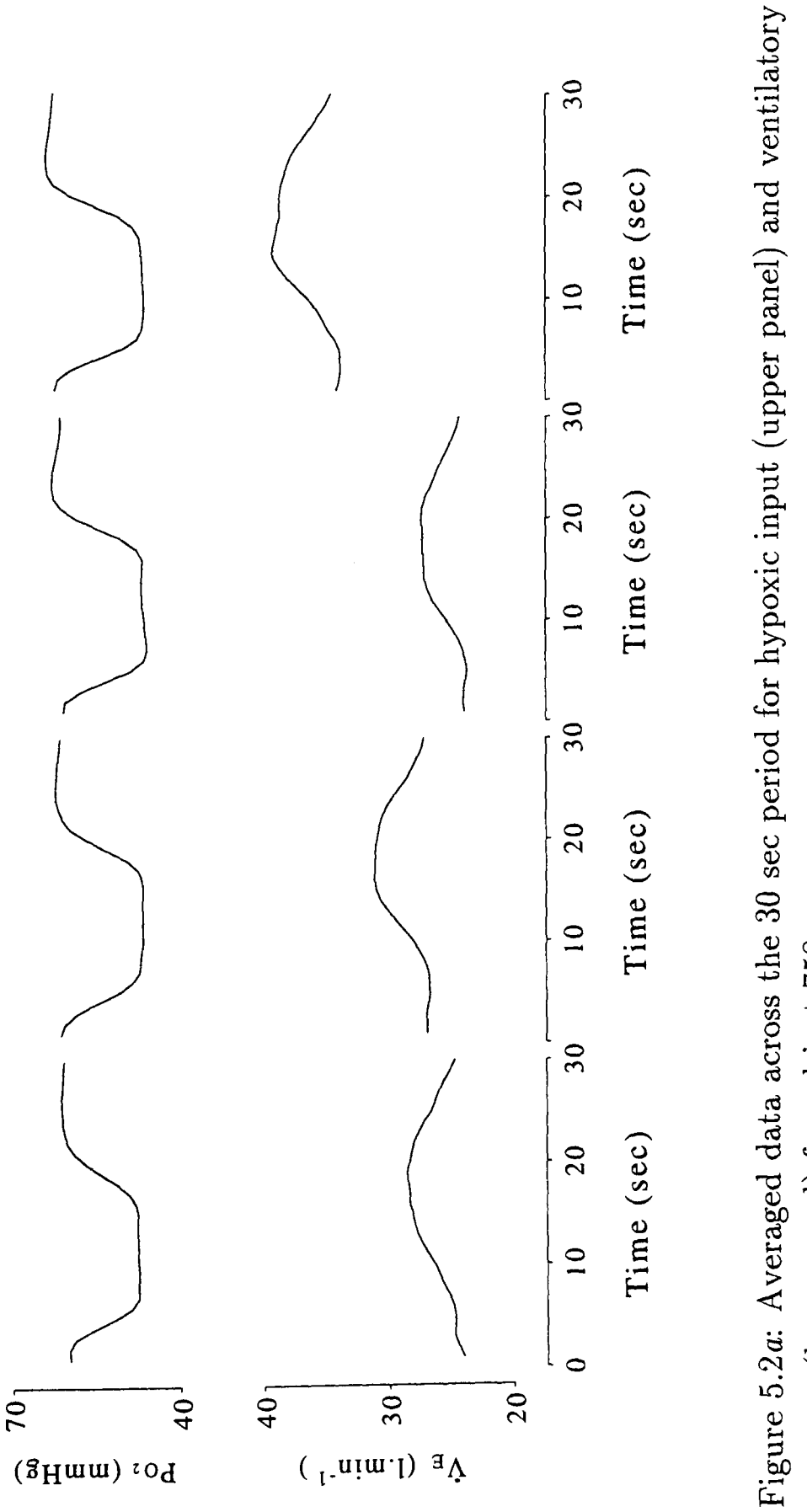


Figure 5.2*a*: Averaged data across the 30 sec period for hypoxic input (upper panel) and ventilatory response (lower panel) for subject 758.

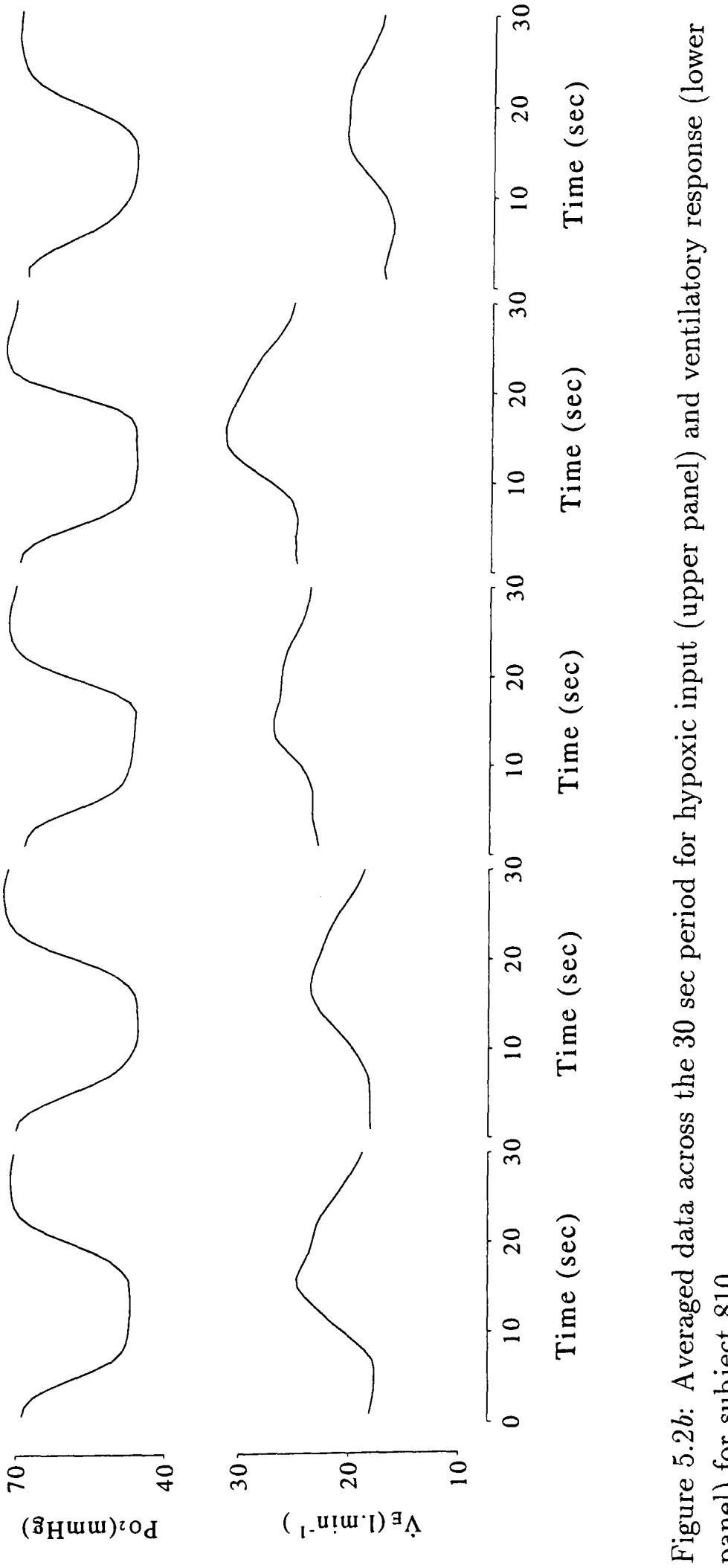


Figure 5.2*b*: Averaged data across the 30 sec period for hypoxic input (upper panel) and ventilatory response (lower panel) for subject 810.

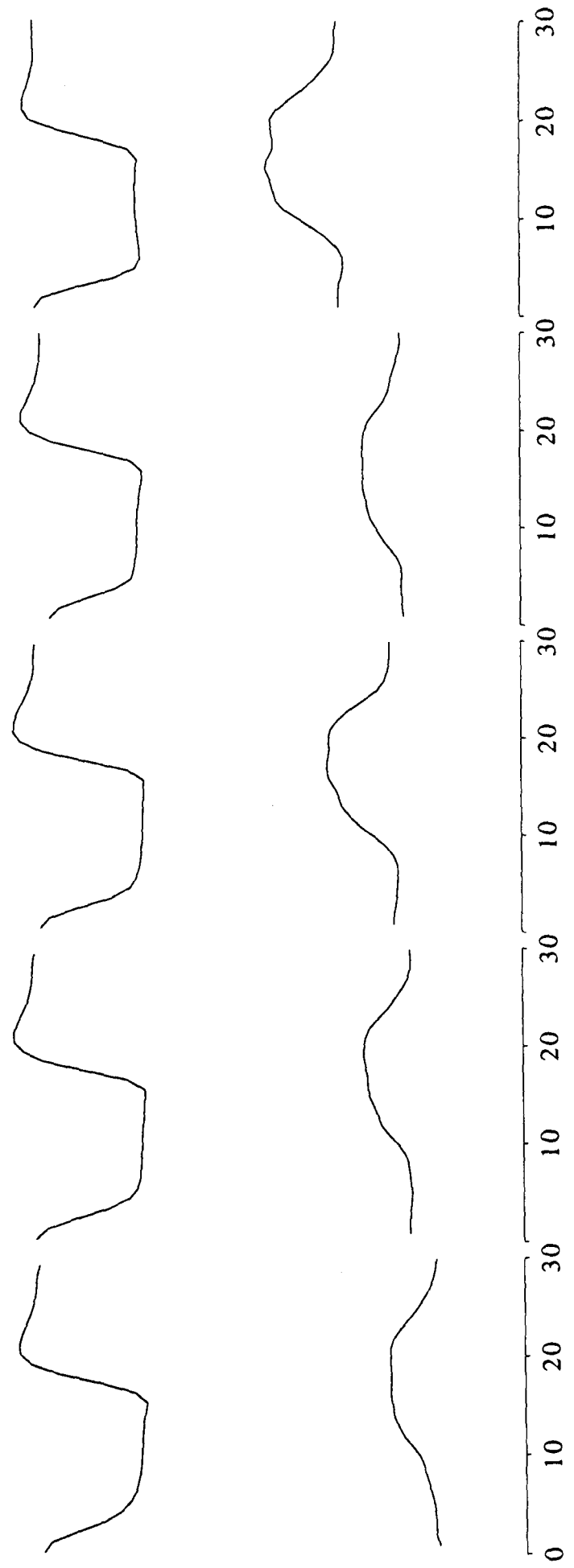


Figure 5.2*c*: Averaged data across the 30 sec period for hypoxic input (upper panel) and ventilatory response (lower panel) for subject 818.

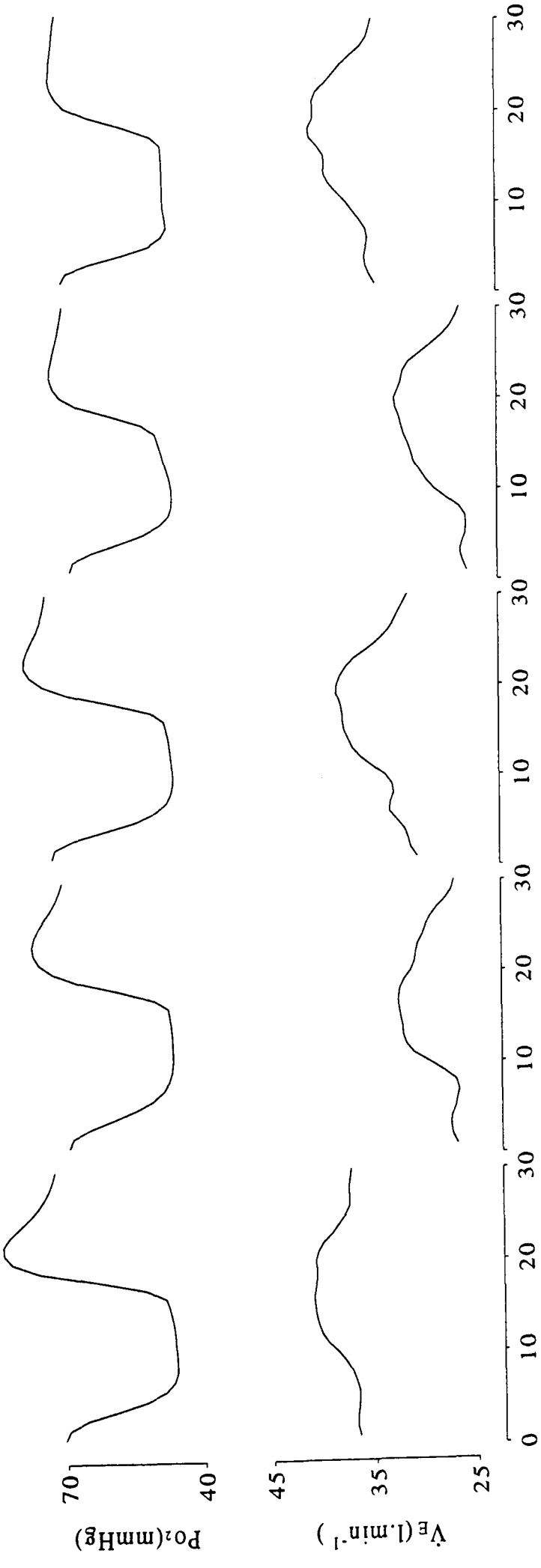


Figure 5.2*d*: Averaged data across the 30 sec period for hypoxic input (upper panel) and ventilatory response (lower panel) for subject 820.

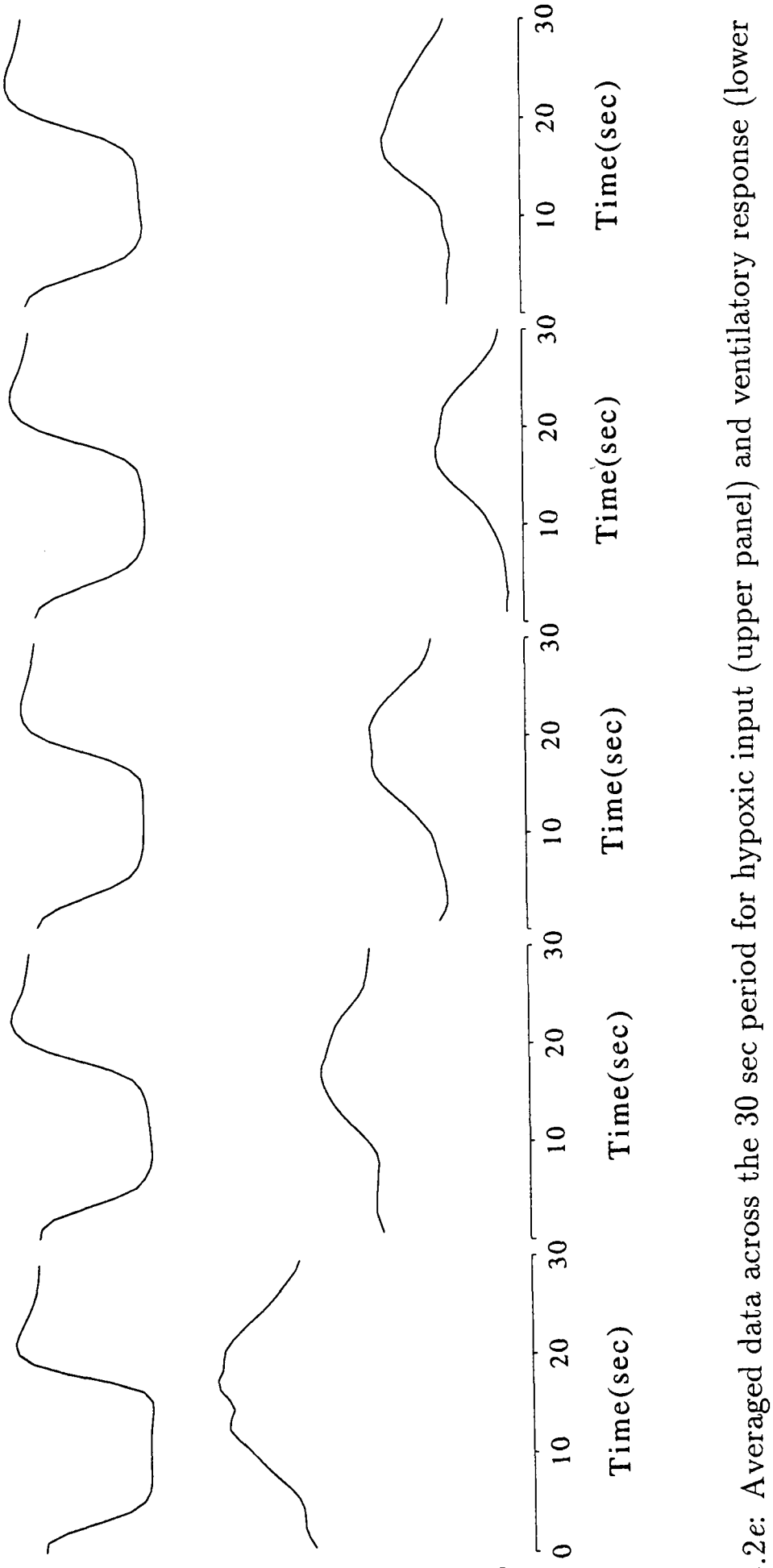


Figure 5.2*e*: Averaged data across the 30 sec period for hypoxic input (upper panel) and ventilatory response (lower panel) for subject 823.

attempts to mimic category averaging through local averaging, which is done in neighbourhoods around the target value. The two main decisions to be made in smoothing are: 1) the way of averaging the data, which really refers to choosing the brand of smoother; and 2) the size of the neighbourhoods to be used, which is usually expressed in terms of a smoothing parameter. Intuitively, large neighbourhoods will produce an estimate with low variance but potentially high bias, with the converse for small neighbourhoods.

There are various kinds of smoother in existence which could be used. Smoothing splines have been shown to be efficient and effective when applied to respiratory data (Jacob, 1995). Thus, a cubic smoothing spline was adopted in this study and implemented using "S-plus" statistical software. The parameter to be chosen for the smoother is the degree of freedom *df*. Briefly, a smoother is given in a form that $\hat{\mathbf{m}} = \mathbf{S}\mathbf{y}$, where $\hat{\mathbf{m}}$ denotes the estimated smoother, $\mathbf{y}$ denotes the data sequence with the length being $n$ and $\mathbf{S}$ is an $n \times n$ matrix called the smoother matrix, with the property that $\mathbf{S} \times \mathbf{1} = \mathbf{1}$, and the smoothing parameter *df* is defined as $df = trace(\mathbf{S})$ (Hastie and Tibshirani, 1990). Once the smoothing parameter (*df*) is decided, a lowpass filter can be built up to determine the smoother ($\hat{\mathbf{m}}$) given the original data sequence ($\mathbf{y}$). The "de-trended" data can thus be obtained simply by subtracting the smoother sequence from the data sequence.

To remove the drift effectively without losing the periodic information contained within the data, the smoothing parameter *df*, which is related to the size of neighbouring data, was taken as half of the number of the hypoxic cycles contained within the data (Jacob, 1995). In this study, the number of cycles during the 30 min of experimental period was equal to 60, and so a value of *df* was chosen as 30.

### 5.2.3 Dynamic models

*First-order linear model.*

To describe the fast component of ventilatory response to acute hypoxia, a first-order proportional dynamic model was proposed by Clement and Robbins (1993*a*). In this model, the total ventilation, $\dot{V}_E$, is considered as a combination of a peripheral component $\dot{V}_P$ and a central component $\dot{V}_C$:

$$\dot{V}_E = \dot{V}_P + \dot{V}_C \tag{5.1}$$

where the central component remains constant during isocapnic hypoxia and the peripheral component is linearly related to the hypoxic stimulus during steady state:

$$\dot{V}_P = g_P \cdot Hyp \tag{5.2}$$

The hypoxic function (Hyp) is the haemoglobin desaturation function taken from Severinghaus (1979) such that

$$Hyp = 1.0 - (\frac{23400}{P_{O_2}^3 + 150 \cdot P_{O_2}} + 1)^{-1} \tag{5.3}$$

A single first-order dynamic for this form of model can thus be written as:

$$d\dot{V}_P/dt = (1/T_P)(g_P \cdot Hyp(t - d_p) - \dot{V}_P) \tag{5.4}$$

where $g_P$ and $T_P$ denote the gain term and the time constant of the dynamic respectively and $d_p$ denotes the time delay, Thus, the parameters to be estimated for the dynamic model are $\dot{V}_C$, $g_P$, $T_P$ and $d_p$, with the difference equations for this model being:

$$\begin{aligned} (\dot{V}_P)_{n+1} &= g_P \cdot Hyp(t_n - d_p) \\ &\quad -(g_P \cdot Hyp(t_n - d_p) - (\dot{V}_P)_n)e^{-(t_{n+1}-t_n)/T_P} \qquad (5.5) \\ (\dot{V}_E)_n &= (\dot{V}_C)_n + (\dot{V}_P)_n \qquad (5.6) \end{aligned}$$

where $t_n$ refers to the time of the $n^{th}$ breath.

*Model with a rate-sensitive component.*

The dynamic model established by Clement and Robbins predicts an overall symmetric output of the ventilatory response to the square wave hypoxic input. However, the experimental data sometimes (but not always) show some asymmetry in the averaged ventilatory records, as shown in some plots in Fig. 5.2. To describe such an asymmetry, Medina-Alvarez (1993) explored an extended model by incorporating a non-linear rate-sensitive component into the simple model. The total ventilation in this modified model, is again expressed as a combination of a peripheral part and a central part, $\dot{V}_E = \dot{V}_P + \dot{V}_C$. However, in this case the peripheral part in this description arises as a combination of two components, one being a proportional component and another being a rate-sensitive component:

$$\dot{V}_E = \dot{V}_P + \dot{V}_C = \dot{V}_p + \dot{V}_r + \dot{V}_C \tag{5.7}$$

where $\dot{V}_p$ and $\dot{V}_r$ represent the proportional and the rate-sensitive components respectively, and the steady-state values for these components are given as:

$$\dot{V}_p = g_p \cdot Hyp \tag{5.8}$$

$$\dot{V}_r = g_r \cdot \frac{dHyp}{dt} \tag{5.9}$$

with the restriction that $\dot{V}_r \geq 0$. Assuming the two components share the same pure delay, the dynamics of these components can be written as:

$$d\dot{V}_p/dt = (1/T_p)(g_p \cdot Hyp(t - d_p) - \dot{V}_p) \tag{5.10}$$

$$d\dot{V}_{r_0}/dt = (1/T_r)(g_r \cdot dHyp(t - d_p)/dt - \dot{V}_{r_0}) \tag{5.11}$$

$$\dot{V}_r = max(\dot{V}_{r_0}, 0) \tag{5.12}$$

The parameters to be estimated in this form of dynamic model are thus the central ventilatory component $\dot{V}_C$, the peripheral gains $g_p$ and $g_r$, the time constants $T_p$

and $T_r$ for the proportional and the rate-sensitive components respectively, and the common pure delay for the two components $d_p$.

The difference equations for this model can be written as:

$$\begin{aligned}
(\dot{V}_p)_{n+1} &= g_p \cdot Hyp(t_n - d_p) \\
&\quad -(g_p \cdot Hyp(t_n - d_p) - (\dot{V}_p)_n)e^{-(t_{n+1}-t_n)/T_p} \qquad (5.13) \\
(\dot{V}_{ro})_{n+1} &= g_r \cdot \Delta Hyp(t_n - d_p) \\
&\quad -(g_r \cdot \Delta Hyp(t_n - d_p) - (\dot{V}_{ro})_n)e^{-(t_{n+1}-t_n)/T_r} \qquad (5.14) \\
(\dot{V}_r)_n &= max((\dot{V}_{r_0})_n, 0) \qquad (5.15) \\
(\dot{V}_E)_n &= (\dot{V}_C)_n + (\dot{V}_p)_n + (\dot{V}_r)_n \qquad (5.16)
\end{aligned}$$

### 5.2.4 Fitting procedures

After the drift had been estimated by a smoother and removed from the original data, two time-invariant dynamic models described in the previous session were examined. The data obtained during the first 12 min of the cyclic hypoxia were discarded before any model fitting was performed. Only the data for the remaining 18 min were used when the "oscillation" may be considered to have come close to a "steady state".

*Simple least-square parameter estimations.*

A simple least-squares fitting technique was employed by Clement and Robbins (1993*a*) and Medina-Alvarez (1993) in applying their models to the experimental data. With this technique, the objective function to be minimised is

$$J = \sum_{n=1}^{m} (j(n))^2 \qquad (5.17)$$

where

$$j(n) = \dot{V}_{E.meas}(n) - \dot{V}_{E.det}(n) \tag{5.18}$$

where $\dot{V}_{E.meas}$ denotes the measured value and $\dot{V}_{E.det}$ is the output of the deterministic dynamic model. In this study, this fitting procedure was initially used in order to examine the effects of incorporating a more complicated noise model (see below).

*Fitting deterministic models incorporating a noise structure.*

As demonstrated in our previous study (see chap.3), ventilatory variations in successive breaths during steady breathing are correlated, and the structure of this correlation can be modelled using a parallel noise process:

$$x(n+1) = fx(n) + v(n) \tag{5.19}$$

$$y(n) = x(n) + w(n) \tag{5.20}$$

where $x(n)$ and $y(n)$ are the system state and observation for the parallel noise component at the $n^{th}$ breath; $f$ is the system gain; and $v(n)$ and $w(n)$ are mutually independent white Gaussian noise processes with means of zero and a constant variance ratio of $R_v/R_w$. The model output ($\dot{V}_{E.out}$) for the ventilatory response to the stimulus can be written as the sum of the deterministic component ($\dot{V}_{E.det}$) and the stochastic component ($x$):

$$\dot{V}_{E.out}(n) = \dot{V}_{E.det}(n) + x(n) \tag{5.21}$$

In order to estimate the stochastic component $x(n)$, a Kalman filter algorithm was employed. The prediction and update values for the system state of the noise component were calculated as follows:

$$\hat{x}(n+1 \mid n) = f\hat{x}(n \mid n) \tag{5.22}$$

$$\hat{x}(n+1 \mid n+1) = \hat{x}(n+1 \mid n) + K(n+1)(y(n+1) - \hat{x}(n+1 \mid n)) \tag{5.23}$$

and the prediction and update of a modified variance are given by

$$P'(n+1 \mid n) = fP'(n \mid n)f + R_v/R_w \tag{5.24}$$

$$P'(n+1 \mid n+1) = (1-K(n+1))P'(n+1 \mid n)(1-K(n+1)) + K(n+1)K(n+1) \tag{5.25}$$

where

$$K(n+1) = P'(n+1 \mid n)[P'(n+1 \mid n)+1]^{-1} \tag{5.26}$$

is the Kalman gain at the $(n+1)^{th}$ breath.

The physiological parameters of the deterministic model along with the two parameters of the stochastic model $(f, R_v/R_w)$ can now be estimated by minimising the sum of the squared prediction errors of the model which is given by

$$J = \sum_{n=1}^{m} (j(n))^2 \tag{5.27}$$

where

$$j(n) = \dot{V}_{E.meas}(n) - (\dot{V}_{E.det}(n) + \hat{x}(n \mid n-1)) \tag{5.28}$$

where $\dot{V}_{E.meas}$ denotes the measured value. This was achieved using a standard Numerical Algorithms Group (NAG; Oxford, UK) subroutine (E04FDF) that finds an unconstrained minimum of a sum of squared residuals.

Data (experimental and model output) were interpolated every 1 sec after model fitting, and the average ventilatory responses were calculated for a single 30 sec hypoxic cycle to give an illustration of the fitting result.

### 5.2.5 Statistical analysis for the residuals

Statistical analysis was performed on the residuals sequences after model fitting to assess the adequacy of each model.

*Whiteness of residuals.*

A "portmanteau" test for examining whiteness was performed on residuals sequences obtained from model fittings to test if they were purely random (Box and Jenkins, 1976). The statistic was defined as

$$Q = n \sum_{k=1}^{K} \hat{\gamma}_k^2 \sim \chi_K^2 \tag{5.29}$$

where $n$ is the number of observations used to compute the likelihood; $\hat{\gamma}_k$ is the estimated autocorrelation value for the sequence of residuals with a lag of $k$; $K$ is an integer, the exact choice of which is arbitrary (it was selected as 10 in this study).

*Comparison of goodness of fit.*

Once the whiteness of the residuals had been checked, the improvement of the fit with the extended (rate-sensitive) model compared with the original simple model was assessed using an F-ratio test on the sum of squared prediction errors. The $F$ statistic is of the form

$$F = \frac{(RSS_1 - RSS_2)/(df_1 - df_2)}{RSS_2/df_2} \sim F(df_1 - df_2, df_2) \tag{5.30}$$

where $RSS_1$ and $df_1$ refer to the residual sum of squares and the degrees of freedom for the original model, and $RSS_2$ and $df_2$ refer to the residual sum of squares and the degrees of freedom for the extended model. Tests were conducted on a subject-by-subject basis, and so the sum of squares and degrees of freedom were accumulated across the individual repeats of the protocol and fits of the model on each individual subject.

*The distribution of large breaths.*

As observed in the experimental records, there are some occasional big breaths during the cyclic hypoxic breathing. Should these big breaths deviate from the

model predictions, then they will result in large residuals. To determine whether or not these big breaths occur during a certain phase of the stimulus cycle, we selected those big residuals which exceed 2 standard deviations and then analysed whether they are evenly distributed over the 30 sec of stimulus period. A $\chi^2$-test was chosen for this purpose:

$$\chi^2 = \sum_{i=1}^{n} \frac{(O_i - E)^2}{E} \sim \chi^2_{n-1} \tag{5.31}$$

where $O_i$ denotes the value for the observation of the $i^{th}$ segment and $E$ denotes the expected value. The value of $n$ was chosen as 5, resulting in the length of each segment being 6 sec. On the null hypothesis (the large breaths are evenly distributed), $\chi^2$ follows the $\chi^2_{n-1}$ distribution. This test was performed on the accumulated data from all the experimental data sets. The residuals sequences for the the total stochastic component (*i.e.* $\dot{V}_{E.meas} - \dot{V}_{E.det}$), as well as the prediction errors were examined for both the simple proportional model and the extended model.

## 5.3 Results

### 5.3.1 Smoothing

The original ventilatory data clearly show an irregular slow drift with time. Using a cubic spline smoother with the parameter *df* chosen to be 30, the ventilatory data over the time span of the 30 min of cyclic hypoxia were smoothed. Fig. 5.3 gives an example of smoothing. The cyclic hypoxic stimulus is plotted in the upper panel, while the smoother (middle dashed line, middle panel) and the 95% confidence intervals (dotted lines, middle panel) were plotted along with the original data. The variation in the smoother is much less changeable than the hypoxic input and the ventilatory output signals. The lower panel shows the ventilatory data after the drift has been removed.

### 5.3.2 Comparison between fitting techniques

Dynamic models were fitted to the ventilatory data after the slow drift had been removed. To avoid any transient responses during the first stage after the hypoxic stimulus had been introduced, the data collected during the first 12 min were discarded, and only the remaining data obtained during the later stage of 18 min were used.

Two different fitting techniques, the simple least-square fitting technique and the Kalman filter algorithm incorporating a parallel noise structure, were compared. After fitting the model to the data using a least-square technique, the residuals sequences mostly appeared to be correlated. When a parallel noise structure was incorporated into the model, using a Kalman Filter, the correlation within the residuals sequence could be mostly removed. These appearances were tested using a portmanteau test, as described in the Methods session. The comparison between the least-square fitting technique and the Kalman filter algorithm is made for the

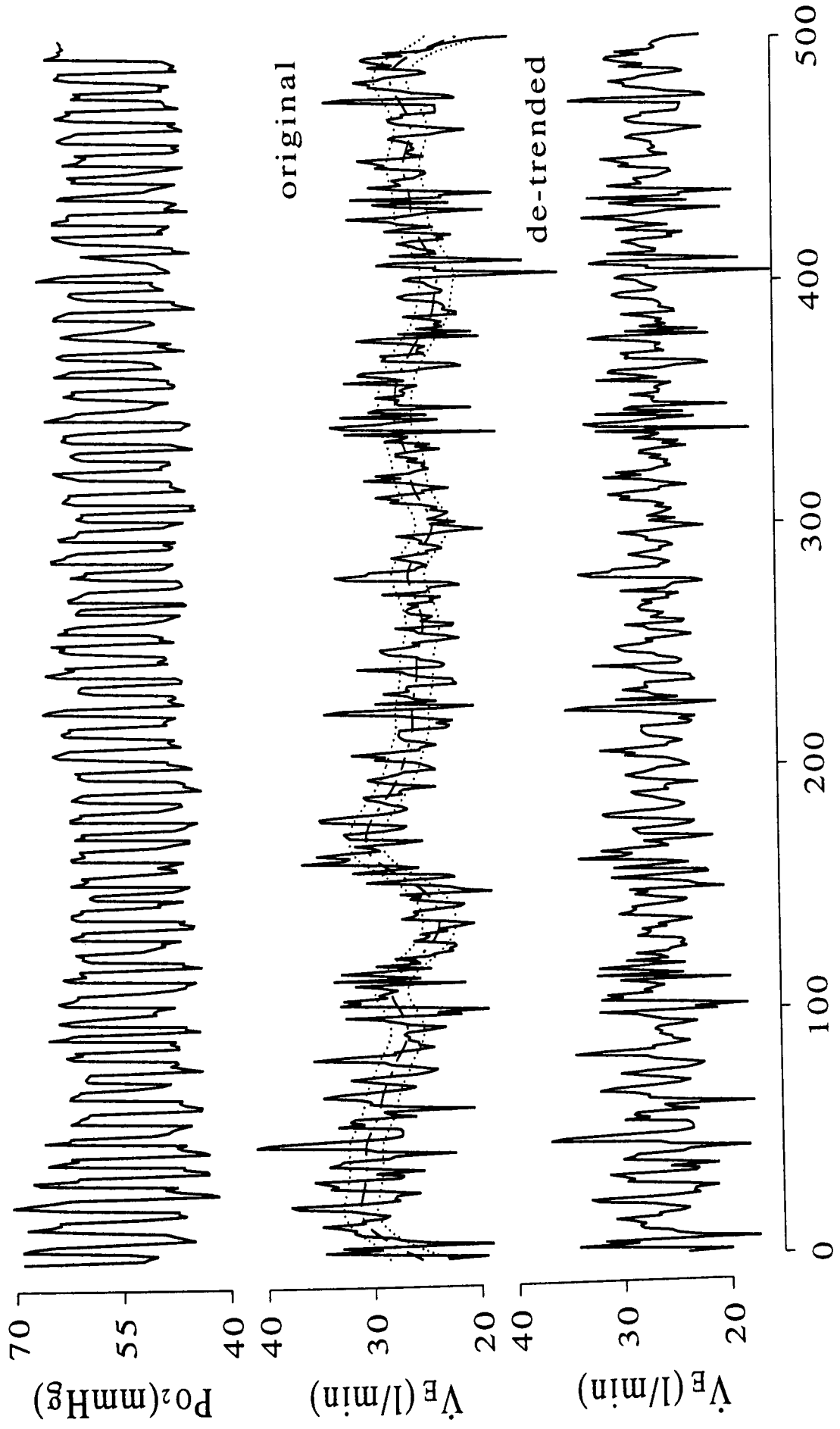


Figure 5.3: An example experimental record and corresponding smoothed data. Upper panel: hypoxic stimulus. Middle panel: original ventilatory record (solid line) and the smoother (dashed line for the smoother and dotted lines for the 95% confidence intervals). Lower panel: ventilatory data after the slow drift in the baseline has been removed.

simple proportional model. There were 5 out of 24 sets of residuals sequences which could be accepted as uncorrelated from the least-square fitting procedure, while for the Kalman filtering algorithm, there were 19 out of 24 sets of residuals sequences which could be accepted as uncorrelated. The average auto-correlation functions for the residuals for each subject for both fitting algorithms are plotted in Fig. 5.4, with 95% confidence intervals. The parameter values for this simple model (from both fitting algorithms) are listed in table 5.1. In general, there are no substantial deviations in the parameters estimated using the two different algorithms.

Table 5.1: Median parameter values for each subject for the proportional model, without and with incorporating the parallel noise structure.

| Subject | $\dot{V}_c$ l/min | $g_p$ l/min | $T_p$ sec | $T_d$ sec |
|---|---|---|---|---|
| 758 | 22.0 (21.9) | 46.6 (47.3) | 3.0 (3.0) | 5.4 (5.2) |
| 810 | 14.8 (14.8) | 50.0 (51.8) | 0.1 (3.1) | 5.6 (4.1) |
| 818 | 26.7 (26.7) | 52.2 (54.7) | 2.5 (2.6) | 5.6 (5.4) |
| 820 | 29.6 (29.4) | 46.3 (47.9) | 2.8 (2.8) | 5.4 (5.4) |
| 823 | 36.2 (36.0) | 48.3 (45.0) | 3.3 (3.1) | 6.2 (6.5) |

The values in brackets are the parameters estimated incorporating a noise structure, using a Kalman filter algorithm.

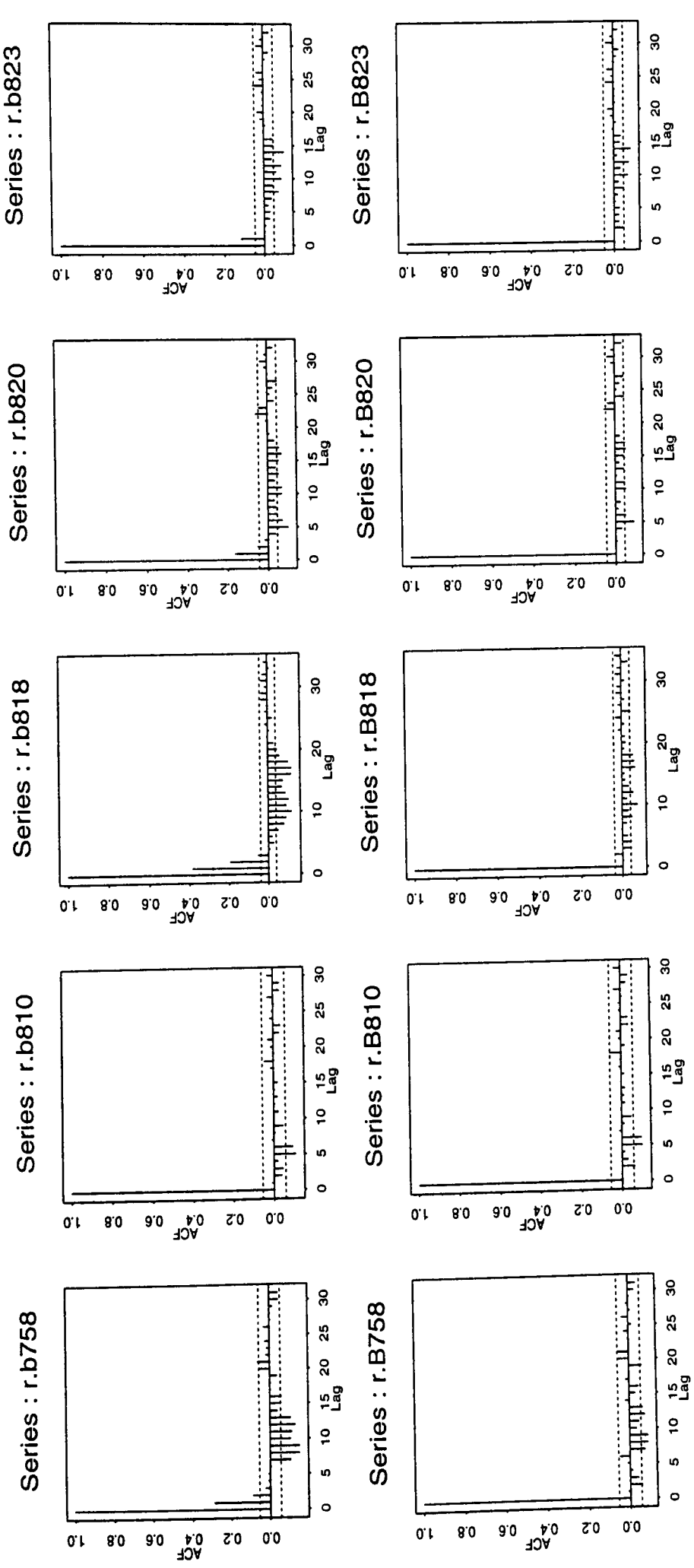


Figure 5.4: Auto-correlation functions for accumulated residuals from the simple proportional model for each subject. Upper panel: residuals from the least-square fitting procedure. Lower panel: prediction errors from the Kalman filter.

### 5.3.3 Comparison between Models

An example of the breath-by-breath data along with the output from the simple proportional model fitted with a parallel noise structure is shown in Fig. 5.5. The upper panel represents the cyclic hypoxia and the ventilatory data are shown in the lower panel (the dashed line represents the experimental observation and the solid line represents the deterministic part of the model). Due to the existence of the noise, it is difficult to judge by inspecting these plots how well the model describes the experimental data. However, a visual impression that these plots gave was that there are some large breaths occuring, which are not well described by the model. It is not clear whether or not these breaths are related (in any form) to the cyclic hypoxia.

To get a better picture of the deterministic response of the model, an alternative way of looking at the data is to average the data sequence across a single 30 sec period of the cyclic hypoxia. The averaged data, for both the experimental observations and the deterministic part of the simple proportional model, are illustrated in Fig. 5.6 for each individual subject. The upper panel represents the cyclic hypoxic input, the lower panel represents the peripheral response $\dot{V}_P$ (dashed lines represent experimental results and solid lines represent the model output).

Generally, the model gives a reasonable description of the data. However, the asymmetry of the ventilatory response and the "peakiness" that Clement and Robbins observed can be seen clearly for subjects 758, 810 and 823. This is not fully described by the model. In these subjects, the data show a large deviation from the model prediction at around 12-18 sec into the cycle.

A non-linear rate-sensitive component which only responds to the step into hypoxia, as described in the Methods session, was incorporated into the original model, in order to determine whether such a model could give a better description of the

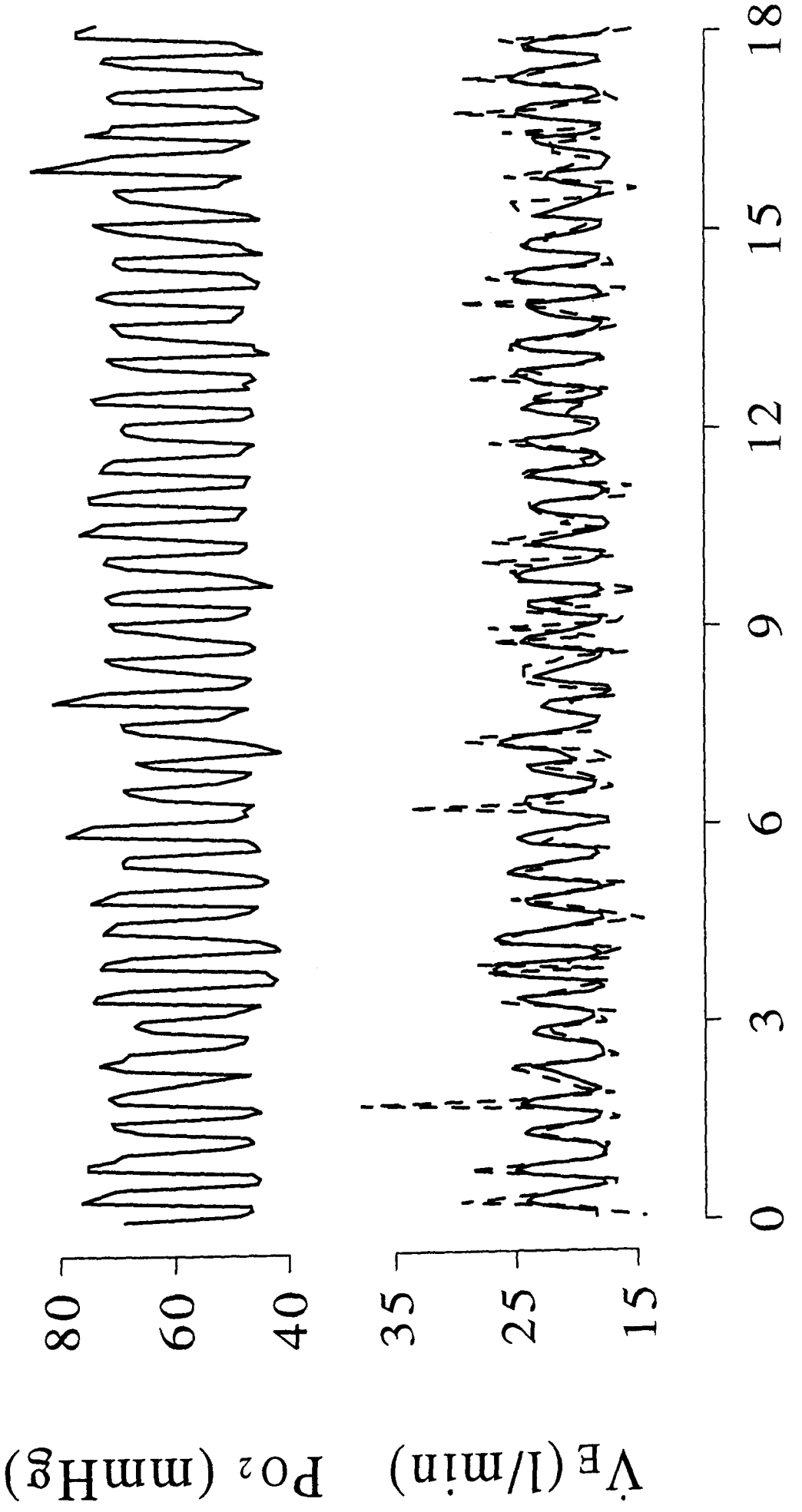


Figure 5.5: An example of the fitting result for the simple model. The upper panel represents the hypoxic input; the lower panel represents the ventilatory response (dashed line for experimental record, solid line for the deterministic part of the model output).

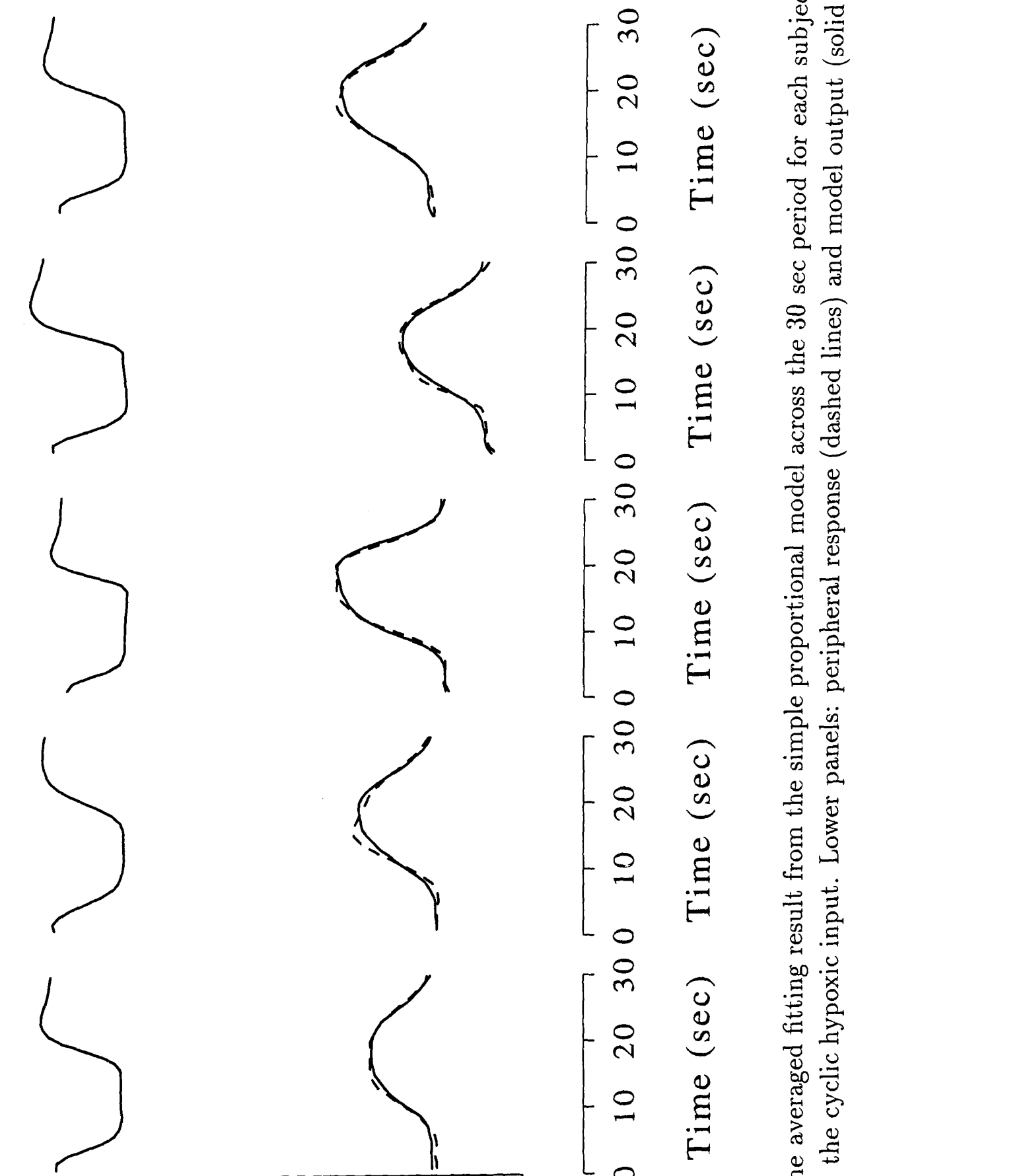


Figure 5.6: The averaged fitting result from the simple proportional model across the 30 sec period for each subject. Upper panels: the cyclic hypoxic input. Lower panels: peripheral response (dashed lines) and model output (solid lines).

data. This extended model, incorporating a parallel noise structure, was fitted using a Kalman filter algorithm. One example of breath-to-breath data from this extended model is plotted in Fig. 5.7. The upper panel shows the results from the simple model and the lower panel shows the results from the extended model. The dashed lines and the solid lines represent the experimental data and the model output from the deterministic parts respectively. This gives an illustration that the large breaths still do not appear to be modelled well by the rate-sensitive model.

A comparison of the two models based on the averaged peripheral response is shown in Fig. 5.8. The upper panels show the fitting results from the simple model and the lower panels show the fitting results from the extended model. Averaged ventilatory data are shown by dashed lines and the model outputs from the deterministic parts for both models are shown by solid lines. For subject 810, the extended model appears to have some improved the fit, while for the other subjects, any improvement in fit is not particularly apparent from these plots.

The estimated parameter values for both models are listed in table 5.2 as median values for each subject. The parameters of the proportional component changed little after adding in the rate-sensitive component. The parameters values for the rate-sensitive component show considerable variation between individuals.

### 5.3.4 Statistical analysis

For further comparison between the two models, statistical analyses were performed to examine whether the extended model yields a better description of the experimental data.

*Whiteness test.*

A whiteness test was first applied on the prediction errors from both models (fitted with a Kalman filter), before any comparisons between these errors were

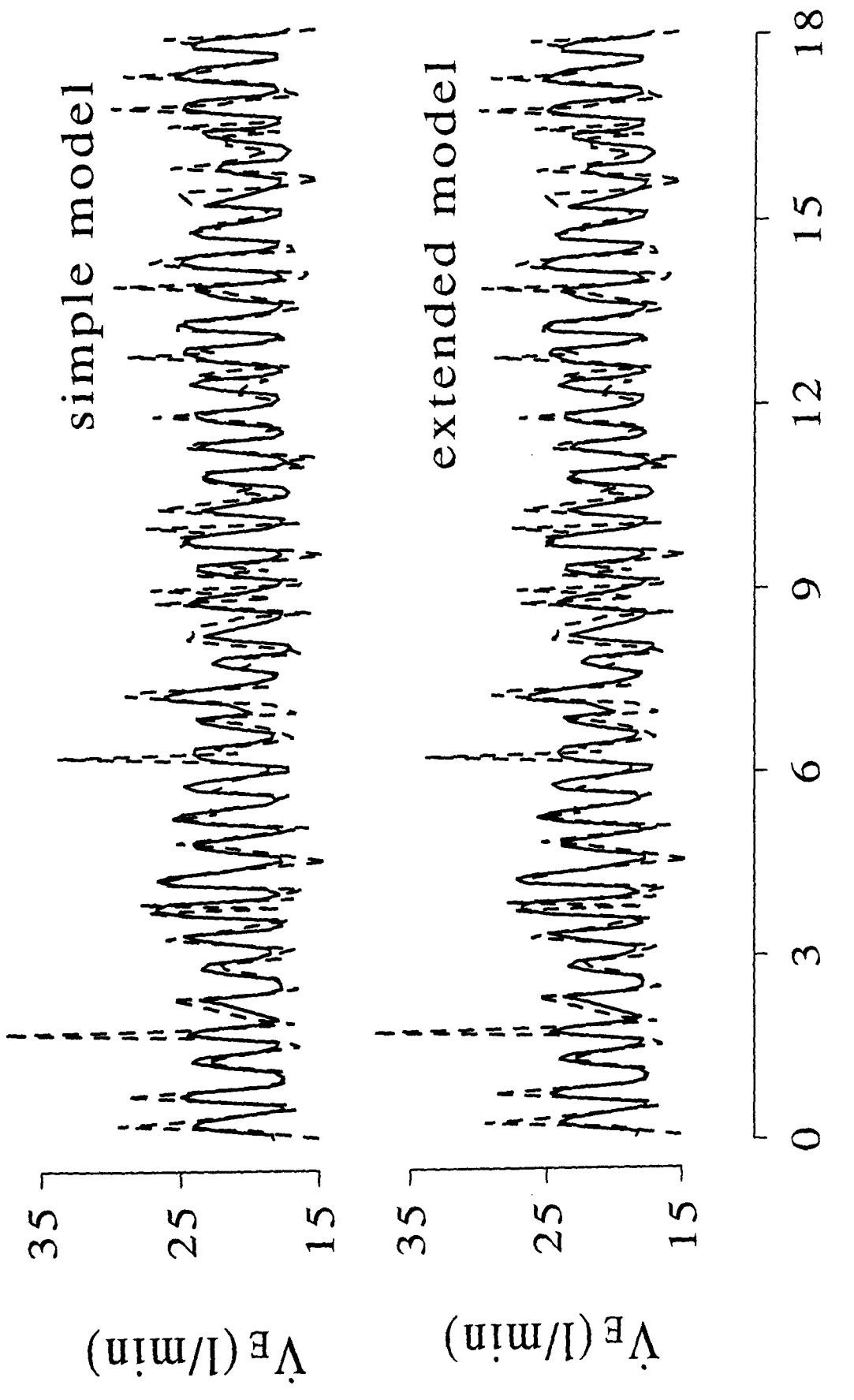


Figure 5.7: A comparison between the two models made on a single set of data. Upper panel: the result from the simple model. Lower panel: the result from the extended model. The dashed lines are for the experimental data and the solid lines are for the deterministic part of the model outputs.

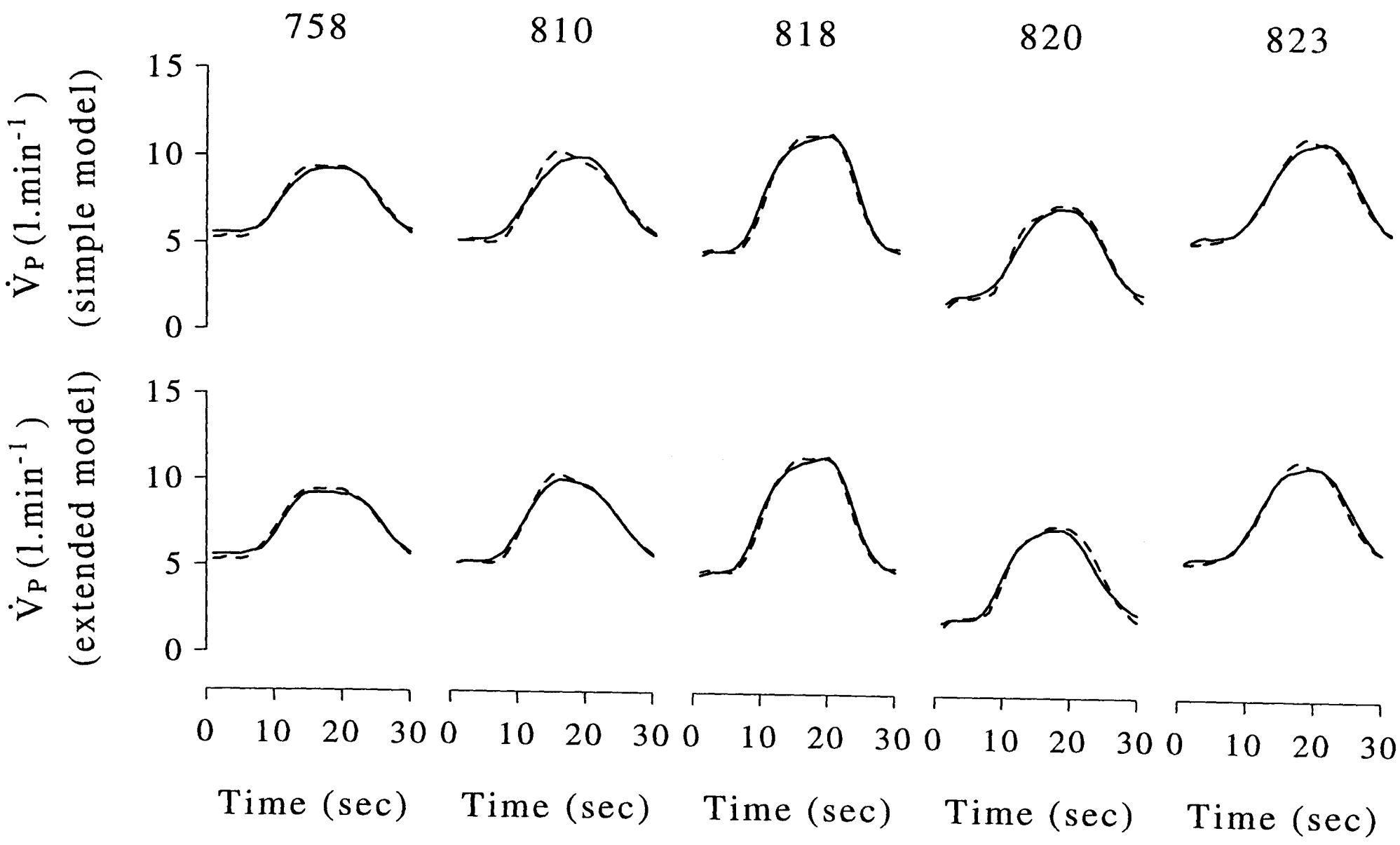


Figure 5.8: The comparison between the two models for the averaged peripheral response across the 30 sec period for each subject. Upper panels: the result from the simple model; lower panels: the result from the extended model. The dashed lines are for the experimental data and the solid lines are for the deterministic part of the model outputs.

Table 5.2: Median parameter values for each subject for the proportional model and for the extended model. The estimates were made incorporating the parallel noise structure.

| | Subject | $\dot{V}_c$ l/min | $g_p$ l/min | $T_p$ sec | $g_r$ l/min | $T_r$ sec | $d_p$ sec |
|---|---|---|---|---|---|---|---|
| *Original* | 758 | 21.9 | 47.3 | 3.0 | | | 5.2 |
| *model* | 810 | 14.8 | 51.8 | 3.1 | | | 4.1 |
| | 818 | 26.7 | 54.7 | 2.6 | | | 5.4 |
| | 820 | 29.4 | 47.9 | 2.8 | | | 5.4 |
| | 823 | 36.0 | 45.0 | 3.1 | | | 6.5 |
| *Extended* | 758 | 21.9 | 46.0 | 4.0 | 124.4 | 134.9 | 5.3 |
| *model* | 810 | 15.7 | 35.8 | 3.5 | 189.4 | 9.6 | 4.2 |
| | 818 | 26.7 | 52.9 | 2.6 | 0.1 | 3.2 | 5.4 |
| | 820 | 29.4 | 48.6 | 2.9 | 144.3 | 23.9 | 6.0 |
| | 823 | 36.1 | 38.9 | 3.9 | 75.0 | 7.9 | 6.6 |

made. The results show that 19 out of 24 of the prediction errors from the simple model, and 20 out of 24 of the ones from the extended model can be accepted as uncorrelated.

*F-ratio test.*

Since the prediction errors are essentially uncorrelated, an F-ratio test (requires uncorrelated residuals) can be performed on the squared prediction error from the Kalman filter to judge if the model output was substantially improved by adding in the extra component. The results show that for the two subjects (810 and 820) with the largest values for $g_r$, the extended model yields significantly better results than the original model. For the other three subjects, there is no significant improvement in the fit.

*$\chi^2$-test on the distribution of the large breaths.*

The ventilatory behaviour during cyclic hypoxia includes some occasional big breaths. To examine if these big breaths are related to the input function, a $\chi^2$-test was performed on the relative residuals (the ratio of the residual to the model predicted value) sequences for both the deterministic component of the model only and for the prediction errors from the Kalman filter, for both models.

The analysis was done on the accumulated data across all the experiments. The 30 sec duration of the input cycle was divided into 5 segments, with each segment being of 6 sec duration. The number of the large relative residuals that exceeded $2\sigma$ which occured in each of the 6 sec periods is listed in table 5.3. In general, the large relative residuals occur most frequently during period 3, which corresponds to the late part of the response to the onset of the hypoxic stimulus. This was significant at $P<0.05$ from the $\chi^2$-test for the residuals from the deterministic part of the models. However, for the prediction errors from the Kalman filter, the large

relative residuals can all be accepted as evenly distributed for both models, although the largest number remains in period 3.

Table 5.3: The distribution of large relative residuals exceeding $2\sigma$ for the deterministic component of the model and for the prediction errors. The results of $\chi^2$-tests are also shown.

| Model | 0-5s | 6-11s | 12-17s | 18-23s | 24-29s | total | P |
|---|---|---|---|---|---|---|---|
| Original (deter. part) | 49 | 44 | 62 | 28 | 42 | 225 | $< 0.05$ |
| Extended (deter. part) | 45 | 44 | 61 | 31 | 42 | 223 | $< 0.05$ |
| Original (pred. error) | 43 | 40 | 54 | 37 | 39 | 231 | $> 0.05$ |
| Extended (pred. error) | 45 | 41 | 48 | 42 | 35 | 211 | $> 0.05$ |

These results suggest that the occasional big breaths occur most frequently during a certain period of the input cycle, in a way which cannot be described by the deterministic part of either model. These large breaths can to some extent be described by the noise model.

## 5.4 Discussion

### 5.4.1 Nature of the experimental data

*Smoothing of the ventilatory data.*

As illustrated in Fig. 5.1, although the change in end-tidal $P_{O_2}$ shows little drift along time, the ventilatory data collected during cyclic hypoxia show a substantial drift in an irregular form. This drift is considerably slower than the periodic response to the hypoxic stimulus. Such an irregular baseline drift was not observed during steady-state breathing as studied in the previous chapters. However, the drift in this slow irregular form was consistently observed during the ventilatory response to cyclic acute hypoxia. Although the mechanism causing such a drift is not clear, its existence may affect the estimation of the model parameters during mathematical model fitting. A cubic spline smoother was thus applied to remove the drift in the ventilatory data. To avoid destroying the periodic response to the hypoxic stimulus, the parameter *df* of the smoother was empirically chosen at a value which equals half of the numbers of the cycles in the data set. As shown in Fig. 5.3, the baseline drift was effectively removed. Although to some extent a deformation in the data sequence might be caused by employing such an additive model, the major benefit of performing such a smoothing is that it yields a "steadier" data sequence, more appropriate to fitting a time-invariate model, and less likely to result in bias in the parameter estimates.

*Selection of data to be analysed.*

As described in the methods session, the data during the first 12 min of the cyclic hypoxic stimulus were discarded and only the data collected during the remaining 18 min were used for model fitting. The purpose of this was to allow time for development of hypoxic ventilatory decline before any data were used for analysis.

From the previous study of Chap. 4, median values of the time constants for the two possible mechanisms of HVD were estimated as 361 sec for the chemoreflex loop dependent component and as 232 sec for the chemoreflex loop independent component. Comparing the time duration of 12 min (720 sec) with the longer time constant (361 sec), it can be calculated that the development of this component of HVD will be 86% complete.

### 5.4.2 Model fitting technique and goodness of fit

Since the stochastic variations in ventilation are intrinsically correlated, one benefit of using cyclic stimuli to study the ventilatory response to acute hypoxia is that the effect of the noise is reduced by "averaging" the data across the repeated cycles. Such "averaging" was efficient in reducing the effect of noise, and was used by Clement and Robbins (1993*a*) to make a comparison of the goodness of fit between the different models by inspecting the averaged data. However, without describing the existing noise structure properly, simply fitting the deterministic model using a least-square fitting technique might cause some bias in the estimates for the parameters of the deterministic model. Statistical comparisons between models are also hard to make due to the existence of correlation in the residuals sequences. A parallel noise structure, as suggested by a previous study (see Chap.3), was used in this chapter to describe the correlation in ventilatory variations. Using a Kalman filter algorithm, the parameters of both the deterministic part and the stochastic part of the model can be estimated. The advantages of this algorithm are that: 1) any bias in the parameter estimates should be removed (provided that the bias is caused by the noise processes within the system); and 2) by providing white residuals, it allows for the goodness of fit between the different models to be compared more rigourously than if correlation is present.

### 5.4.3 Validity of the models and the physiological explanations

*The proportional model.*

A simple first order dynamic model has been used to describe the peripheral compartment of the ventilatory response to a change in $CO_2$ (Swanson and Bellville, 1975; Bellville *et al*, 1979). Since during acute hypoxia, only the peripheral chemoreflex loop is involved, this first order model was employed in studies of the ventilatory response to cyclic hypoxia. Robbins (1984) used a similar structure to predict the ventilatory response to sinusoidal hypoxia and found that it was not fully satisfactory, and that features additional to those included in the model would be required to describe the ventilatory response in full. Using a least-square fitting technique, the first order proportional model was further examined by Clement and Robbins (1993*a*), by fitting it to the ventilatory data collected during square-wave hypoxia. As reported by the authors, this simple model failed describe the asymmetry at the on- and off-transient of the ventilatory response to hypoxia.

This model was examined more carefully in this study, in the sense that it was fitted to the data after the slow baseline drift had been removed and using a model of the noise structure implemented via a Kalman filter algorithm. The main result repeats that of Clement and Robbins (1993*a*), confirming that the deterministic part of the model can not adequately predict the asymmetry shown in the averaged data.

The parameter values for the simple model were estimated in this study using both simple least-square approach and a Kalman filter algorithm. Generally, the parameter values with both approaches lay in similar range to those reported by Clement and Robbins (1993*a*). This suggests that neither the variations in baseline ventilation nor the fitting technique had much effect on the parameter values. However, in comparison with the previous study modelling the ventilatory response to sustained hypoxia (Chap. 4), there are some marked differences observed in the

parameter values. In particular, the value of the central component $\dot{V}_C$ appears higher from this study than that from the results of Chap. 4 (median value of 26.7 l/min *v.s.* 13.6 l/min); and the value of the time constant for the peripheral component appears shorter in this study (median value of 3.0 sec *vs.* median values of 14.0 and 4.5 sec for the on- and off-transients respectively). The higher value for $\dot{V}_C$ in this study(like the baseline variability) is hard to explain, particularly since the end-tidal $P_{CO_2}$ was only raised slightly (around 2 Torr above eucapnia) in both studies. The differences in time constants, depending upon frequency of stimulation, has been commented on before by Clement and Robbins (1993*a*). The large values of the time constants for the sustained hypoxia are in keeping with the presence of a second slower component to the peripheral chemoreflex response, which has been reported in anaesthetised cats by Berkenbosch *et al.* (1991*b*).

*The rate-sensitive model.*

The main imperfection of the proportional model was that it failed to describe the asymmetry in the ventilatory response to cyclic hypoxia, which implies that some other mechanisms in addition to a linear component should be investigated. In a previous study, Black *et al.* (1971) showed that a sudden change of hypoxic stimuli can cause an overshoot in the response of the carotid sinus nerve, while the sinus nerve discharge displayed a decline without undershoot on the removal of the stimulus. This suggests that a rate-sensitive component which only responds at the step into hypoxia might underlie the asymmetry. This suggestion has been made previously by Robbins (1984) and Clement and Robbins (1993*a*), but in neither study was such a model fit to the data. Such an extended model was explored briefly by Medina-Alvarez (1993), using a least-square technique, on the data collected from one of the subjects (810). The results suggested that the extended model improved the fit to the asymmetry in the data. However, with residuals which were highly

correlated, it was difficult to perform a proper statistical analysis.

In this study, the introduction of the rate-sensitive component into the model does not change the value of the parameters relating to the proportional component very much. The parameter values obtained for the rate-sensitive component show considerable variation between the subjects.

The F-ratio test suggests that this extended model yields a better fit to the data for only two out of the five subjects. Inspection of Fig. 5.8 suggests that there may be some improvement in describing the asymmetry, but the peakiness of the data is still detectable. Inspection of the data and model fit before averaging, together with the results of the $\chi^2$-test for large breaths, suggests that the peakiness may arise from large breaths not related in a simple way to either the proportional or the differential response to the input.

### 5.4.4 Large breaths and alternative models

The results from this study showed that neither a simple proportional model nor an extended model is adequate in describing the ventilatory response to cyclic acute hypoxia. The particular feature that remains to be explored is the occurrence of large breaths within a certain part of the hypoxic cycle, and these may in fact induce the peakiness in the averaged response that has not been described fully by either model. One possibility is that the large breaths are associated with a specific phase relationship between the onset of the hypoxic stimulus at the carotid body and the on-going respiratory cycle. In work carried out on responses to sudden chemical changes at the carotid body, Black and Torrance (1967) demonstrated that the effect on respiration depends on the phase of respiration at which the chemical change occurs. Thus, to predict the ventilatory response during cyclic hypoxia, a dynamic model with time-varying parameters might be required.

Alternatively, it might be that these large breaths are related to the "normal"

large breaths that can be seen during steady breathing in humans (Patil *et al.*, 1990). It could be that the probability of these occurring varies with the hypoxic drive, and in this case some stochastic model with a varying probability (dependent on input function) for the occurrence of large breaths is required.

# Chapter 6

# References

夫唯不盈　故能敝而成新

老子・十五

## References

1. Ackerson, L. M., R. H. Jones, and E. N. Bruce. Adaptive multivariate autoregressive modelling of respiratory cycle variables. In: *Respiratory Control – A Modeling Perspective,* New York: Plenum, pp. 309-316, 1989.

2. Anderson, B. D. O., and J. B. Moore. Optimal Filtering. Englewood Cliffs: Prentice-hall, Inc., 1979.

3. Andronikou, S., M. Shirahata, A. Mokashi and S. Lahiri. Carotid body chemoreceptor and ventilatory responses to sustained hypoxia and hypercapnia in the cat. *Respir. Physiol.* 72:361-374, 1988.

4. Armitage, P., and G. Berry. Statistical methods in medical research (Second Edition). Oxford: Blackwell Scientific Publications, pp. 194-196, 1987.

5. Asmussen, E., and M. Nielsen. Ventilatory response to $CO_2$ during work at normal and at low oxygen tensions. *Acta Physiol. Scand.* 39:27-35, 1957.

6. Bascom, D.A., I.D. Clement, D.A. Cunningham, R. Painter and P.A. Robbins. Changes in peripheral chemoreflex sensitivity during sustained, isocapnic hypoxia. *Respir. Physiol.* 82:161-176, 1990.

7. Bascom, D.A. Some Factors Affecting Respiration in Man. *D.Phil. Thesis.* University of Oxford. 1991.

8. Bascom, D.A., J.J. Pandit, I.D. Clement and P.A. Robbins. Effects of different levels of end-tidal $P_{O_2}$ on ventilation during isocapnia in humans. *Respir. Physiol.* 88:299-311, 1992.

9. Bellville, J.W., B.J. Whipp, R.D. Kaufman, G.D. Swanson, K.A. Aqleh and D.M. Wiberg. Central and peripheral chemoreflex loop gain in normal and carotid body-resected subjects. *J. Appl. Physiol.* 46:843-853, 1979.

10. Bellville, J. W., D. S. Ward, and D. Wiberg. Respiratory system: modelling and identification. In: *System & control encyclopaedia.* Oxford: Pergamon Press, pp. 4055-4062, 1988.

11. Benchetrit, G., and T. Pham Dinh. Analyse d'une étude statistique de la ventilation cycle par cycle chez l'homme au repos. *Biométrie Humaine.* 8:7-19, 1973.

12. Benchetrit, G., and F. Bertrand. A short-term memory in the respiratory centres: statistical analysis. *Respir. Physiol.* 23:147-158, 1975.

13. Berkenbosch, A. and J. DeGoede. Actions and interactions of $CO_2$ and $O_2$ on central and peripheral chemoreceptive structures. In: *Neurobiology of the Control of Breathing.* New York: Raven, pp. 9-17, 1986.

14. Berkenbosch, A., C.N. Olievier J. DeGoede and E.W. Kruyt. Effect on ventilation of papaverine administered to the brain stem of the anaesthetised cat. *J. Physiol. (London)* 443:457-468, 1991*a*.

15. Berkenbosch, A., J. DeGoede, D.S. Ward, C.N. Olievier and J. Van Hartevelt. Dynamic response of the peripheral chemoreflex loop to changes in end-tidal $O_2$. *J. Appl. Physiol.* 71:1123-1128, 1991*b*.

16. Black, A.M.S. and R.W. Torrance. Chemoreceptor effects in the respiratory cycle. *J. Physiol. (London)* 189:59-61P, 1967.

17. Black, A.M.S., D.I. McCloskey and R.W. Torrance. The responses of carotid body chemoreceptors in the cat to sudden changes of hypercapnic and hypoxic stimuli. *Respir. Physiol.* 13:36-49, 1971.

18. Boetger Mann, C., K.A. Aqleh and D.S. Ward. Asymmetry in the ventilatory response to a bout of hypoxia in human beings. In: *Respiratory Control.* Plenum Publishing Co. New York, pp. 217-223, 1989.

19. Bolton, D.P.G., and J. Marsh. Analysis and interpretation of turning points and run lengths in breath-by-breath ventilatory variables. *J. Physiol. (London)* 351:451-459, 1984.

20. Box, G. E. P., and G. M. Jenkins. Time Series Analysis – Forecasting and Control (Revised Edition), San Francisco: Holden-Day, pp. 290-293, 1976.

21. Chambers, J. M., W. S. Cleveland, B. Kleiner, and P. A. Tukey. Graphical Methods for Data Analysis. Belmont, California: Wadsworth, pp. 191-238, 1983.

22. Cherniack, N.S. Sleep apnea and its cause. *J. Clin. Invest.* 73:1501-1506, 1984.

23. Clement, I.D. Some Factors Affecting Respiration in Man. *D.Phil. Thesis.* University of Oxford. 1992.

24. Clement, I.D. and P.A. Robbins. Dynamics of the ventilatory response to hypoxia in humans. *Respir. Physiol.* 92:253-275, 1993*a*.

25. Clement, I.D. and P.A. Robbins. Latency of the ventilatory chemoreflex response to hypoxia in humans. *Respir. Physiol.* 92:277-287, 1993*b*.

26. Cummin, A.R.C., J. Alison, M.S. Jacobi, V.I. Iyawe and K.B. Saunders. Ventilatory sensitivity to inhaled carbon dioxide around the control point during exercise. *Clin. Sci.* 71:17-22, 1986.

27. Cunningham, D.J.C., D. Spurr and B.B. Lloyd. The drive to ventilation from arterial chemoreceptors in hypoxic exercise. In: *Arterial Chemoreceptors.* Blackwell Scientific Publication, Oxford. pp. 301-323, 1968.

28. Cunningham, D. J. C., P. A. Robbins and C. B. Wolff. Interaction of respiratory responses to changes in alveolar partial pressures of $CO_2$ and $O_2$ and in arterial $pH$. In: *Handbook of Physiology – the Respiratory System II.* American Physiological Society, pp. 475-528, 1986.

29. Dahan, A., I. C. W. Olievier, A Berkenbosch, and J. DeGoede. Modelling the dynamic ventilatory response to carbon dioxide in healthy human subjects during normoxia. In: *Respiratory Control – A Modeling Perspective.* New York: Plenum, pp. 265-273, 1989.

30. Dahan, A., J. DeGoede, A Berkenbosch and I.C.W. Olievier. The influence of oxygen on the ventilatory response to carbon dioxide in man. *J. Physiol. (London)* 428:485-499, 1990.

31. DeGoede, J., N. van der Hoeven, A. Berkenbosch, C.N. Olievier and J.H.G.M. van Beek. Ventilatory responses to sudden isocapnic changes in end-tidal $O_2$ in cats. In: *Modelling and Control of Breathing.* Elsevier Science Publishing Co. Inc. Amsterdam, pp. 37-45, 1983.

32. DeGoede, J., and A. Berkenbosch. Dynamic end-tidal forcing technique: modelling the ventilatory response to carbon dioxide. In: *Modelling And Parameter Estimation in Respiratory Control.* New York: Plenum, pp. 59-69, 1989.

33. Easton, P.A., L.J. Slykerman and N.R. Anthonisen. Ventilatory response to sustained hypoxia in normal adults. *J. Appl. Physiol.* 61:906-911, 1986.

34. Easton, P.A., L.J. Slykerman and N.R. Anthonisen. Recovery of the ventilatory response to hypoxia in normal adults. *J. Appl. Physiol.* 64:521-528, 1988*a*.

35. Easton, P.A., and N.R. Anthonisen. Carbon dioxide effects on the ventilatory response to sustained hypoxia. *J. Appl. Physiol.* 64: 1451-1456, 1988*b*.

36. Edelman, N.H., P.E. Epstein, S. Lahiri and N.S. Cherniack. Ventilatory responses to transient hypoxia and hypercapnia in man. *Respir. Physiol.* 17:302-314, 1973.

37. Fitzgerald, R.S. and S. Lahiri. Reflex responses to chemoreceptor stimulation. In: *Handbook of Physiology: Sec. 3, Vol. II, Part I.* pp. 313-362, 1986.

38. Gallman, E.A. and D.E. Millhorn. Two long-lasting central respiratory responses following acute hypoxia in glomectomized cats. *J. Physiol. (London)* 395:333-347, 1988.

39. Gardner, W.N. The pattern of breathing following step changes of alveolar partial pressures of carbon dioxide and oxygen in man. *J. Physiol. (London)* 300:55-73, 1980.

40. Georgopoulos, D., S. Walker and N.R. Anthonisen. Increased chemoreceptor output and ventilatory response to sustained hypoxia. *J. Appl. Physiol.* 67:1157-1163, 1989.

41. Haldane, J.S., and J.G. Priestley. The regulation of the lung-ventilation. *J. Physiol. (London)* 32:225-266, 1905.

42. Haldane, J.S., J.C. Meakins and J.G. Priestley. The respiratory response to anoxaemia. *J. Physiol. (London)* 52:420-432, 1919.

43. Harvey, A. C. Forecasting, Structural Time Series Models and the Kalman Filter. Cambridge: Cambridge University Press, 1989.

44. Hastie, T.J., and R.J. Tibshirani. Generalized Additive Models. Chapman & Hall, 1990.

45. Holtby, S.G., D.J. Berezabsky and A.N. Anthonisen. Effect of 100% $O_2$ on hypoxic eucapnoic ventilation. *J. Appl. Physiol.* 65:1157-1162, 1988.

46. Howse, B.P.A., M.E. McIntyre and P.A. Robbins. Modifications to a cycle ergometer for studying the transition from rest to exercise in man. *J. Physiol. (London)* 417:7P, 1989.

47. Howson, M.G., S. Khamnei, D.F. O'Connor and P.A. Robbins. The properties of a turbine device for measuring respiratory volumes in man. *J. Physiol. (London)* 382:12P, 1986.

48. Howson, M.G., S. Khamnei, M.E. McIntyre, D.F. O'Connor and P.A.Robbins A rapid computer-controlled binary gas-mixing system for studies in respiratory control. *J. Physiol. (London)* 394:7P, 1987.

49. Jacob, G. Physiological Studies of Breathing. *M.Sc. Dissertation.* University of Oxford. 1995.

50. Jain, S.K., S. Subramanian, D.B. Julka and A. Guz. Search for evidence of lung chemoreflexes in man: study of respiratory and circulatory effects of phenyldiguanide and lobeline. *Clin. Sci.* 42:163-177, 1972.

51. Jensen J.I. An Analysis of Breath-to-Breath Variability in Steady-States of Breathing in Man. *Ph.D. Thesis.* Aarhus Universitet. Aarhus. Denmark. 1987.

52. Kagawa, S., M.J. Stafford, T.B. Waggener and J.W. Severinghaus. No effect of naloxone on hypoxia-induced ventilatory depression in adults. *J. Appl. Physiol.* 52:1030-1034, 1982.

53. Kay, J.D.S., E.S. Petersen and H. Vejby-Christensen. Mean and breath-by-breath pattern of breathing in man during steady-state exercise. *J. Physiol.* 251:657-669, 1975.

54. Kendall, M. G., and A. Stuart. The Advanced Theory of Statistics (Third Edition). London: Charles Griffin, 1969.

55. Khamnei, S. Some Factors Affecting Respiration in Man. *D.Phil. Thesis.* University of Oxford. 1990.

56. Khamnei, S. and P.A. Robbins. Hypoxic depression of ventilation in humans: alternative models for the chemoreflexes. *Respir. Physiol.* 81:117-134, 1990.

57. Khatib, M.F., Y. Oku and E.N. Bruce. Contribution of chemical feedback loops to breath-to-breath variability of tidal volume. *J. Appl. Physiol.* 83:115-128, 1991.

58. Kronenberg, R., F.N. Hamilton, R. Gabel, R. Hickey, D.J.C. Read and H. Severinghaus. Comparison of three methods for quantitating respiratory response to hypoxia in man. *Respir. Physiol.* 16:109-125, 1972.

59. Lahiri, S. Depressant effect of acute and chronic hypoxia on ventilation. In: *Morphology and Mechanisms of Chemoreceptors.* Nanchetan Press Ltd. pp.

138-146, 1976.

60. Lee, L.-Y. and H. Milhorn. Central ventilatory responses to $O_2$ and $CO_2$ at three levels of carotid chemoreceptor stimulation. *Respir. Physiol.* 25:319-333, 1975.

61. Lenfant, C. Time-dependent variations of pulmonary gas exchange in normal man at rest. *J. Appl. Physiol.* 22:675-684, 1967.

62. Li, K., J. Ponte and C.L. Sadler. Carotid body chemoreceptor response to prolonged hypoxia in the rabbit: effects of domperidon and propranolol. *J. Physiol.* 430:1-11, 1990.

63. Ljung, L. System Identification – Theory for the User. Englewood Cliffs: Prentice-Hall, Inc., 1987.

64. Lloyd, B.B., M.G.M. Jukes and D.J.C. Cunningham. The relation between alveolar oxygen pressure and the respiratory response to carbon dioxide in man. *Quart. J. Exp. Physiol.* 43:214-227, 1958.

65. Long, W.Q., G.G. Giesbrecht and N.R. Anthonisen. Ventilatory response to moderate hypoxia in awake chemodenervated cats. *J. Appl. Physiol.* 74:805-810, 1993.

66. Long, W., D. Lobchuk and N.R. Anthonisen. Ventilatory response to $CO_2$ and hypoxia after sustained hypoxia in awake cats. *J. Appl. Physiol.* 76:2262-2266, 1994.

67. Lugliani, R., B.J.Whipp, C. Seard, and K. Wasserman. Effect of bilateral carotid-body resection on ventilatory control at rest and during exercise in man. *New Engl. J. Med.* 285:1105-1111, 1971.

68. Macfarlane, D.J. Some Factors Affecting Breathing in Man. *D.Phil. Thesis.* University of Oxford. 1985

69. Masson, R.G. and S. Lahiri. Chemical control of ventilation during hypoxic exercise. *Respir. Physiol.* 22:241-262, 1974.

70. Medina-Alvarez, R. Nonlinear Modelling on Respiratory System Data. *M.Sc. Dissertation.* University of Oxford. 1993.

71. Miescher-Rüsch, F. Bemerkungen zur Lehre von den Athembewegungen. *Archiv f. Anat. u. Physiol.* 6:355-379, 1885.

72. Miller, J.P., D.J.C. Cunningham, B.B. Lloyd and J.M. Young. The transient respiratory effects in man of sudden changes in alveolar $CO_2$ in hypoxia and in high oxygen. *Respir. Physiol.* 20:17-31, 1974.

73. Millhorn, D.E., F.L. Eldridge, J.S. Kiley and T.G. Waldrop. Prolonged inhibition of respiration following acute hypoxia in glomectomized cats. *Respir. Physiol.* 57:331-340, 1984.

74. Modarreszadeh, M., E.N. Bruce and B. Gothe. Nonrandom variability in respiratory cycle parameters of humans during stage 2 sleep. *J. Appl. Physiol.* 69:630-639, 1990.

75. Morrill, C.G., J.R. Meyer and J.V. Weil. Hypoxic ventilatory depression in dogs. *J. Appl. Physiol.* 38:143-146, 1975.

76. Neubauer, J.A., T.V. Santiago, M.A. Posner and N.H. Edelman. Ventral medullary pH and ventilatory responses to hyperperfusion and hypoxia. *J. Appl. Physiol.* 58:1659-1668, 1985.

77. Neubauer, J.A., J.E. Melton, and N.H. Edelman. Modulation of respiration during brain hypoxia. *J. Appl. Physiol.* 68: 441-451, 1990.

78. Nielsen, M. and H. Smith. Studies on the regulation of respiration in acute hypoxia. *Acta Physiol. Scand.* 24:293-313, 1951.

79. Padget, P. The respiratory response to carbon dioxide. *Am. J. Physiol.* 83:384-394, 1928.

80. Painter, R., S. Khamnei and P. Robbins. A mathematical model of the human ventilatory response to isocapnic hypoxia. *J. Appl. Physiol.* 74:2007-2015, 1993.

81. Pandit, J.J., and P.A. Robbins. The ventilatory effects of sustained isocapnic hypoxia during exercise in humans. *Respir. Physiol.* 86:393-404, 1991.

82. Pandit, J.J., and P.A. Robbins. Ventilation and gas exchange during sustained exercise at normal and raised $CO_2$ in man. *Respir. Physiol.* 88:101-112, 1992.

83. Pandit, J.J. The Effects of Exercise on the Chemical Control of Breathing in Man. *D.Phil. Thesis.* University of Oxford. 1993.

84. Patil, C.P., K.B. Saunders and B.M. Sayers. Timing of deep breaths during rest and light exercise in man. *Clin. Sci.* 78:573-578, 1990.

85. Pflüger, E. Ueber die Ursache der Athembewegungen, sowie der Dyspnoë und Apnoë. *Pflügers Archiv für die gesamte Physiologie des menchen und der Thiere.* 1:60-106, 1868.

86. Priban, I.P. An analysis of some short-term patterns of breathing in man at rest. *J. Physiol. (London)* 166:425-434, 1963.

87. Priestley, M. B., and S.S Rao. A testing of non-stationarity of time-series. *J. Royal Stat. Society, Ser.B,* 31: 140-149, 1969.

88. Priestley, M. B. Spectral Analysis and Time Series. London: Academic Press, pp. 449-471, 1981*a*.

89. Priestley, M. B. Spectral Analysis and Time Series. London: Academic Press, pp. 821-848, 1981*b*.

90. Priestley, M. B. Non-linear and Non-Stationary Time Series Analysis. London: Academic Press, 1991.

91. Rebuck, A.S., and E.J.M. Campbell. A clinical method for assessing the ventilatory response to hypoxia. *Amer. Rev. Resp. Dis.* 109:345-350, 1974.

92. Reynolds, W.J., H.T. Milhorn and G.H. Holloman. Transient ventilatory response to graded hypercapnia in man. *J. Appl. Physiol.* 33:47-54, 1972.

93. Robbins, P.A., G.D. Swanson, A.J. Micco and W.P. Schubert. A fast gas-mixing system for breath-to-breath respiratory control studies. *J. Appl. Physiol.* 52:1358-1362, 1982.

94. Robbins, P.A. The ventilatory response of the human respiratory system to sine waves of alveolar carbon dioxide and hypoxia. *J. Physiol. (London)* 350:461-474, 1984.

95. Severinghaus, J.W. Proposed standard determination of ventilatory responses to hypoxia and hypercapnia in man. *Chest.* 70(Supplement):129-131, 1976.

96. Shea, S.A., J. Walter, K. Murphy and A. Guz. Evidence for individuality of breathing patterns in resting healthy man. *Respir. Physiol.* 68:331-344, 1987.

97. Shore, E.T., R.P. Millman, D.A. Silage, D.-C. Chung and A.I. Pack. Ventilatory and arousal patterns during sleep in normal young and elderly subjects. *J. Appl. Physiol.* 59:1607-1615, 1985.

98. Stoll, P.J. Respiratory system analysis based on sinusoidal variations of $CO_2$ in inspired air. *J. Appl. Physiol.* 27:389-399, 1969.

99. Swanson, G.D. and J.W. Bellville. Hypoxic-hypercapnic interaction in human respiratory control. *J. Appl. Physiol.* 36:480-487, 1974.

100. Swanson, G.D. and J.W. Bellville. Step changes in end-tidal $CO_2$: methods and implications. *J. Appl. Physiol.* 39:377-385, 1975.

101. Tobin, M.J., M.J. Mador, S.M. Guenther, R.F. Lodato and M.A. Sackner. Variability of resting respiratory drive and timing in healthy subjects. *J. Appl. Physiol.* 65:309-317, 1988.

102. Van Beek, J.H.G.M., A. Berkenbosch, J. DeGoede and C.N. Olievier. Effect of brain stem hypoxaemia on the regulation of breathing. *Respir. Physiol.* 57:171-188, 1984.

103. Vizek, M., C.K. Pickett and J.V. Weil. Biphasic ventilatory response of adult cats to sustained hypoxia has central origin. *J. Appl. Physiol.* 63:1658-1664, 1987.

104. Ward, D.S., A. Berkenbosch, J. DeGoede and C.N. Olievier. Dynamics of the ventilatory response to central hypoxia in cats. *J. Appl. Physiol.* 68:1007-1113, 1990.

105. Ward, D.S., A. Dahan and C.B. Mann. Modelling the dynamic ventilatory response to hypoxia in humans. *Ann. Biomed. Eng.* 20:181-194, 1992.

106. Weil, J.V., E. Byrne-Quinn, I.E. Sodal, J.S. Kline, R.E. McCullough and G.F. Filley. Augmentation of chemosensitivity during mild exercise in normal man. *J. Appl. Physiol.* 33: 813-819, 1972.

107. Weil, J.V. and C.W. Zwillich. Assessment of ventilatory response to hypoxia. *Chest.* 70(Supplement):124-128, 1976.

108. Weiskopf, R.B., and R.A. Gabel. Depression of ventilation during hypoxia in man. *J. Appl. Physiol.* 39:911-915, 1975.

## Publications associated with this thesis

1. Liang, P.-J., J.J. Pandit and P.A. Robbins. Non-stationarity of breath-by-breath ventilation and approaches to modelling the phenomenon. In: *Modeling and Control of Ventilation.* New York: Plenum, pp.117-121, 1995.

2. Liang, P.-J., J.J. Pandit and P.A. Robbins. The statistical properties of breath-to-breath variations in ventilation of human subjects. *Journal of Applied Physiology* (In press).

3. Liang, P.-J., D.A. Bascom and P.A. Robbins. A comparison of two models of the ventilatory response to sustained isocapnic hypoxia in humans. *Journal of Applied Physiology* (Accepted subject to revision).

## Published abstracts

1. Liang, P.-J., J.J. Pandit and P.A. Robbins. Non-stationarity of breath-by-breath ventilation during "steady breathing" in humans. *Journal of Physiology (London)*, 480.P:51P, 1994.

2. Liang, P.-J., J.J. Pandit and P.A. Robbins. Non-stationarity of respiratory variability and possible model structures for the noise processes. *Clinical and Experimental Pharmacology and Physiology*, 22(3):A42, 1995.

3. Liang, P.-J., D.A. Bascom and P.A. Robbins. Dynamic models of the human ventilatory response to sustained hypoxia. *Journal of Physiology (London)*, 487.P:109P, 1995.

4. Liang, P.-J., I.D. Clement and P.A. Robbins. Dynamics of the fast component of the ventilatory response to acute hypoxia in humans. *Journal of Physiology (London)*, 494.P:93-94P, 1996.